UNIVERSITY OF CALIFORNIA
SANTA CRUZ

STRUCTURAL AND FUNCTIONAL ASSESSMENTS OF VISION AND TOUCH IN SEA OTTERS, *ENHYDRA LUTRIS*

A dissertation submitted in partial satisfaction
of the requirements for the degree of

DOCTOR OF PHILOSOPHY

in

ECOLOGY AND EVOLUTIONARY BIOLOGY

by

Sarah McKay Strobel

September 2019

The Dissertation of Sarah McKay Strobel
is approved:

Professor Jim Estes, chair

Professor Bruce Lyon

Professor Pete Raimondi

Tim Tinker, Ph.D.

Quentin Williams
Acting Vice Provost and Dean of Graduate Studies

TABLE OF CONTENTS

LIST OF TABLES

Chapter 3

LIST OF FIGURES

Chapter 1

Chapter 2

Chapter 3

STRUCTURAL AND FUNCTIONAL ASSESSMENTS OF VISION AND TOUCH IN SEA OTTERS, *ENHYDRA LUTRIS*

Sarah McKay Strobel

ABSTRACT

The proximate mechanisms underlying foraging behavior in sea otters (*Enhydra lutris*) are relatively unknown despite decades of research focused on the biology and ecology of this top predator. Sea otters prey on infaunal or visually cryptic benthic invertebrates, but maintain a high rate of capture to consume a quarter of their body mass each day. Consequently, sea otter sensory systems have been shaped by selective pressures for accurate and efficient detection of prey location and assessment of prey quality. This dissertation describes a series of behavioral experiments with trained sea otters and anatomical studies from post-mortem sea otters to assess the visual and tactile capabilities of this species in the context of underwater foraging behavior. Chapter 1 focuses on the visual sense and potential adaptations for foraging in marine environments and low light. This material comprises quantitative and qualitative descriptions of pupil mobility, retinal photoreceptor distribution, and tapetal morphology to assess low-light sensitivity relative to previously demonstrated amphibious acuity. We find that sea otter pupils adjust in size to variable light levels and sea otter retinas retain features that enhance sensitivity in low light. However, pupillary dynamic size range and visual acuity in low light are limited relative to other marine carnivores, likely due to a smaller absolute eye size, non-specialized circular pupil shape, and a reliance on a narrow

range of pupil sizes to adequately deform the lens to retain visual acuity under water. Given that sea otters forage successfully across a wide range of light levels and for buried prey, the conclusions from Chapter 1 motivated subsequent investigations of whether sea otter touch abilities are sensitive enough to compensate for the loss of visual focus in low light. The results presented in Chapters 2 are drawn from a comprehensive series of four experiments with a trained sea otter to directly measure in-air and underwater tactile sensitivity for paws and facial vibrissae. These studies provide a behavioral means to evaluate predictions based on previous research of sea otter brain and vibrissal morphology. We find that sea otter paw and vibrissal sensitivities are comparable to other tactile specialists, but paw-based touch is especially acute and comparable to human hands. Additionally, sea otter decision times were reliably less than 250 ms for paw and 500 ms for vibrissae, which suggests that sea otters can make fast and accurate decisions based on information received through touch. Chapter 3 builds on the behavioral results from Chapter 2 to investigate the density and distribution of sensory receptors and associated circulatory structures in sea otter glabrous (*i.e.*, hairless) skin—paw pads, flipper digit pads, lips, and the rhinarium—and to link the degree of neural investment to differential sensitivity and use of these regions in observed sea otter behavior. We confirm the presence of two mammalian mechanoreceptor types—Merkel cells and Pacinian corpuscles—and find that their densities, as well as corresponding neural and blood supply, were highest in the paw digit tips and substantially lower in other glabrous skin. This pattern of increased neural investment is consistent with the areas of the

paw primarily used for texture discrimination in Chapter 2, which suggests that the distal paw serves as a tactile fovea in sea otters. As a body of work, this dissertation combines structural and functional approaches to provide a more comprehensive assessment of the visual and tactile systems in sea otters. The findings from these studies not only contribute foundational knowledge about the sensory biology of sea otters, but also offer a mechanistic framework to interpret behavioral patterns and energy expenditure observed in wild sea otters across variable environmental conditions.

DEDICATION

To my mischievous kelp weasel collaborators

Odin, Selka, Charlie

and 836-18, 839-18, 844-18, 849-19,

and to Rio

who warms our hearts with each ice cube

ACKNOWLEDGMENTS

How can I sufficiently thank the people who have contributed to my growth as a scientist, mentor, and person throughout this strange process of earning a doctorate? I must first firmly acknowledge that this dissertation and my identity as a scientist would not have been possible without Dr. Colleen Reichmuth. Her guidance over the last seven years has made me a humbler researcher, a better communicator, and a kinder human being. Although her signature is on this page due to University regulations of committee structure, her approval means as much to me as the signatures on the cover page.

The Dissertation of Sarah McKay Strobel is approved:

Colleen Reichmuth, Ph.D.

The remaining members of my committee—Drs. Tim Tinker, Jim Estes, Bruce Lyon, and Pete Raimondi—encouraged me to pursue multiple research directions while providing helpful guidance to keep me from straying too far off the path. Dr. Tim Tinker welcomed me to the sea otter community to me and then gave me the freedom to explore it from a new perspective. Conversations with Tim pushed me to expand my quantitative skills without forgetting about natural history, which has made me a more well-rounded scientist. Dr. Jim Estes was always present as a guiding hand to place my research questions into the broader context of ecology. He makes it a point to always treat graduate students as colleagues, and his

encouragement has helped me feel that I have a place in the research world. Dr. Bruce Lyon's direct feedback has greatly improved the clarity of my writing for all three chapters. His early assurances about my ways of thinking helped substantially to fight the ever-present feelings of imposter syndrome throughout graduate school. Dr. Pete Raimondi juggles what seems like an infinite number of professional responsibilities while remaining patient and kind to any person who knocks on his door. His willingness to sit down with me on short notice to discuss statistical approaches was instrumental in developing the analyses for Chapter 2 and 3. Dr. Rita Mehta swooped in like a fairy research godmother and adopted me into her lab over my last year. Her inclusive approach to mentorship has made me feel that I am worth investing in, and she has been an invaluable cheerleader for my professional development.

I owe the completion of this dissertation to many other mentors outside of academia. Dr. Melissa Miller, Laird Henkel, and the team at the Marine Wildlife Veterinary Care and Research Center have been incredibly open to collaboration and were directly or indirectly involved in all three chapters. Andy Johnson, Michelle Staedler, Karl Mayer, Dr. Michael Murray, Chris DeAngelo, and their teams at the Monterey Bay Aquarium were patient teachers who helped me find my own voice in the sea otter community.

Keeping a smile on one's face through the rigors of graduate school is not possible without the mutual support among fellow graduate students. Dr. Peter Cook inspired me to think big and welcomed me as a colleague despite my first-year naiveté. Dr. Christin Murphy's generosity was singlehandedly responsible for

launching my graduate research career. I have greatly admired Dr. Jillian Sills as my academic big sister—she taught me the satisfaction of careful, attentive methodology and the importance of a good bottle of red wine. As my academic big brother, Dr. Kane Cunningham taught me to advocate for my scientific ideas in a kind manner. I don't know how she does it, but Dr. Caroline Casey brings a grounded and compassionate perspective even when the world feels like it's spinning out of control—I would be a far worse person without her friendship. I value the openness of Kirby Parnell, Brandi Ruscher-Hill, and Holly Herman-Sorenson to having honest conversations about the ups and downs of graduate school, and Dr. Sarah Kienle was always ready with a genuine laugh and an invitation to pick-me-up lunch. To the one-and-only Ross Christopher Nichols, with whom I can debate at length the architecture of the perfect nachos. He has been a shoulder to lean on at my lowest and a cheerleader to celebrate with at my highest. No one but he is capable of maintaining the spirit of Natchek all year round.

The Pinniped Cognition and Sensory Systems Lab is a weird time vortex—I've never seen another lab that accomplishes so much research and mentorship with as few resources. My fondest memories of the last seven years are with my cohort-turned-family—Tristin, Claire, Shelby, Katie, Ross, Skyla, Karli, Jenn, Brendan, Megan, Vanessa, and Andrew. They made Santa Cruz home. In addition to my cohort, an absurdly large number of volunteer research assistants and interns at the lab have had a hand in some part of my dissertation research, from developing creative sea otter enrichment to sitting in uncomfortable positions for long periods of

time during data collection. They volunteered 15-40 hours of their time each week and deserve significant recognition. Each day with this special group of people holds years of memories, including incredible joys and deep sadnesses. They helped me identify my strengths, work on my weaknesses, and ultimately discover the person who I want to be.

The cyclical nature of the research community cannot function without the dedicated commitment of long-term staff. Dr. Dave Casper tirelessly provides veterinary care for our animal colleagues and performed a life-saving surgery on a young shark-bitten sea otter who profoundly altered my life a couple years later. Jenna Sullivan at the Pinniped Cognition and Sensory Systems Laboratory has maintained a positive spirit of comradery in the program despite big changes that challenged us all personally and professionally. Sonny Knaub was a patient and supportive mentor who always pushed me to be a better trainer. Asila Ghoul established a collaborative relationship with the Monterey Bay Aquarium and the sea otter community, as a whole; her early efforts and encouragements opened the door for me to pursue sea otter research. I deeply respect Traci Kendall, Beau Richter, Courtney Ribeiro-French, and the entire team in Dr. Terrie Williams's Marine Mammal Physiology Lab, who have become dear colleagues in the shared pursuit of animal care and training. Maria Choy, Jody Bruner, Randolph Skrovan, and Nate Randolph at Long Marine Lab provided administrative and facility support. In the EEB department, Sarah Amador patiently guided me through administrative hoops and made time for many encouraging chats over the last few years, and Jacqueline

Rose for coordinating the room for my public defense. I am grateful to the funding agencies that supported the research summarized in this dissertation, including the National Science Foundation, Friends of Long Maine Lab, The Graduate Assistantship in Areas of National Need Fellowship, the Earl & Ethyl Myers Oceanographic and Marine Biology Trust Award, the Sea Otter Foundation and Trust, and the EEB department here at UCSC.

My mother and father have been supportive of my academic pursuits since I announced my plans to be a marine biologist on a family road trip in 1996. Thank you for teaching me a strong work ethic and guaranteeing me the independence to pursue work that excites me. My little big sister Paich has quietly looked out for me my whole life, and she has dropped everything to visit Santa Cruz when I just needed a sister's hand to hold. Randomly assigned acquaintances transformed into dear friends throughout college—Kay, Lizzie, Annie, Kelley, and Elizabeth—continue to remind me who I am outside of science.

I want to acknowledge my partner: local hero and lifestyle bike racer Zach Wick, who values the person I am and challenges me to be the person I could be. He constantly encourages me to take my hands of the brakes and just send it. I sure am a lucky lady to have him rooting for me.

Finally, I cannot finish my degree without thanking my non-human family. Learning from my fissiped friends, Charlie, Odin, and Selka, and my pinniped partners, Rio, Ronan, Natchek, Nayak, Noatak, Siku, Sprouts, Amak, and Tunu, has

been, paws and flippers down, the most rewarding experience and greatest adventure of my life.

The text of this dissertation includes a reprint of the following previously published material:

Strobel, S.M., Sills, J.M., Tinker, M.T., and Reichmuth, C.J. 2018. Active touch in sea otters: in-air and underwater texture discrimination thresholds and behavioral strategies for paws and vibrissae. *Journal of Experimental Biology* 221(18): jeb181347. doi:10.1242/jeb.181347.

Co-author Dr. Colleen Reichmuth directed and supervised the research that forms the basis for this dissertation. Co-author Dr. Jillian Sills provided technical support regarding experimental design and data collection. Dr. Tim Tinker provided expertise in designing the Bayesian statistical analyses that estimated sensitivity thresholds. I (Sarah McKay Strobel) designed all experiments, trained the sea otter subject for all research behaviors, collected and analyzed all experimental data, and was responsible for manuscript preparation.

All procedures performed in studies involving animals were in accordance with institutional ethical standards. All applicable international, national, and institutional guidelines for the care and use of animals were followed under USFWS Permit MA186914-1 and MA186914-2 and the Institutional Care and Use Committees at

University of California Santa Cruz (Reicc1304, Reicc1603, and Reicc1701) and Monterey Bay Aquarium (13-02). All research with human subjects was conducted with the approval and oversight of the University of California Santa Cruz's Institutional Review Board (Protocol #2786). Post-mortem samples were collected under Letters of Authorization from the United States Fish and Wildlife Service (08EVEN00-2016-B-0187 and 08EVEN00-2017-B-0045).

INTRODUCTION

Living organisms sense the environment to obtain nutrients, perform essential life history functions, and avoid danger. Across and within taxa, responses to perceived information range along a behavioral spectrum from simple, immediate positive or negative taxis to complex decision-making and future planning. Over evolutionary time, selection should favor organisms with appropriate and efficient responses to their environment. However, an individual rarely exists in one environmental state throughout its lifetime. Instead, external transitions (*e.g.*, seasons, migrations, microhabitats) and/or internal transitions (*e.g.*, ontogeny, learning) can pose conflicting selective pressures on the morphology and function of sensory systems.

In the case of amphibious mammals, two critical resources are spatially separated—food resources underwater and oxygen at the surface. Since air and seawater differ substantially in physical properties that influence the transmission of light, sound, chemicals, and vibrations, the sensory systems of these species show variation in form and function depending on their relative importance in air or underwater. Unlike other aquatic carnivores, amphibious marine mammals are secondarily adapted to the marine environment, having undergone major evolutionary transitions from the terrestrial to aquatic habitat 25-27 Ma (seals and sea lions), 1-3 Ma (sea otters), 1-1.5 Ma (polar bears) (Berta et al. 2015). This mixed evolutionary

history is important to consider, as it directly constrains the base material upon and time frame in which selection can act across extant species (Estes 1989).

Sea otters, *Enhydra lutris*, are an amphibious marine mammal species that historically ranged continuously from Baja California northward along the Pacific rim to the Alaskan archipelago and Japan (Bodkin 2015). Heavily depleted during the 19th-century fur trade (Kenyon 1969), sea otters now exist in fragmented populations along the western coastline of North America (Kenyon 1969; Riedman and Estes 1990; Bodkin 2015). Sea otters differ from other aquatic carnivores in their use of the aqueous environment, use of terrestrial substrate, time spent at the water's surface, and mobility of their prey resources. Sea otters do not depend on the terrestrial environment for life history functions, unlike polar bears, pinnipeds, amphibious mustelids, and freshwater otters, who require access to land or ice for reproduction (Estes 1989). Sea otters make shallow foraging dives and rest in air at the water's surface for extended periods of time, unlike pinnipeds, who spend extended periods of time underwater when at sea and typically haul out to rest (*e.g.*, Feldkamp et al., 1989; Le Boeuf et al., 2000). Sea otters primarily consume sessile or slow-moving marine invertebrates (Riedman and Estes 1990), unlike pinnipeds and many freshwater otters, who capture fast-swimming fish using vision and vibration-sensitive vibrissae (Walls 1942; Jamieson and Fisher 1972; Green 1977; Dehnhardt et al. 2001), and polar bears, who use a highly sensitive olfactory system to prey upon Arctic seals in air (Stirling and Latour 1978). Sea otters' unique use of the aquatic environment and the strong selective pressure to forage efficiently given their high

baseline metabolic demands (Costa and Kooyman 1982) make for an interesting case study to examine how terrestrial-based sensory systems can adapt to function amphibiously over a relatively short evolutionary time period. Since underwater observations of foraging behavior in sea otters are scarce and difficult to obtain (Shimek 1977; Hines and Loughlin 1980), focused research on their sensory capabilities can provide context to identify the mechanisms underlying high foraging efficiency measured from observations of sea otters at the water's surface (Estes et al. 2003; Bodkin et al. 2004, 2007).

While sea otter sensory biology is still relatively unstudied, experimental and morphological studies over the last decades have assessed the auditory, chemoreceptive, visual, and tactile systems to some degree. Although morphology of the outer and middle ear show features associated with streamlining for an aquatic environment, sea otter hearing seems mostly adapted to detect air-borne sounds at the water's surface rather water-borne sounds while diving (Ghoul and Reichmuth 2014a, b). Chemoreceptive sensitivity and its role in intraspecific communication seem reduced in sea otters relative to terrestrial and amphibious mustelids (Gittleman 1991; Hammock 2005; Van Valkenburgh et al. 2011), although anecdotal evidence suggests that chemical cues remain an important source of information in social interactions, predator avoidance, and prey quality assessments (Kenyon 1969; Estes 1989; Riedman and Estes 1990; Kvitek et al. 1991; Kvitek and Bretz 2004). Sea otter vision has been classified as intermediate between terrestrial and aquatic carnivores based on studies of acuity, spectral sensitivity, and accommodation (Walls 1942; Mass and

Supin 2000, 2007). Their visual sensitivity in low-light conditions commonly encountered by diving mammals is unknown. Observations of populations at high latitudes report subtle behavioral changes in response to ambient light levels, which suggests that visual cues may play a role in underwater foraging behavior or in-air predator avoidance (Estes et al. 1982; Esslinger et al. 2014). Touch has long been considered a promising avenue for research in sea otters, given expanded allocation of tissue in the somatosensory cortex (Radinsky 1968) and obvious modifications to the vibrissal array (Marshall et al. 2014) and forefeet morphology (Pocock 1928; Kenyon 1969). In addition, the infaunal habitat and cryptic behavior of their invertebrate prey, field-based observations of underwater foraging behavior (Shimek 1977; Hines and Loughlin 1980) and paw-based tool use during prey handling at the water's surface (Hall and Schaller 1964; Fujii et al. 2015) suggest that touch is highly useful to maintain high foraging efficiency required by high daily metabolic needs (Costa and Kooyman 1982). However, touch sensitivity has not been assessed for either the vibrissal array or glabrous skin on their forefeet (*i.e.*, paws). Other specialized sensory systems, such as electroreception or magnetoreception, have remain untested for this species, as little in their ecology and behavior suggests that these senses have developed.

This dissertation aims to improve our understanding of sensory biology in sea otters from the perspective of foraging behavior and differential use of in-air and underwater environments. I integrate structural and functional approaches to assess the visual and tactile systems of sea otters. This whole-animal strategy provides an

opportunity to examine the links between morphology, sensitivity, and behavior within the constraints imposed by an amphibious lifestyle and to integrate sensory biology within the framework of foraging ecology for this aquatic top predator.

Chapter 1 of this dissertation assesses amphibious vision in sea otters, specifically the tradeoff between sensitivity in low-light conditions and acuity in bright-light conditions. Although vision is the best studied sense in sea otters, key data gaps remain; this chapter aims to address these research areas and resolve previously equivocal conclusions on visual function in the species. I evaluate the morphology of the sea otter retina and tapetum lucidum using histology and photography, and I measure the pupillary response of trained sea otters to changes in ambient light levels and spectral properties. This chapter concludes with a comparative discussion of sea otters relative to other terrestrial and aquatic carnivores and considers sea otters' degree of investment in low-light sensitivity and acuity within the context of their unique in-air and underwater behaviors.

Chapter 2 of this dissertation uses behavioral psychophysics to measure the in-air and underwater sensitivity of the tactile system (*e.g.*, paws and vibrissae) to textural differences in a young, healthy sea otter trained with positive reinforcement techniques. I measure performance as percent correct response in a two-alternative choice procedure in each experimental condition. I apply a novel Bayesian statistical technique to fit a psychometric curve and interpolate relative difference threshold for each condition. Additionally, I use model comparison to assess if thresholds differ between paw or vibrissae and between air or under water. In addition to sensitivity

measurements, I analyze the sea otter's exploration strategy and decision time using video footage from each experimental session. To directly compare sea otters to humans and compare this study to the larger body of research on human touch, I also measure human hand sensitivity, strategy, and decision time using the same experimental procedure and stimuli as the sea otter. I fit psychometric curves to the human data using the same Bayesian approach, and I assess the effects of difficulty, species, and media on strategy and decision time using generalized linear mixed effects models and linear mixed effects models. This chapter concludes with a comparison of the sea otter's performance with other aquatic and terrestrial touch specialists and relates her strategy to species-specific evolutionary pressures for quick processing of tactile information to make efficient decisions while foraging.

Chapter 3 of this dissertation uses histology to describe and quantify the morphology of the tactile system within sea otter glabrous skin: paw pads, rhinarium pad, lips, and flipper digit pads. In collaboration with the sea otter stranding response team and veterinary staff at the Monterey Bay Aquarium, I collect glabrous skin structures from deceased sea otters. I section and process the tissues for histology and work closely with the Veterinary Histology lab at University of California Davis for tissue staining. After imaging the stained tissues with light microscopy, I identify presence or absence of mechanoreceptive structures and calculate their density. Using generalized mixed effect models and custom contrasts with equal weighting, I assess differences in mechanoreceptor density across and within glabrous skin structures. Additionally, I describe gross morphology of the skin texture and thickness and

speculate on its contribution to touch function given the thermoregulatory demands of sea otters as a small-bodied mammal in an aquatic environment. This chapter directly complements the behavioral measurements of touch in Chapter 2 and previous histological descriptions of the sea otter vibrissal system (Marshall et al. 2014) to assess the sea otter tactile system from structure to function.

Given limited direct observations of foraging behavior in free-ranging sea otters, the significance of this dissertation extends beyond the assessment of a single sense in a single species. Taken together, these three chapters contribute new data that advance our understanding of sensory biology, behavior, and ecology in a coastal predator and highlight the importance of using multiple methods to interpret the influence of abiotic cues on foraging behavior. More broadly, this study contributes to our understanding of trade-offs associated with amphibious vision in mammals, and how different phylogenetic and ecological pressures can drive species to different evolutionary solutions.

REFERENCES

Berta A, Sumich JL, Kovacs KM (2015) Marine Mammals: Evolutionary Biology, 3rd edn. Academic Press, London

Bodkin JL (2015) Historic and Contemporary Status of Sea Otters in the North Pacific. In: Larson SE, Bodkin JL, VanBlaricom GR (eds) Sea Otter Conservation. Academic Press, London, pp 43–61

Bodkin JL, Esslinger GG, Monson DH (2004) Foraging depths of sea otters and implications to coastal marine communities. Mar Mammal Sci 20:305–321

Bodkin JL, Monson DH, Esslinger GG (2007) Activity budgets derived from time–depth recorders in a diving Mammal. J Wildl Manage 71:2034–2044 . doi: 10.2193/2006-258

Costa DP, Kooyman GL (1982) Oxygen consumption, thermoregulation, and the effect of fur oiling and washing on the sea otter, Enhydra lutris. Can J Zool 60:2761–2767 . doi: 10.1139/z82-354

Dehnhardt G, Hanke W, Bleckmann H (2001) Hydrodynamic trail-following in harbor seals (Phoca vitulina). Science (80-) 293:102–104

Esslinger GG, Bodkin JL, Breton AR, et al (2014) Temporal patterns in the foraging behavior of sea otters in Alaska. J Wildl Manage 78:689–700 . doi: 10.1002/jwmg.701

Estes JA (1989) Adaptations for Aquatic Living by Carnivores. In: Gittleman JL (ed) Carnivore behavior, ecology, and evolution. Cornell University Press, Ithaca, pp 242–282

Estes JA, Jameson RJ, Rhode EB (1982) Activity and prey selection in the sea otter: influence of population status on community structure. Am Nat 120:242–258

Estes JA, Riedman ML, Staedler MM, et al (2003) Individual variation in prey selection by sea otters: patterns, causes and implications. J Anim Ecol 72:144–155

Feldkamp SD, DeLong RL, Antonelis GA (1989) Diving patterns of California sea lions, Zalophus californianus. Can J Zool 67:872–883

Fujii JA, Ralls K, Tinker MT (2015) Ecological drivers of variation in tool-use frequency across sea otter populations. Behav Ecol 26:519–526 . doi: 10.1093/beheco/aru220

Ghoul A, Reichmuth C (2014a) Hearing in sea otters (Enhydra lutris): Audible frequencies determined from a controlled exposure approach. Aquat Mamm 40:243–251 . doi: 10.1578/AM.40.3.2014.243

Ghoul A, Reichmuth C (2014b) Hearing in the sea otter (Enhydra lutris): auditory profiles for an amphibious marine carnivore. J Comp Physiol A Neuroethol Sens Neural Behav Physiol 200:967–81 . doi: 10.1007/s00359-014-0943-x

Gittleman JL (1991) Carnivore olfactory bulb size: allometry, phylogeny and ecology. J Zool 225:253–272 . doi: 10.1111/j.1469-7998.1991.tb03815.x

Green J (1977) Sensory perception in hunting otters, Lutra lutra. Otters, J Otter Trust 13–16

Hall KRL, Schaller GB (1964) Tool-using behavior of the California sea otter. J Mammal 45:287–298

Hammock J (2005) Structure, function and context: the impact of morphometry and ecology on olfactory sensitivity. Massachusetts Institute of Technology and Woods Hole Oceanographic Institution

Hines AH, Loughlin TR (1980) Observations of sea otters digging for clams at Monterey Harbor, California. Fish Bull 78:159–163

Jamieson GS, Fisher HD (1972) The pinniped eye: a review. In: Harrison RJ (ed) Functional Anatomy of Marine Mammals, Vol. 1. Academic Press, London, pp 245–261

Kenyon K (1969) The sea otter in the eastern Pacific ocean. Washington, D.C.

Kvitek R, Bretz C (2004) Harmful algal bloom toxins protect bivalve populations from sea otter predation. Mar Ecol Prog Ser 271:233–243 . doi: 10.3354/meps271233

Kvitek RG, Degange AR, Beitler MK (1991) Paralytic shellfish poisoning toxins mediate feeding behavior of sea otters. Limnol Oceanogr 36:393–404

Le Boeuf BJ, Crocker DE, Costa DP, et al (2000) Foraging ecology of northern elephant seals. Ecol Monogr 70:353–382

Marshall CD, Rozas K, Kot B, Gill VA (2014) Innervation patterns of sea otter (Enhydra lutris) mystacial follicle-sinus complexes. Front Neuroanat 8:1–8 . doi: 10.3389/fnana.2014.00121

Mass AM, Supin AY (2007) Adaptive features of aquatic mammals' eye. Anat Rec 290:701–715 . doi: 10.1002/ar.20529

Mass AM, Supin AY (2000) Ganglion cells density and retinal resolution in the sea otter, Enhydra lutris. Brain Behav Evol 55:111–119 . doi: 10.1159/000006646

Pocock RI (1928) Some external characters of the sea-otter (Enhydra lutris). Proc Zool Soc London 98:983–991

Radinsky LB (1968) Evolution of somatic sensory specialization in otter brains. J Comp Neurol 134:495–506 . doi: 10.1002/cne.901340408

Riedman ML, Estes JA (1990) The sea otter (Enhydra lutris): behavior, ecology, and natural history. Biol Rep 90:1–136

Shimek S (1977) The underwater foraging habits of the sea otter, Enhydra lutris. Calif Fish Game 63:120–122

Stirling I, Latour PB (1978) Comparative hunting abilities of polar bear cubs of different ages. Can J Zool 56:1768–1772

Van Valkenburgh B, Curtis A, Samuels JX, et al (2011) Aquatic adaptations in the nose of carnivorans: evidence from the turbinates. J Anat 218:298–310 . doi: 10.1111/j.1469-7580.2010.01329.x

Walls GL (1942) The vertebrate eye and its adaptive radiation. Hafner, New York

CHAPTER 1

ADAPTATIONS FOR AMPHIBIOUS VISION IN SEA OTTERS:

STRUCTURAL AND FUNCTIONAL OBSERVATIONS

ABSTRACT

Sea otters (*Enhydra lutris*) are amphibious mammals that balance opposing selective forces exerted by air and water on vision. Although sea otters maintain equal in-air and underwater acuity, their lens-based accommodative mechanism requires a small pupil that may limit sensitivity across variable light levels. In this study we combine anatomical and behavioral methods to assess the tapetum lucidum, retina, and pupil dynamics in sea otters. We compare aspects of these structures to those of terrestrial and aquatic carnivores. The tapetum lucidum in sea otters resembles that of terrestrial carnivores. A heavily rod-dominated retina appears similar to the ferret and domestic cat, but methodological difficulties precluded a quantitative assessment. Pupil size in two trained sea otters changed 55- to 86-fold in air from bright day to dark night ambient light levels, which is a smaller range relative to pinnipeds when accounting for differing light conditions. Given previous work, our results suggest that sea otters have retained but not necessarily enhanced features for low-light vision, which may be constrained by pupil shape and absolute eye size. Sea otters certainly have functional vision in air and under water, but we cannot conclude if they compensate for underwater acuity lost in dim conditions when pupil dilation reduces accommodation effectiveness. This research helps to resolve mixed clues regarding amphibious vision in an important coastal predator and contributes to our understanding of how differing phylogenetic and ecological pressures can drive species to different evolutionary solutions in the visual domain.

INTRODUCTION

Sensory cues convey critical information about food availability, social interactions, competition, and predation threat across taxa. Physical properties of the environment directly affect the transmission of these cues, and species exhibit adaptations to process light, sound, chemicals, and vibrations appropriately for their habitats. When a species inhabits disparate physical environments, however, it must balance the opposing selective forces acting on its sensory systems. For vision, transmission of light differs between air and water, and maintenance of visual acuity when transitioning between the two transparent media presents an optical challenge for the two major refractive structures of the vertebrate eye: the cornea and the lens. In air, focusing power largely derives from the different refractive indices of cornea and air. As a result, terrestrial animals largely depend on the cornea for focusing power and typically rely less on the lens. Underwater, however, corneal power is lost given the similar refractive indices of the cornea and water, and thus aquatic species rely almost exclusively on lenticular accommodation. Amphibious vertebrates require adaptations to overcome the differences between the two media and support functional vision in air and under water. These adaptations include altered corneal curvature, changes in the lens shape and position, and changes in pupil shape and location to enable light to reach different parts (and different curvatures) of the lens. Some of these adaptations are static, such as flattened areas of the cornea and spherical lenses in seals and other pinnipeds (Walls 1942; Welsch et al. 2001) and double pupils in some fishes that use simultaneous amphibious vision (Walls 1942;

Sivak 1976). Conversely, accommodative mechanisms can be dynamic, shifting in each medium to retain acuity. Examples include muscle-based lenticular deformation in some pursuit-diving birds (Goodge 1960; Levy and Sivak 1980; Sivak et al. 1985; Katzir and Howland 2003) and high pupil mobility (*i.e.*, large range between minimum and maximum sizes) in some semiaquatic snakes (Schaeffel and de Queiroz 1990), pinnipeds (Walls 1942; Levenson and Schusterman 1997), and even some populations of humans that rely on aquatic resources obtained by diving (Gislen et al. 2003).

Amphibious vertebrates encounter a more variable range of light levels than obligate terrestrial or aquatic vertebrates. In air, amphibious vertebrates may experience both extended photopic (bright light) and scotopic (low light) conditions due to a polyphasic activity pattern (*i.e.*, multiple active and rest periods within 24 hours). While diving, the same animals experience rapid light changes on descent and ascent, as well as persistent low light levels at depth. To increase the amount of light processed by the retina in low light, species can develop large eyes and a higher proportion of rods in the retinal photoreceptor array. Additionally, species can increase the surface area or thickness of the tapetum lucidum, which comprises layers of reflective cells located behind the retina. To constrain the amount of light processed by the retina in bright conditions, species can develop pupils capable of drastically decreasing size and/or changing shape.

Sea otters (*Enhydra lutris*) are amphibious marine mammals closely related to terrestrial carnivores like weasels, badgers, and wolverines. As the heaviest

mustelid species, but one of the smallest marine mammals (the less aquatic marine otter *Lutra feline* is smaller (Valqui 2012)), sea otters have an extremely high baseline metabolic rate relative to other mammals (Costa and Kooyman 1982) and must devote substantial time to foraging to compensate for heat loss to the aquatic environment.. Sea otters hunt under water along the seafloor for invertebrate prey and occasionally fish, making repeated shallow, short dives (Riedman and Estes 1990; Bodkin et al. 2004; Thometz et al. 2016). Since they are unable to process prey under water, sea otters return to the surface after each dive to handle and consume captured prey, typically only spending a few minutes in air before diving again (see, *e.g.*, Ralls et al. 1995; Bodkin et al. 2004; Hughes et al. 2013; Thometz et al. 2016). These rapid transitions occur repeatedly as sea otters forage up to 11 hours throughout a 24-hour period (Garshelis et al. 1986; Bodkin et al. 2007; Thometz et al. 2016). When not foraging, sea otters rest, groom, and socialize at the surface, which reduces thermoregulatory costs but exposes them to extended periods of bright light during day and low light during night.

The degree to which sea otters rely on vision across air, water, and varying light levels is difficult to interpret based on observational studies of wild individuals. Activity patterns are typically polyphasic and not clearly delineated by ambient light levels (Ralls et al. 1995; Gelatt et al. 2002; Bodkin et al. 2004; Tinker et al. 2008). Foraging success seems unaffected by decreased light levels at night (Ralls et al. 1995; Jolly 1997; Wilkin 2003), however some sea otters shift foraging activity to maximize daylight hours during winter at high latitudes (Esslinger et al. 2014) or to

take advantage of fishes' reduced vision during dawn and dusk (Estes et al. 1982). Sea otter prey can be visually cryptic, and the extractive foraging techniques used by sea otters disperse sediment in the water column (Shimek 1977; Hines and Loughlin 1980), which likely inhibits vision beyond initial patch localization. Even when extractive techniques are unnecessary for prey capture, sea otters often forage in turbid estuarine and coastal habitats where visibility is poor.

Anatomical evidence, although sparse and incomplete, provides clues to resolve the role of vision in sea otter behavior. The position, size, and spectral sensitivity of the sea otter eye is best suited for in-air vision. Typical of most carnivores, sea otters have forward-facing eyes that enable a large field of binocular vision, a narrow range of monocular vision, and a relatively large blind area at the back of the head. Unlike polyphasic pinnipeds and nocturnal terrestrial mammals, sea otters eyes are not enlarged in the absolute sense or relative to body size (Estes 1989; Howland et al. 2004). Sea otters possess dichromatic color vision common in mammals, in contrast to derived cone monochromacy in some nocturnal mammals, all semiaquatic pinnipeds, and fully aquatic cetaceans (Jacobs 1993; Peichl et al. 2001; Levenson et al. 2006). Sea otters have retained a tapetum lucidum posterior to the retina (Riedman and Estes 1990)—a common vertebrate feature that allows for amplification of available light at low light levels. Tapetal structure, fundic-surface-area coverage, and thickness can vary widely across carnivores and relate to feeding behavior or compensate for reflectance interference from other eye structures

(Braekevelt 1986; Ollivier et al. 2004), but these tapetal properties have not been assessed in sea otters.

Despite sharing similarities with terrestrial mammals, sea otters exhibit a definite adaptation to maintain vision under water: a powerful accommodative mechanism that relies on strong ciliary body musculature to move the lens anteriorly against the iris and into the circular pupillary margin, which deforms the anterior surface of the lens into a more rounded shape (Murphy et al. 1990). This method of accommodation enables equal acuity across media and is also used by the North American river otter (*Lontra canadensis*) (Ballard et al. 1989) and some amphibious bird species that actively pursue fish prey under water (Walls 1942; Sivak et al. 1977; Ballard et al. 1989; Katzir and Howland 2003). Sea otter visual acuity is two to three times better than terrestrial and amphibious mustelids in photopic conditions (Neumann and Schmidt 1959; Balliet and Schusterman 1971; Schusterman and Barrett 1973; Sinclair et al. 1974; Dunstone and Sinclair 1978; Wight et al. 1988) and is more comparable to a distantly related group of amphibious mammals, the pinnipeds, which comprise sea lions, true seals, and walrus, *Odobenus rosmarus* (Gentry and Peterson 1967; Schusterman and Balliet 1970b, a; Mass 1992; Mass and Supin 1992, 2005, 2010; Supin and Mass 2003; Weiffen and Mo 2006; Hanke and Dehnhardt 2009; Hanke et al. 2009). However, the same mechanism that maintains acuity under water can limit low-light sensitivity (Schusterman and Barrett 1973). Since the sea otter pupil needs to remain small to induce sufficient lens deformation

under water, and a small pupil functions best in photopic conditions, underwater acuity may sharply decrease with declining light levels.

The extent to which sea otters balance tradeoffs in amphibious vision (visual acuity across media vs. sensitivity across variable light levels) is not well understood despite species-typical and comparative data from observational and anatomical studies (reviewed in Estes 1989). In this study, we contribute new data to evaluate the adaptations that support amphibious vision in sea otters. We address data gaps using functional and structural approaches: pupillometry to measure how the pupils of live sea otters respond to changes in brightness properties of light, and histology of preserved sea otter eyes to describe tapetal structure and photoreceptor density. Given the lens-based accommodative mechanism and circular pupil shape in sea otters, we suspect that the dynamic range of pupil size is limited. If vision in low-light is useful to sea otters, then we expect to find adaptations that compensate for constraints imposed by their method of accommodation, such as a robust tapetum lucidum or a higher rod-to-cone proportion than mustelids and diurnal terrestrial mammalian carnivores. These data allow us to assess the selective pressures shaping amphibious vision in sea otters relative to terrestrial mustelids that share a similar phylogeny, as well as semi-aquatic marine mammals that share a similar ecology.

MATERIALS AND METHODS

Tapetum Lucidum

To describe structural properties of the tapetum lucidum that may enhance low light vision, we made observations of tapetal appearance in a living sea otter

(*Enhydra lutris*, n=1) using photographic methods and in deceased sea otters (n=2) using histology. We photographed the eyes of a three year-old adult female sea otter (Selka: USGS 6511-12R, MBA 595-12) at Long Marine Laboratory, University of California Santa Cruz, Santa Cruz, CA. The sea otter was trained to receive eyedrops and hold still in a fixed location. We photographed the eyes under two conditions: (1) using flash photography with a DSLR camera in ambient light, and (2) using a fundic camera while she received a routine veterinary exam under anesthesia. Prior to flash photography, we administered two drops of a topical anticholinergic mydriatic medication (tropicamide ophthalmic solution USP, 1%, Bausch & Lomb Incorporated, Tampa, FL). Prior to the veterinary exam, we increased the tropicamide dosage to five drops to circumvent opioid-induced miosis while under anesthesia.

For the *ex situ* measurements of tapetal properties, we excised a left eye and a right eye from two adult male sea otters that were humanely euthanized following stranding. We placed each eye in Davidson's solution (Electron Microscopy Sciences, Hatfield, PA, USA) within 10 min of death. Following at least 48h fixation at room temperature, we placed each eye in 10% neutral buffered formalin. We hemisected the eyes at the ora serrata using a razor blade and removed all vitreous humor using forceps and spring scissors. Gross observations of the tapetal coverage within the fundus were noted. We sectioned two retinas to visualize ocular structures in cross section. The posterior eyecups underwent standard paraffin embedment and were sectioned at 5µm. We mounted sections on gelatinized slides and stained them routinely with Hematoxylin and Eosin.

Photoreceptor Density

To assess retinal adaptations for low-light vision, we excised a left eye from one adult male sea otter and a and a right eye from another adult male sea otter that were humanely euthanized following stranding. We placed each eye in Davidson's solution (Electron Microscopy Sciences, Hatfield, PA, USA) within 10 min of death. Following at least 48h fixation at room temperature, we placed each eye in 10% neutral buffered formalin. We dissected the eyes along the limbus to separate the posterior segment. The posterior segment was cryoprotected in sequentially increased sucrose solutions: 10% sucrose in phosphate buffered saline (PBS) for 1 hour, 20% sucrose for 1 hour, and then 30% sucrose overnight until the tissue sank. The tissue was embedded by submerging in Optimal Cutting Temperature gel (OCT, Sakura Finetek USA, Inc., Torrance, CA, USA) and slowly freezing over dry ice and 100% ethanol. We took serial 14µm cryosections along the horizontal plane of the segment. Additionally, a single eye was prepared for flat-mount analysis. The eye was fixed as above; thereafter, we removed the anterior segment and carefully dissected the retina by removing the fibrous and vascular tunics.

We slide-mounted and stained sections according to a previously published protocol (Mowat et al., 2013). Briefly, sections were rehydrated with PBS and then placed for 2 hours in blocking solution to block potential nonspecific binding sites in the tissue sample. Sections were incubated in primary antibody for 4 hours, rinsed, and incubated in secondary antibody for 2 hours (Supp Table 1). We evaluated cone arrestin and PNA as primary stains for cones, and we ran tandem sections without

primary stains as negative controls. Sections were slide-mounted using mounting media containing DAPI nuclear counterstain, which targets all photoreceptor nuclei. The retina for the flat-mount preparation was placed in a well of a 6-well culture plate and submerged in blocking solution for 2 h, followed by primary antibody overnight, and then secondary antibody for 2 h. The retina was laid flat on a slide and mounted as above. We used fluorescent and confocal microscopes to image cross-section and flat-mount slides then qualitatively evaluated images for their response to primary stains and use in determining rod-to-cone proportions.

Pupillometry

To measure dynamic range (*i.e.*, pupil size range from minimum to maximum size) we measured pupil size in response to varying light levels in living sea otters. This noninvasive measurement technique has been used across vertebrates to infer spectral sensitivity and quantify pupil mobility (Banks and Munsinger, 1974; De Groot and Gebhard, 1952; Hughes, 1977; Levenson and Schusterman, 1997; Munsinger and Banks, 1974; Werner, 1970; Wilcox and Barlow, 1975). Here, we trained two sea otters to position in ambient light conditions and controlled light exposures at Long Marine Laboratory, University of California Santa Cruz. The subjects were the same 3-year-old adult female and an 11-year-old adult male (Odin: USGS 3857-03, MBA Repo). Both sea otters were trained to position their heads in a fixed location and remain immobile for up to 45s.

We used a battery-powered infrared-sensitive black-and-white camera (APPRO, 30 fps) equipped with a macro lens (50mm f1.8) to film from 15cm the right eye of each sea otter (Fig. 1a) in bright and dark conditions. An infrared (IR) LED array comprising five LEDs (940nm, Lumex, Palatine, IL) provided light for the camera under dark conditions (Fig. 1a). We used a viewing monitor (Haier, Fig. 1c) to observe the sea otter's eye during data collection; the light emitted from the screen was blocked from the sea otter, and video recordings were stored to DVD. Each sea otter completed up to three sessions per experimental period (one day or one night), and we waited 15-20min between sessions to ensure that the sea otter's pupil returned to baseline dark-adapted size (Calderone and Jacobs, 2003; Levenson and Schusterman, 1999). The set-up remained in the same location and orientation during testing. We measured ambient light in foot candles using a luxometer (Goldilux® foot-candle meter, response accuracy ±3%).

To measure dynamic range, we filmed the sea otters under ambient day and night conditions. In addition to the IR light (940nm) that remained on for consistency across all sessions, we artificially increased the light in the day condition by exposing the sea otters to a broadband light (white) emitted from a battery-powered LED array 27cm away from and at the same height as the sea otter's eye (Fig. 1a). Sessions during the lowest light conditions (night) were performed outdoors after sundown or before dawn to ensure natural dark-adaptation, and sessions performed during brightest light conditions (day) were performed outdoors at midday. To confirm that the sea otters were insensitive to IR light used to provide light for the camera, we

completed two tests at night with the male sea otter. The first test (low-to-high IR) began with 15s of the IR light at low intensity to allow the camera to focus on the pupil, immediately followed by a step-wise increase of the IR light to the maximum intensity for 15s. If the sea otter was sensitive to this IR light, we expected to see a decrease in pupil size immediately following the step-wise increase. The second test (off-on IR) lasted for an additional 15s, beginning with 5s of maximum IR light to allow the camera to focus on the pupil, followed by turning off the IR light for 30s to allow the pupil to dilate following potential light exposure, then immediately followed by turning on the IR light at the maximum intensity for 10s. If the sea otter was sensitive to the IR light, we expected to see a decrease in pupil size immediately after we turned on the IR light in the third stage.

To provide gross estimation of spectral sensitivity at longer wavelengths, we exposed the male sea otter to two light treatments at night that differed in wavelength: 630nm (orange) and 640nm (red). We also exposed the sea otter to the broadband (white) as a positive control and 940nm (IR) as a negative control. The LED array corresponding to each treatment comprised a five-LED-circuit with comparable typical luminous intensity and viewing angle (Supp. Table 2). We measured each array's illuminance using the luxometer at the location of the sea otter's eye (Supp. Table 2). After the sea otter positioned in the fixed location (Fig. 1b), each session began when the camera focused on the pupil. Each session lasted for 30s: the first 15s of a session comprised the negative control immediately followed by 15s exposure to a light treatment or the positive control (white). We presented the stimulus at full

intensity in a step-function rather than a gradual increase in brightness. Additionally, we filmed the sea otter during 30s of continuous IR to monitor pupil size across the full time frame as the light treatments.

To measure pupil size across all conditions, we calibrated the scaling factor for each session. We presented a scale at eye level at the end of each session, moving it towards and away from the camera over the course of a few seconds. Upon reviewing the footage, we selected an in-focus image of the scale for size calibration. We inferred that the position of this in-focus scale was the same as the sea otter's eye, since we did not adjust the lens during a session. We then selected frames in which the pupil was in-focus to represent each second of the session for analysis. We did not select more than one frame per second, so due to slight movements of the sea otter and the extremely low level of ambient light, some seconds did not contain any frames that met criteria for image selection. We saved selected frames as PNG images and measured horizontal and vertical pupil diameters (Fig. 2a) and pupil area (Fig. 2b) using the image-analyzing software ImageJ (Rasband 1997).

We report differences in horizontal and vertical measurements of pupil diameter, and how these scaled with pupil area to recommend the most accurate proxy for pupil size. For the dynamic range measurements, we calculated means and standard errors for pupil area separately in the male and female sea otters. For the IR tests and light treatments, we calculated a pre-treatment mean (first 15s) and a post-treatment mean (final 10s to exclude the pupil's initial constriction response) for each session. Using a one-way analysis of variance, we found an effect of session on pre-

treatment pupil area for the 630nm (orange), continuous IR, and low-to-high IR test, which discouraged us from pooling sessions. Instead, we kept sessions as separate replicates and used the stats package in R (R Core Team, Vienna, Austria) to run a one-sided, paired *t*-test to compare three pairs of pre-treatment means and post-treatment means within each light treatment and the low-to-high IR control. We visually confirmed the required assumptions of normality and homoscedasticity. We report means and standard errors for pre-treatment and post-treatment for all replicates.

RESULTS

Tapetum Lucidum

Based on *in situ* and *ex situ* observations and measurements, we confirm that the tapetum of sea otters is a cellular type located in the anterior choroid posterior to the retina. The sea otter retina is holangiotic with retinal vessels extending throughout the fundus and onto the optic nerve head (Fig. 3b). The dorsal retinal epithelium is nonpigmented with gradually increasing pigmentation towards the periphery (Fig. 3d). The tapetum is a semicircular shape and is restricted to the superior choroid, covering ~40% percent of the fundus (Fig. 3b,c). The tapetum comprises 7-8 layers and measures 46 µm thick in the central retina (Fig. 4a) but thins towards the periphery (Fig. 4b). In photos with flash photography, the tapetum lucidum reflects a green-yellow color (Fig. 3a). In photos taken with the fundic camera, the tapetum reflects three ill-defined semi-circular zones that surround the optic disc (Fig. 3b).

The optic disc is off-white with three pairs of primary venules and arteries emanating from near a small physiologic cup and extending radially. The optic disc is surrounded by a narrow bright green ring called the conus papillaris (Fig. 3b). The central zone is blue-green and lightly mottled with yellow; this mottling becomes denser in the transition to the middle zone, which is yellow heavily mottled with orange (Fig. 3b). The orange mottling becomes denser in the transition to the peripheral zone (Fig. 3b).

For flash photography, dilation occurred within 1 h from two drops of topical 1% tropicamide (see Fig. 3a). For the veterinary exam, dilation occurred within 35 min from five drops of topical 1% tropicamide, but it was counteracted after administration of anesthetic drugs, despite the increased tropicamide dosage. To encourage further dilation, we administered two additional drops in each eye of the anesthetized sea otter, and dilation re-occurred within 30 min; this effect was still apparent 7 h later. Normal pupillary response returned within 24 h. During the veterinary exam, we opportunistically measured intraocular pressure (IOP) using a TonoVet tonometer. The otter's IOP measured 9 mmHg in the right eye and 11 mmHg in the left eye, generally considered in the normal reference range for other carnivores.

Photoreceptor Density

We achieved only partial success in determining rod-to-cone proportions in the sea otter retina using IHC on both cross-section and flat-mount preparations.

DAPI nuclear counterstaining positively stained a dense network of outer segment nuclei, suggesting densely packed photoreceptor cells. Cone arrestin did not show staining of cones in test or control slides despite testing of multiple antibody concentrations and conditions. PNA showed positive staining of the inner/outer segment region of cones in cross-sections viewed with fluorescent microscopy and of individual cone cells in the flat-mount viewed with confocal microscopy. Few PNA-labeled cones suggested that photoreceptor distribution is heavily rod-dominant across the retina, although PNA-labeled cones subjectively increased in the area of the central retina. Overall high density of photoreceptors and evident outer segment deterioration during processing did not allow specific cell counting.

We supplemented our gross observations of photoreceptor density from IHC by examining the H&E-stained cross-sections used for tapetal measurements. Photoreceptor distribution was heavily rod dominated in cross-sections from the central (Fig. 4a,5) and peripheral retina with lower overall photoreceptor density in the peripheral retina (Fig. 4a,b). The ratio of outer nuclear layer thickness to inner nuclear layer thickness (ONL/INL) ranged from 0.62 in central retina to 1.00 at periphery. As a side observation, contrary to previous reports (Mass and Supin 2000), we did not find evidence of physical attachment between the lens and iris based on histology.

Dynamic Range of Pupils and Insensitivity to IR light

The sea otters' pupils remained round under day and night conditions in air (Fig. 6), confirming early observations (Walls 1942; Mass and Supin 2000). On

average, we were able to select in-focus frames for 7-15 seconds in dynamic range assessments and for over 80% of each session for the IR tests and light treatments. Calculating pupil area from the horizontal diameter consistently underestimated area, whereas calculating pupil area from the vertical diameter consistently overestimated area. Thus, we report values for pupil area from direct area measurements. The two sea otters differed in their dynamic ranges. In the male sea otter, pupil area increased 55-fold from day (0.47 ± 0.009 mm^2, Fig. 6a) to night (25.7 ± 0.12 mm^2, Fig. 6b). In the female sea otter, pupil area increased 86-fold from day (0.28 ± 0.008 mm^2, Fig. 6c) to night (24.2 ± 0.23 mm^2, Fig. 6d). For the night condition, ambient light consistently fell below the sensitivity of the luxometer and registered at 0 foot candles; for the day condition, ambient light registered 600-9200 foot candles during testing with Selka and 415-430 foot candles during testing with Odin.

The sea otter's mean pupil area was not significantly smaller after an abrupt increase in IR intensity in the first IR test (Table 1, Fig. 7a,b), and mean pupil area was stable upon transition from darkness to IR exposure in the second IR test (Fig. 7c). The sea otter's mean pupil area also remained constant across 30 s when continuously exposed to the IR (940 nm) negative control (Table 1, Fig. 8a,b). However, the sea otter's mean pupil area decreased significantly after exposure to 630 nm (orange) and 640 nm (red) light treatments and the broadband (white) positive control (Table 1, Fig. 8a). Constriction began immediately upon light exposure and lasted 2-6 seconds before stabilizing (Fig. 8b), and the magnitude of constriction decreased as wavelength increased (Table 1, Fig. 8a,b).

DISCUSSION

The combined results from our behavioral and histological investigations suggest that sea otter have retained features for low-light vision within the constraints of their proportional eye size. However, the lack of quantitative data for photoreceptor densities prevents definitive conclusions on whether these features are enhanced to maintain sensitivity across variable light levels to the same extent that their accommodative mechanism is enhanced to maintain amphibious acuity. The measurements of tapetal thickness and pupillary dynamic range and the descriptions of photoreceptor density in this study help interpret observations from wild sea otter populations and suggest that selective pressures for enhancing acuity are stronger than those for enhancing absolute sensitivity, both under water and in air, similar to conclusions by Estes (1989). Since the prey of sea otters are either slow-moving or sessile, contrast discrimination contributes more to vision-based foraging than motion sensitivity. Although contrast discrimination is limited to photopic conditions in shallow daytime foraging, the tactile abilities of sea otter front paws and facial whiskers are sensitive enough to compensate for limited visual sensitivity during deeper dives, turbid conditions, and nighttime foraging (Strobel et al. 2018). In air, enhanced low-light sensitivity confers fewer advantages to sea otter grooming, resting, and social behaviors than enhanced acuity confers for predator-avoidance behaviors. Predators hunting diurnally from air or land, including bald eagles, coyotes, and brown bears, as well as humans prior to the legal protections enacted in the last century (Riedman and Estes 1990; Monson and DeGange 1995; Liapunova

and Miklukho 1996) can exert significant pressure on behavioral patterns in this species (see *e.g.*, Esslinger et al. 2014).

Dynamic range decreased relative to amphibious carnivores

Results from pupillometry confirm that the sea otter pupil is mobile in size but not shape. The size difference between the constricted and dilated pupil (1.2-1.9% of maximum area) at first seems consistent to those reported for assessments in northern elephant seals (*Mirounga angustirostris*, 0.2% of maximum area), harbor seals (*Phoca vitulina*, 1.4% of maximum area) and California sea lions (*Zalophus californianus*, 3.8% of maximum area) unless one considers the brightness ranges under which pupil size was assessed. If the sea otters in this study were tested across the narrower range of brightness levels as the seals and sea lion (Levenson and Schusterman 1997), we strongly suspect that the size difference between the constricted and dilated pupil would be much larger (*i.e.*, smaller pupil dynamic range) than that reported here. Unlike sea otters, pinnipeds have a stenopaic pupil, larger absolute eye size, and a need to overcome the myopic effect of a flattened cornea in air, which all contribute to their large pupil size range. Differing measurements for the two sea otters likely resulted from differences in ambient brightness levels, not age. The female sea otter experienced brighter light levels during day testing than the male sea otter, and her pupil size was more consistent with his for the lower range of ambient light during her testing (600-700 foot candles). His pupil appeared well constricted during day testing, but during night testing his pupil appeared less dilated

relative to the iris than in the female. The male sea otter may have experienced brighter light levels during night testing, which were not apparent during ambient light measurements, since luxometers calculate brightness based only on the visual spectrum. Although the male sea otter was almost nine years older than the female, he did not show evidence of decreased visual acuity during daily training sessions or lens occlusion in the right eye during veterinary exams (S.M. Strobel, *pers. obs.*).

Balancing the demands of amphibious vision resembles a zero-sum game for sea otters, since the same adaptation that facilitates acuity across media can limit sensitivity across variable light levels. Although we conducted these behavioral assessments in air, we suspect that pupil mobility would be comparable or slightly less under water. While submerged, sea otters rely on lens protrusion through the pupil for accommodation. Pupil size is thus limited at either extreme, since the lens cannot sufficiently protrude through a too wide or too narrow pupil aperture. This trade-off is heightened in low-light conditions, since underwater acuity requires a small pupil to adequately deform the lens, but low-light vision requires a wide pupil to gather light. A similar trade-off has been suggested for some diving birds, who show a tight coupling between pupil constriction and accommodation (Levy and Sivak 1980; Sivak et al. 1985) and limited pupil size range (Sivak et al. 1985), even with changing light levels (Katzir and Howland 2003).

Tapetum lucidum comparable to terrestrial carnivores

Our measurements of tapetal thickness and distribution in sea otters are consistent with a visual system biased towards acuity over sensitivity. Tapetal

thickness (7-8 layers, 46 μm) is greater than another amphibious, freshwater mustelid (Braekevelt 1989) but comparable to terrestrial mustelids (Braekevelt 1981; Tjälve and Frank 1984; Wen et al. 1985) and terrestrial carnivores (Lesiuk and Braekevelt 1983; Wen et al. 1985; Yamaue et al. 2015). In contrast, amphibious pinnipeds have the thickest tapetums known among vertebrates (20-50 layers, 110-500 μm) (Walls 1942; Nagy and Ronald 1970; Jamieson and Fisher 1971; Braekevelt 1986; Kastelein et al. 1993; Welsch et al. 2001; Smodlaka et al. 2016), which may provide more reflectance, and thus improve photon capture, in scotopic environments, relative to sea otters. Furthermore, the restriction of the tapetum lucidum to the dorsal fundus and just slightly below the optic disc in sea otters is similar to the pattern found in terrestrial and amphibious fres mustelids (Braekevelt 1981; Tjälve and Frank 1984) and walruses (Kastelein et al. 1993), but less than the almost-full fundus coverage found in many pinniped species (Johnson 1901; Jamieson and Fisher 1971; Braekevelt 1986; Mass 2004, 2009; Miller et al. 2010; Smodlaka et al. 2016). Given that sea otters are benthic foragers and spend prolonged periods at the surface instead of in the water column, they may process light cues based on a horizontal horizon instead of the three-dimensional aquatic light environment experienced by other amphibious marine mammals (Ollivier et al. 2004). A dorsal coverage of the fundus is likely sufficient to increase luminance to the ventral visual field during underwater foraging and in-air behaviors.

Tapetal fundic coverage in sea otters is consistent with the spatial distribution of the visual streak, previously described in the sea otter retina to lie just dorsal to the

optic nerve in the mid-temporal retina (Mass and Supin 2000). The visual streak is a band of high ganglion cell density affording acute visual sampling of the visual field that it subtends (Moore et al. 2017), so its spatial coupling with the tapetum likely aids acuity in low-light along the horizontal plane. The range of colors represented in the sea otter tapetum resemble those in fundi described for the Eurasian otter (*Lutra lutra*) and the pine marten (*Martes martes*) (Johnson 1901, 1968) with a few key differences. The turquoise color present in the sea otter's central zone is not reported for the Eurasian otter or pine marten, but is consistently described for pinniped species (Mass 2004; Smodlaka et al. 2016), and extends more superior to the optic disk before transitioning to warmer colors. Additionally, the bright green ring surrounding the optic disc (*i.e.*, the peripapillary conus) in sea otters is similar to the harbor seal (Johnson 1901). Although tapetal color has been shown to change seasonally in Arctic reindeer (*Rangifer ratandus*), presumably to adjust retinal sensitivity to match consistent high-light conditions in summer and low-light conditions in winter (Stokkan et al. 2013), the relationship between tapetal color and function is not well understood. A comparative investigation of tapetal color in amphibious and marine mammal species that exhibit a wide range of diving depths would help to determine if blue-shifted tapetal colors are adaptive for an aquatic lifestyle.

Qualitatively rod-dominant retinas

Our histological results suggest that the sea otter eye has a high photoreceptor density, is heavily rod-dominant, and is qualitatively similar to the ferret and

domestic cat. The pattern of DAPI-stained photoreceptors and PNA-stained cones suggests that high overall rod density decreases slightly toward the central retina as cone density increases, consistent with an area centralis, as reported in many mammalian species. However, since stains that have successfully been applied in other mammals were only partially successful for sea otters, only qualitative consideration of photoreceptor densities is possible. We cannot conclude whether sea otter photoreceptor density and distribution compensate for a smaller pupil range, a thinner tapetum, and eyes proportional to body size. The ONL/INL ratio in sea otters is intermediate between the corresponding measurements for diurnal and crepuscular eyes in fishes (Munz and Mcfafuand 1973; Yu Wang et al. 2011). Further studies are needed to determine how retinal organization, in addition to the accommodative mechanism, influences amphibious vision in sea otters relative to other carnivores.

Spectral sensitivity consistent with predictions

By monitoring pupil constriction in response to the addition of light with progressively longer wavelength, we confirm that sea otters are insensitive to near-infrared light (940 nm) but display sensitivity to the upper wavelengths tested—640 nm (red) and 630 nm (orange). These results validate our use of near-infrared light as perceived darkness to assess pupil size and are consistent with the presence of the M/L cone, demonstrating that sea otters show sensitivity to wavelengths ~95 nm longer than its peak sensitivity inferred from retinal mRNA cone opsin sequences (545 nm) (Levenson et al. 2006). As sea otter M/L cone inferred sensitivity is only 7-

15 nm lower than that in mustelids and pinnipeds, we expect that these species would also show sensitivity to the wavelengths of light presented here.

Study Limitations

This study combines results from anatomical and behavioral methods to contribute to our understanding of sea otter vision. However, our conclusions are limited by difficulties in adapting histological methods to a species in which they have not previously been validated and by variability inherent in behavioral assessments of live animals. We plan to build upon our staining protocols to improve rod-cone differentiation across the sea otter retina that will lead to a quantitative metric of rod-to-cone proportions. The pupillometry results highlight the importance of testing multiple subjects due to inter-individual variation. Our decision to assess pupil dynamics across the extremes of ambient light conditions typically experienced by sea otters introduced environmental variability that makes our results difficult to compare beyond broad generalizations to other species tested in experimentally controlled and/or unreported light conditions.

Future Directions

Anatomical and behavioral studies of sea otters are needed to assess how vision may function during search behavior in low-light conditions under water and adjust to rapid and extreme changes in light levels during repeated dives. *In situ* rapid-flicker electroretinography (ERG) could be performed in anesthetized

individuals to assess visual sensitivity as a function of wavelength. This method provides a functional and comprehensive metric of the peripheral visual system that includes contributions from the cornea, lens, photoreceptors, and tapetum lucidum. To test the suspected coupling of pupil size and accommodation in sea otters, we encourage development of a model that predicts the maximum pupil size that sufficiently decreases the radius of curvature of the lens to retain acuity under water. This model can be tested by monitoring pupil size during behavioral acuity tests in air and under water across controlled, artificial light conditions. Given our findings and those from related species (Balliet and Schusterman 1971), we suspect that acuity decreases more rapidly under water than in air with decreasing light levels and that pupil dynamic range may be smaller under water than in air, since lens protrusion during submersion likely prevents full pupil constriction in photopic conditions.

Since comparisons among sea otters and other amphibious mammals are confounded by absolute eye size, which sets an upper size limit on iris musculature and pupil area, future studies should apply the behavioral and anatomical methods used here to other amphibious and terrestrial mustelids with similar eye sizes to sea otters. A comparative framework would disentangle the contributing effects of pupil shape, accommodative mechanism, and photoreceptor density on minimum and maximum pupil area, since all mustelids share a circular pupil, but presumably only amphibious mustelids exhibit a similar underwater accommodative mechanism as sea otters. Such data would contribute to our understanding of the selective pressures

shaping vision in amphibious species that have differing foraging ecologies but similar evolutionary histories (Estes 1989).

Conclusions

Sea otters have apparently favored enhancing acuity over absolute sensitivity, although they retain typical carnivore features that enable vision in low-light. In-air dynamic size range of the pupil is reduced relative to pinnipeds, and the thickness, fundic coverage, and structure of the tapetum lucidum is most similar to terrestrial carnivores. A consistently circular pupil shape that limits minimum pupil constriction and a proportional eye size that limits maximum pupil dilation may further contribute to reduced pupil mobility in sea otters relative to pinnipeds. We cannot conclude if the qualitatively heavily rod-dominant retinas of sea otters compensate for the limits posed by their unique accommodative ability for underwater vision in variable light conditions.

Although our findings place vision in sea otters as intermediate between terrestrial carnivores and semiaquatic pinnipeds, we suggest that this distinction is not merely a result of their recent evolutionary transition to an aquatic lifestyle, as previous studies have suggested. Instead, sea otters' different use of the aquatic environment relative to other amphibious mammals likely selects for visual acuity in photopic conditions over absolute sensitivity. When visual acuity fails in scotopic conditions at deeper depths and at night, the accurate and rapid tactile sense in sea otters is likely sufficient for benthic foraging.

ACKNOWLEDGMENTS

I acknowledge my co-authors on the soon-to-be-submitted manuscript based on this chapter: Bret Moore, Katie Freeman, Michael Murray, and Colleen Reichmuth. We thank the volunteers and staff at the Cognition and Sensory Systems Lab, especially Caroline Casey, Kane Cunningham, Asila Ghoul, Tianna Grant, Jenna Lofstrom, Jeff Mihok, Ross Nichols, Andrew Rouse, Jillian Sills, and Connor Whalen for their assistance with research. David Levenson provided experimental support, equipment, and advice. We thank Andy Johnson, Erin Lenihan, Karl Mayer, and Marissa Young at Monterey Bay Aquarium for sample collection, logistical support, and access to sea otters. Lilian Carswell at US Fish and Wildlife Service provided assistance in the permitting procedure. Ari Friedlaender and Patrick Robinson provided photographic assistance during pilot testing for this study, and Dr. E.J. Ehrhardt provided gross anatomical assessments of two sea otter eyes that contributed to planning for this study. We also thank the many people who guided the authors in eye dissection and histology in preliminary planning stages of this research, including Corinne Beier and Sasha Sher at University of California Santa Cruz, Martin Glössman at University of Vienna, Austria, and Melissa Miller, Laird Henkel, Francesca Batac, Erin Dodd, Colleen Young and Angie Reed at California Department of Fish and Wildlife's Marine Wildlife Veterinary Care and Research Center. Tim Tinker, Pete Raimondi, Bruce Lyon, and James Estes at the EEB Department at the University of California Santa Cruz contributed to the interpretation of this research. Noe Castaneda, Kat Dale, Sarah Kienle, Chris Law, Rita Mehta, and Kelley Voss provided helpful

suggestions on earlier versions of this manuscript. This work was supported by the National Science Foundation Graduate Research Fellowship Program under grant no. NSF DGE 1339067 and the Department of Education Graduate Assistance in Areas of National Need Fellowship P200A150100. Research costs were supported in part by the Monterey Bay Aquarium's Conservation Program, the Friends of Long Marine Lab, and the Pinniped Cognition and Sensory Systems Lab.

REFERENCES

Ballard K., Sivak JG, Howland HC (1989) Intraocular muscles of the Canadian river otter and Canadian beaver and their optical function. Can J Zool 67:469–474 . doi: 10.1139/z89-068

Balliet RF, Schusterman RJ (1971) Underwater and aerial visual acuity in the Asian "clawless" otter (Amblonyx cineria cineria). Nature 234:305–306

Banks MS, Munsinger H (1974) Pupillometric measurement of difference spectra for three color receptors in an adult and a four-year-old. Vision Res 14:813–817

Bodkin JL, Esslinger GG, Monson DH (2004) Foraging depths of sea otters and implications to coastal marine communities. Mar Mammal Sci 20:305–321

Bodkin JL, Monson DH, Esslinger GG (2007) Activity budgets derived from time–depth recorders in a diving Mammal. J Wildl Manage 71:2034–2044 . doi: 10.2193/2006-258

Braekevelt CR (1986) Fine structure of the tapetum cellulosum of the grey seal (Halichoerus grypus). Arcta anat 127:81–87

Braekevelt CR (1989) Fine structure of the retinal epithelium and tapetum lucidum of the ranch mink Mustela vison. Acta Anat 135:296–302

Braekevelt CR (1981) Fine structure of the tapetum lucidum of the domestic ferret. Anat Embryol (Berl) 163:201–214

Calderone JB, Jacobs GH (2003) Spectral properties and retinal distribution of ferret cones. Vis Neurosci 20:11–7

Costa DP, Kooyman GL (1982) Oxygen consumption, thermoregulation, and the effect of fur oiling and washing on the sea otter, Enhydra lutris. Can J Zool 60:2761–2767 . doi: 10.1139/z82-354

De Groot SG, Gebhard JW (1952) Pupil size as determined by adapting luminance. J Opt Soc Am 42:492–495 . doi: 10.1364/JOSA.42.000492

Dunstone N, Sinclair W (1978) Comparative aerial and underwater visual acuity of the mink, Mustela vison Schreber, as a function of discrimination distance and stimulus luminance. Anim Behav 26:6–13 . doi: 10.1016/0003-3472(78)90002-7

Esslinger GG, Bodkin JL, Breton AR, et al (2014) Temporal patterns in the foraging behavior of sea otters in Alaska. J Wildl Manage 78:689–700 . doi: 10.1002/jwmg.701

Estes JA (1989) Adaptations for Aquatic Living by Carnivores. In: Gittleman JL (ed) Carnivore behavior, ecology, and evolution. Cornell University Press, Ithaca, pp 242–282

Estes JA, Jameson RJ, Rhode EB (1982) Activity and prey selection in the sea otter: influence of population status on community structure. Am Nat 120:242–258

Garshelis DL, Garshelis JA, Kimker AT (1986) Sea otter time budgets and prey relationships in Alaska. J Wildl Manage 50:637–647

Gelatt TS, Siniff DB, Estes JA (2002) Activity patterns and time budgets of the declining sea otter population at Amchitka Island, Alaska. J Wildl Manage 66:29–39

Gentry R, Peterson R (1967) Underwater vision of the sea otter. Nature 216:435–436

Gislen A, Dacke M, Kröger RHH, et al (2003) Superior underwater vision in a human population of sea gypsies. Curr Biol 13:833–836 . doi: 10.1016/S

Goodge WR (1960) Adaptations for amphibious vision in the dipper (Cinclus mexicanus). J Morphol 107:79–91

Hanke F, Dehnhardt G (2009) Aerial visual acuity in harbor seals (Phoca vitulina) as a function of luminance. J Comp Physiol A 195:643–650 . doi: 10.1007/s00359-009-0439-2

Hanke FD, Peichl L, Dehnhardt G (2009) Retinal ganglion cell topography in juvenile harbor seals (Phoca vitulina). Brain Behav Evol 74:102–109 . doi: 10.1159/000235612

Hines AH, Loughlin TR (1980) Observations of sea otters digging for clams at Monterey Harbor, California. Fish Bull 78:159–163

Howland HC, Merola S, Basarab JR (2004) The allometry and scaling of the size of vertebrate eyes. Vision Res 44:2043–65 . doi: 10.1016/j.visres.2004.03.023

Hughes A (1977) The topography of vision in mammals of contrasting lifestyle: comparative optics and retinal organisation. In: Crescitelli F (ed) Handbook of Sensory Physiology, VII-5. Springer-Verlag, Berlin, pp 613–756

Hughes BB, Eby R, Van Dyke E, et al (2013) Recovery of a top predator mediates negative eutrophic effects on seagrass. Proc Natl Acad Sci U S A 110:15313–8 . doi: 10.1073/pnas.1302805110

Jacobs GH (1993) The distribution and nature of colour vision among the mammals. Biol Rev 68:413–471

Jamieson GS, Fisher HD (1971) The retina of the harbour seal, Phoca vitulina. Can J Zool 49:19–23 . doi: 10.1139/z71-005

Johnson GL (1901) Contributions to the comparative anatomy of the mammalian eye, chiefly based on ophthalmoscopic examination. Philos Trans R Soc Biol Charact 1941–82 194:1–82

Johnson GL (1968) Opthalmoscopic studies on the eyes of mammals. Philos Trans R Soc B Biol Sci 254:207–220

Jolly J (1997) Foraging ecology of the sea otter, Enhydra lutris, in a soft-sediment community. University of California Santa Cruz

Kastelein RA, Zweypfenning CVJ, Spekreijse H, et al (1993) The anatomy of the Walrus head (Odobenus rosmarus). Part 3: The eyes and their function in Walrus ecology. Aquat Mamm 19.2:61–92

Katzir G, Howland HC (2003) Corneal power and underwater accommodation in great cormorants (Phalacrocorax carbo sinensis). J Exp Biol 206:833–841 . doi: 10.1242/jeb.00142

Lesiuk TP, Braekevelt CR (1983) Fine structure of the canine tapetum lucidum. J Anat 136:157–164

Levenson DH, Ponganis PJ, Crognale M a, et al (2006) Visual pigments of marine carnivores: pinnipeds, polar bear, and sea otter. J Comp Physiol A 192:833–43 . doi: 10.1007/s00359-006-0121-x

Levenson DH, Schusterman RJ (1999) Dark adaptation and visual sensitivity in shallow and deep-diving pinnipeds. Mar Mammal Sci 15:1303–1313

Levenson DH, Schusterman RJ (1997) Pupillometry in seals and sea lions: ecological implications. Can J Zool 75:2050–2057 . doi: 10.1139/z97-838

Levy B, Sivak JG (1980) Mechanisms of accommodation in the bird eye. J Comp Physiol A 137:267–272

Liapunova RG, Miklukho NN (1996) Essays on the ethnography of Aleuts: at the end of the eighteenth and the first half of the nineteenth century. The University of Alaska Press, Fairbanks, Alaska

Mass AM (2004) A High-Resolution Area in the Retinal Ganglion Cell Layer of the Steller's Sea Lion (Eumetopias jubatus): A Topographic Study. Dokl Biol Sci 396:187–190

Mass AM (2009) Localization of the highest retinal resolution area in the retinal ganglion cell layer of the caspian seal Phoca caspica: A topographic study. Dokl Biol Sci 429:575–578 . doi: 10.1134/S001249660906026X

Mass AM (1992) Retinal topography in the walrus (Odobenus rosmarus divergence) and fur seal (Callorhinus ursinus). In: Thomas JA, Kastelein RA, Supin AY (eds) Marine Mammal Sensory Systems. Plenum Press, New York, NY, pp 119–135

Mass AM, Supin AY (2010) Retinal ganglion cell layer of the caspian seal Pusa caspica: topography and localization of the high-resolution area. Brain Behav Evol 76:144–153 . doi: 10.1159/000320951

Mass AM, Supin AY (1992) Peak density, size and regional distribution of ganglion cells in the retina of the fur seal Callorhinus ursinus. Brain Behav Evol Evol 39:69–76

Mass AM, Supin AY (2000) Ganglion cells density and retinal resolution in the sea otter, Enhydra lutris. Brain Behav Evol 55:111–119 . doi: 10.1159/000006646

Mass AM, Supin AY (2005) Ganglion cell topography and retinal resolution of the Steller sea lion (Eumetopias jubatus). Aquat Mamm 31:393–402 . doi: 10.1578/AM.31.4.2005.393

Miller SN, Colitz CMH, Dubielzig RR (2010) Anatomy of the California sea lion globe. Vet Ophthalmol 13:63–71

Monson DH, DeGange AR (1995) Reproduction, preweaning, and survival of adult sea otters at Kodiak Island, Alaska. Can J Zool 73:1161–1169

Moore BA, Tyrell LP, Kamilar JM, et al (2017) Structure and function of regional specializations in the vertebrate retina. In: Kaas JH (ed) Evolution of Nervous Systems, 2nd edn. Elsevier, Oxford, U.K., pp 351–372

Mowat FM, Breuwer AR, Bartoe JT, et al (2013) RPE65 gene therapy slows cone loss in Rpe65-deficient dogs. Gene Ther 20:545–555 . doi: 10.1038/gt.2012.63

Munsinger H, Banks MS (1974) Pupillometry as a measure of visual sensitivity among infants, young children, and adults. Dev Psychol 10:677–682 . doi: 10.1037/h0036942

Munz FW, Mcfafuand WN (1973) The significance of spectral position in the rhodopsins of tropical marine fishes. Vision Res 13:1829–1874

Murphy CJ, Bellhorn RW, Williams T, et al (1990) Refractive state, ocular anatomy, and accommodative range of the sea otter (Enhydra lutris). Vision Res 30:23–32

Nagy AR, Ronald K (1970) The harp seal, Pagophilus groenlandicus (Emleben, 1777). VI. Structure of retina. Can J Zool 48:367–370

Neumann F, Schmidt H (1959) Optische Differenzierungsleistungen von Musteliden: Versuche an Frettchen und Iltisfrettchen. Z Vgl Physiol 42:199–205

Ollivier FJ, Samuelson D a., Brooks DE, et al (2004) Comparative morphology of the tapetum lucidum (among selected species). Vet Ophthalmol 7:11–22 . doi: 10.1111/j.1463-5224.2004.00318.x

Peichl L, Behrmann G, Kröger RH (2001) For whales and seals the ocean is not blue: a visual pigment loss in marine mammals. Eur J Neurosci 13:1520–8

Ralls K, Hatfield BB, Siniff DB (1995) Foraging patterns of California sea otters as indicated by telemetry. Can J Zool 73:523–531

Rasband WS (1997) ImageJ. U. S. National Institutes of Health, Bethesda, Maryland, USA, https://imagej.nih.gov/ij/, 1997-2018.

Riedman ML, Estes JA (1990) The sea otter (Enhydra lutris): behavior, ecology, and natural history. Biol Rep 90:1–136

Schaeffel F, de Queiroz A (1990) Alternative Mechanisms of Enhanced Underwater Vision in the Garter Snakes Thamnophis melanogaster and T. couchii. Am Soc Ichthyol Herpetol 1:50–58

Schusterman RJ, Balliet RF (1970a) Visual acuity of the harbour seal and the stellar sea lion under water. Nature 226:563–564

Schusterman RJ, Balliet RF (1970b) Conditioned vocalizations as a technique for determining visual acuity thresholds in sea lions. Science (80-) 169:498–501

Schusterman RJ, Barrett B (1973) Amphibious nature of visual acuity in the Asian “clawless” otter. Nature 244:518–519

Shimek S (1977) The underwater foraging habits of the sea otter, Enhydra lutris. Calif Fish Game 63:120–122

Sinclair W, Dunstone N, Poole TB (1974) Aerial and underwater visual acuity in the mink Mustela vison shreber. Anim Behav 22:965–974

Sivak JG (1976) Optics of the eye of the “four-eyed fish” (Anableps anableps). Vision Res 16:521–534

Sivak JG, Hildebrand T, Lebert C (1985) Magnitude and rate of accomodation in diving and nondiving birds. Vision Res 25:925–933

Sivak JG, Lincer JL, Bobier W (1977) Amphibious visual optics of the eyes of the double-crested cormorant (Phalacrocorax auritus) and the brown pelican (Pelecanus occidentalis). Can J Zool 55:782–788 . doi: 10.1139/z77-102

Smodlaka H, Khamas WA, Palmer L, et al (2016) Eye histology and ganglion cell topography of northern elephant seals (Mirounga angustirostris). Anat Rec 299:798–805 . doi: 10.1002/ar.23342

Stokkan K-A, Folkow L, Dukes J, et al (2013) Shifting mirrors: adaptive changes in retinal reflections to winter darkness in Arctic reindeer. Proc Biol Sci 280:20132451 . doi: 10.1098/rspb.2013.2451

Strobel SM, Sills JM, Tinker MT, Reichmuth CJ (2018) Active touch in sea otters: in-air and underwater texture discrimination thresholds and behavioral strategies for paws and vibrissae. J Exp Biol 221:1–14

Supin AM, Mass AY (2003) Retinal topography of the harp seal Pagophilus groenlandicus. Brain Behav Evol 62:212–222 . doi: 10.1159/000073273

Thometz NM, Staedler MM, Tomoleoni JA, et al (2016) Trade-offs between energy maximization and parental care in a central place forager, the sea otter. Behav Ecol 27:1552–1566 . doi: 10.1093/beheco/arw089

Tinker MT, Bentall G, Estes JA (2008) Food limitation leads to behavioral diversification and dietary specialization in sea otters. PNAS 105:560–565

Tjälve H, Frank A (1984) Tapetum lucidum in the pigmented and albino ferret. Exp Eye Res 38:341–351

Valqui J (2012) The marine otter Lontra felina (Molina, 1782): A review of its present status and implications for future conservation. Mamm Biol 77:75–83 . doi: 10.1016/j.mambio.2011.08.004

Walls GL (1942) The vertebrate eye and its adaptive radiation. Hafner, New York

Weiffen M, Mo B (2006) Effect of water turbidity on the visual acuity of harbor seals (Phoca vitulina). Vision Res 46:1777–1783 . doi: 10.1016/j.visres.2005.08.015

Welsch U, Ramdohr S, Riedelsheimer B, et al (2001) Microscopic anatomy of the eye of the deep-diving Antarctic weddell seal (Leptonychotes weddellii). J Morphol 248:165–174

Wen G, Sturman J, Shek J (1985) A comparative study of the tapetum, retina and skull of the ferret, dog and cat. Lab Anim Sci 35:200–210

Werner YL (1970) Extreme adaptatability to light, in the round pupil of the snake, Spalerosophis. Vision Res 10:1159–1164

Wight R, Milliken GW, Ward JP (1988) Assessment of visual acuity, the oblique effect, and the lateral mirror-image confusion effect in the ferret (Mustela putorius furo). Int J Comp Psychol 1:254–267

Wilcox JG, Barlow HB (1975) The size and shape of the pupil in lightly anaesthetized cats as a function of luminance. Vision Res 15:1363–5

Wilkin SM (2003) Nocturnal foraging ecology and activity budget of the sea otter (Enhydra lutris) in Elkhorn Slough, California. San Francisco State University

Yamaue Y, Hosaka YZ, Uehara M (2015) Spatial relationships among the cellular tapetum, visual streak and rod density in dogs. J Vet Med Sci 77:175–179 . doi: 10.1292/jvms.14-0447

Yu Wang F, Yun Tang M, Young Yan H (2011) A comparative study on the visual adaptations of four species of moray eel. Vision Res 51:1099–1108 . doi: 10.1016/j.visres.2011.02.025

TABLES

TABLE 1. Sea otter pupil area (pooled means and standard errors for pre-treatment and post-treatment) for three replicates of five treatments (white, 630 nm, 640 nm, 940 nm) and one control (low-to high IR). For each condition, percent of pre-treatment mean pupil area relative to post-treatment mean pupil area are reported. Statistical outputs (t-statistic, df, and p-value) are calculated from a paired, one-tailed t-test that assesses the mean difference between pre-treatment and post-treatment means. If $p<0.05$, then the post-treatment mean pupil area is significantly smaller than the pre-treatment mean pupil area, which can be interpreted physiologically as a pupillary constriction response

Condition	Pre-treatment mean ± sem (mm^2)	Post-treatment mean ± sem (mm^2)	% pre of post	*t*-statistic	*df*	*p*
	24.2 ± 0.26	6.83 ± 0.22				
White	27.3 ± 0.24	6.99 ± 0.72	27.6	20.1	2	0.0012
	24.9 ± 0.24	7.23 ± 0.71				
	25.8 ± 0.20	15.5 ± 0.19				
630 nm (orange)	25.8 ± 0.24	15.5 ± 0.20	59.1	79.3	2	<0.0001
	24.8 ± 0.26	14.2 ± 0.25				
	24.6 ± 0.08	20.9 ± 0.25				
640 nm (red)	24.9 ± 0.24	22.5 ± 0.37	88.1	8.0	2	0.0076
	24.5 ± 0.37	21.8 ± 0.15				
	29.8 ± 0.18	29.9 ± 0.21				
940 nm (continuous IR)	26.0 ± 0.14	27.1 ± 0.15	101.5	-1.0	2	0.79
	22.8 ± 0.14	22.7 ± 0.13				
	26.9 ± 0.34	24.1 ± 0.20				
940 nm (low-to-high IR)	25.7 ± 0.41	26.6 ± 0.16	93.9	1.3	2	0.17
	25.1 ± 0.24	22.26 ± 0.05				

FIGURES

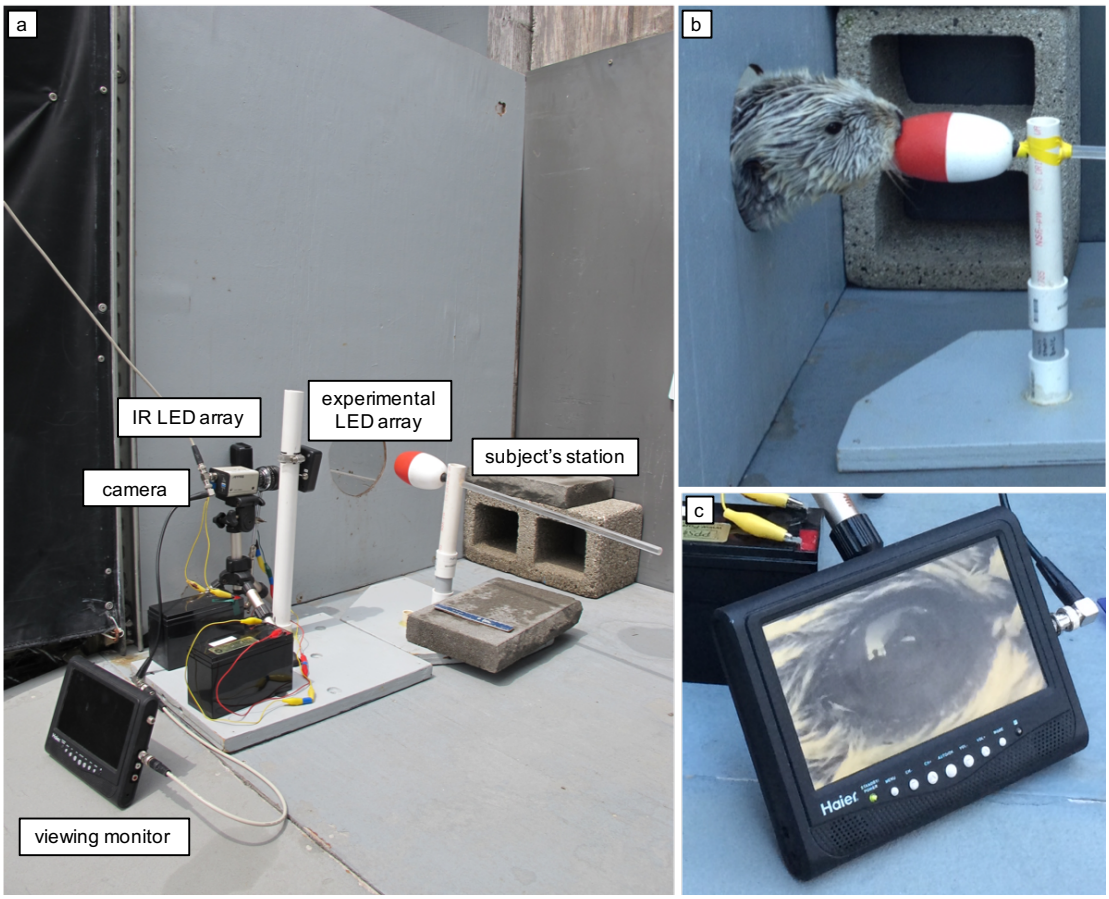

FIGURE 1. Experimental set-up for measurements of sea otter pupil size. (a) The experimental LED array, IR LED array, subject's stationing position, camera, and viewing monitor for the camera operator are depicted during ambient day conditions. (b) Odin the sea otter inserted his head through a protective barrier to contact and maintain firm contact on a station, which ensured consistent positioning during the experimental session and across replicate sessions; for nighttime sessions, a light-blocking box was placed around the sea otter's head to further control for ambient and artificial light. (c) The viewing monitor enabled the camera operator to assess and adjust the camera's focus in real-time prior to data collection and monitor the subject's behavior throughout the session. During ambient night conditions, a visual screen blocked light contamination from the viewing monitor

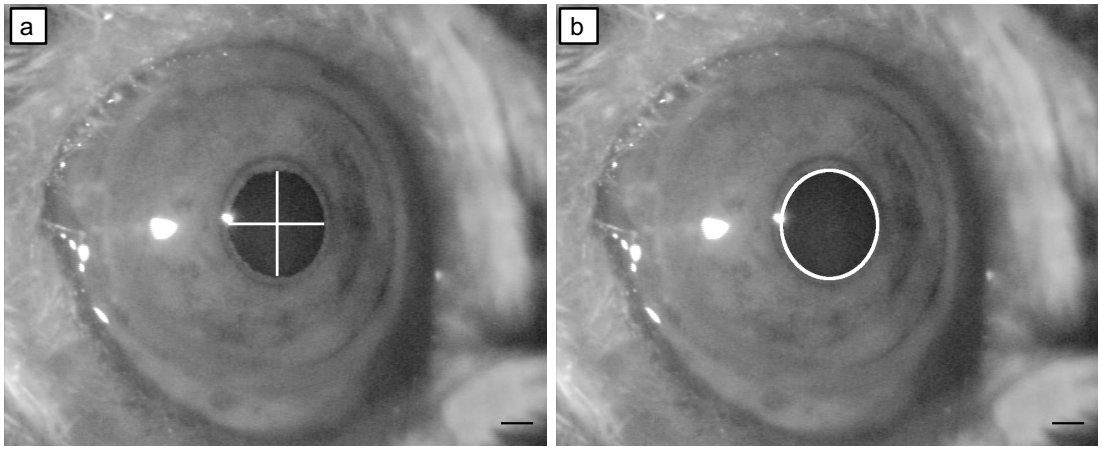

FIGURE 2. Pupil size measurements in the sea otter right eye using the straight line and oval area selection tools in ImageJ: (a) pupil horizontal and vertical diameter, (b) pupil area bounded by the white line

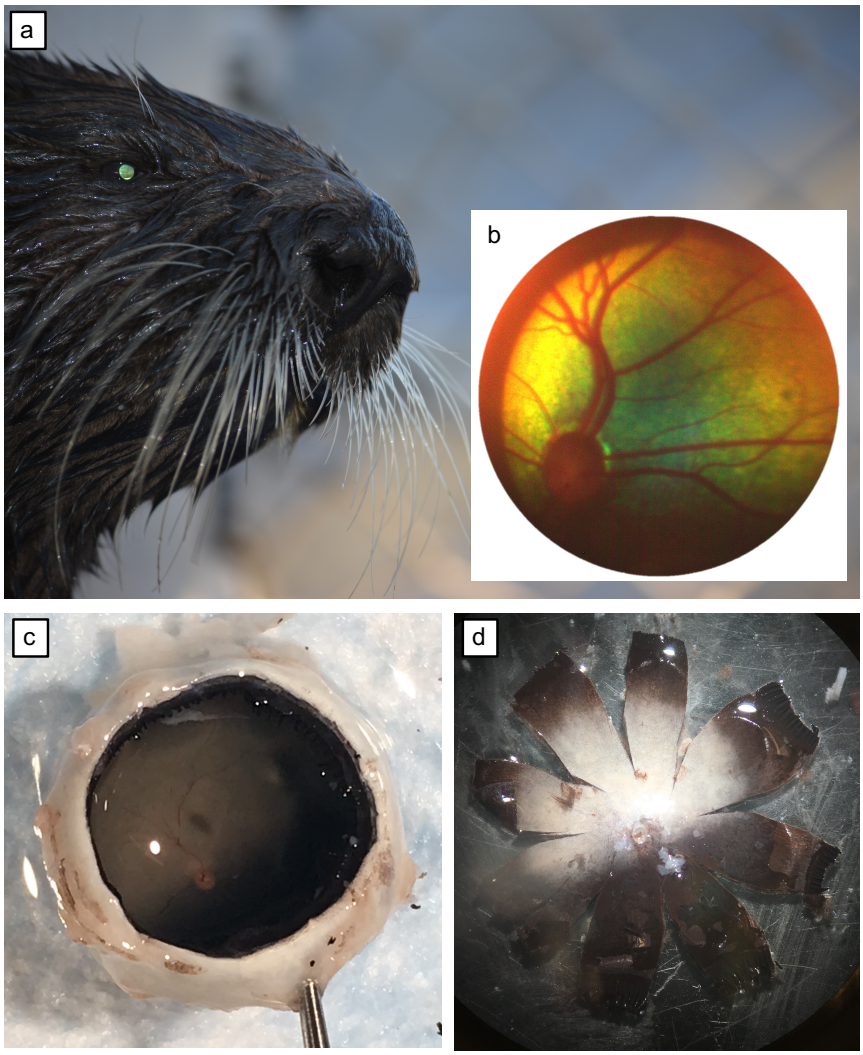

FIGURE 3. The tapetum lucidum shown *in situ* for the female sea otter (a,b) and *ex situ* for a formalin-fixed right eye excised from a deceased sea otter (c,d). (a) At dusk, the tapetum lucidum in the dilated sea otter right eye reflects the camera flash as a green-yellow circle within the pupil. (b) The tapetum lucidum, photographed with a fundic camera in the right dilated eye of the female sea otter under anesthesia, reflects off-white in the optic disc, surrounded by a bright green disc (the peripapillary conus), then a gradient of turquoise, green, yellow, orange, and reddish-brown toward the periphery. The tapetum lucidum extends slightly ventral to the optic disc, into the lower fundus. (c) The eyecup with the cornea, iris, and lens removed. The vitreous humor, retina, retinal pigment epithelium, and choroid are still present. The tapetum lucidum is milky white as a byproduct of fixation; as pictured in situ, it extends slightly into the lower fundus. (d) The retinal pigment epithelium removed from the eyecup but still attached to the choroid. The tapetum lucidum is visible through the transparent portion of the retinal pigment epithelium

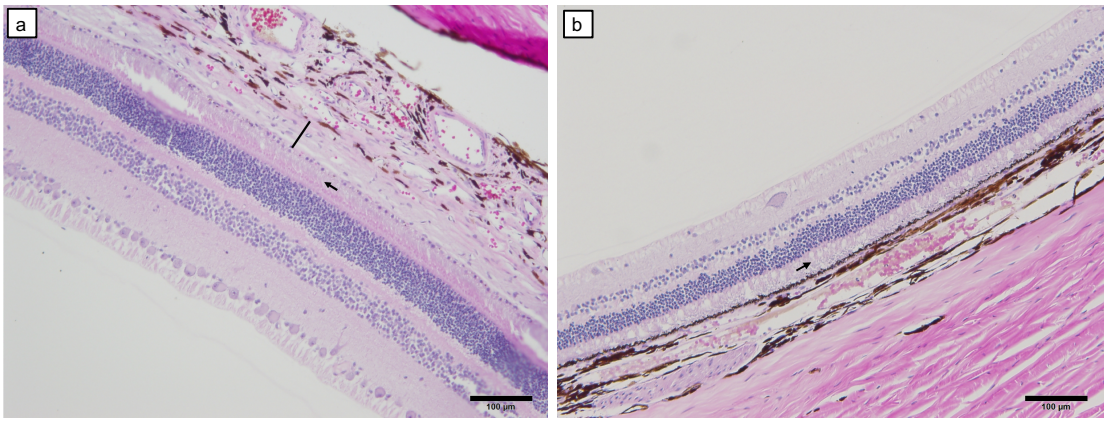

FIGURE 4. H&E-stained retina, tapetum lucidum, choroid, and sclera from the central (a) and peripheral (b) posterior segments of the sea otter eye. The photoreceptor layer (arrow) is noticeably denser in the central retina (a) than in the peripheral retina (b). The tapetum lucidum (line), located posterior to the photoreceptor layer, is thickest in the central posterior segment of the eye (a) and heavily reduced in the peripheral posterior segment of the eye (b)

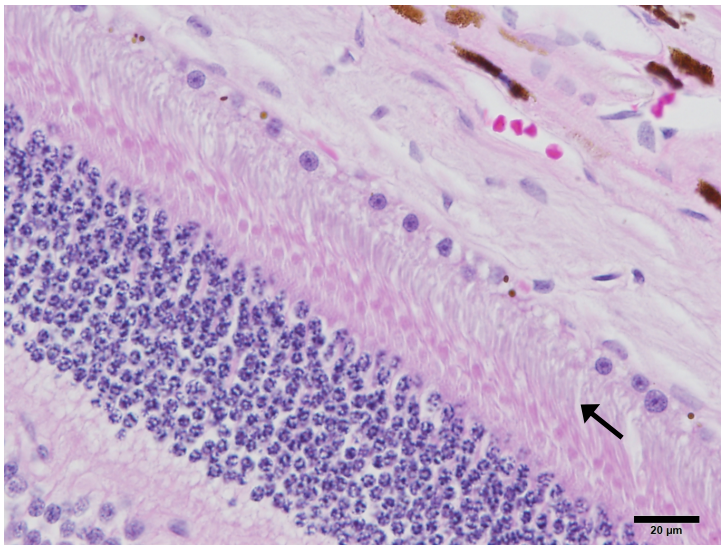

FIGURE 5. H&E-stained retina from the central posterior segment of the sea otter eye. The high density in the photoreceptor layer (arrow) primarily comprises rods with few apparent cones

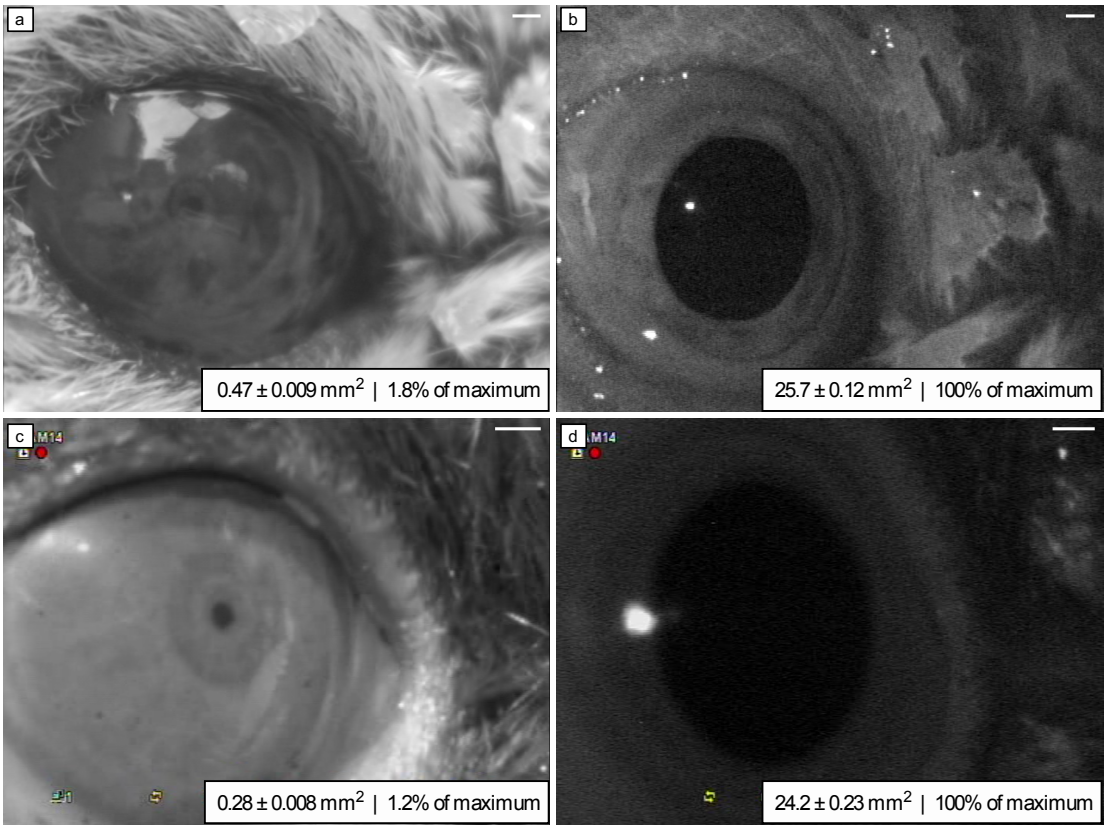

FIGURE 6. Photo representation of dynamic range across day and night in the male sea otter right eye (a,b) and female sea otter right eye (c,d). Mean ± sem, in addition to percent pupil area of maximal pupil area, is reported for day and night for each sea otter in the lower right-hand corner for constricted pupil in day (a,c) and dilated pupil at night (b,c). Scale bar in upper right corner represents 1mm for all photos

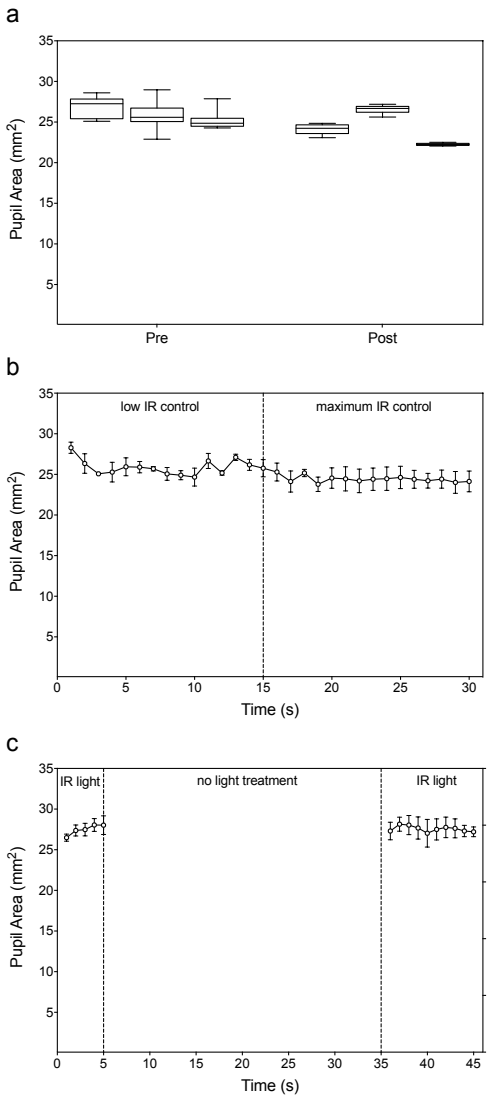

FIGURE 7. Pupil area for the male sea otter right eye during IR controls. (a) Box-and-whisker plots plotted separately for three replicates of low-to-high IR control that report median, upper and lower quartiles, and upper and lower ranges for pre-treatment (calculated from first 15 seconds) and post-treatment (calculated from last 9 seconds to exclude constriction response). (b) Mean ± sem of three replicates is plotted at each second for low-to-high IR control. An abrupt step-function from low IR light intensity to maximal IR light intensity occurred at the 15-second mark, indicated by the vertical dashed line. (c) Mean ± sem of three replicates is plotted at each second for off-on IR control. An abrupt change in light level from maximal IR light intensity to no introduced IR light occurred at the 5-second mark, indicated by the left vertical dashed line. An abrupt change from no introduced IR light to maximal IR light intensity occurred at the 35-second mark, indicated by the right vertical dashed line; no constriction occurred in response to this exposure

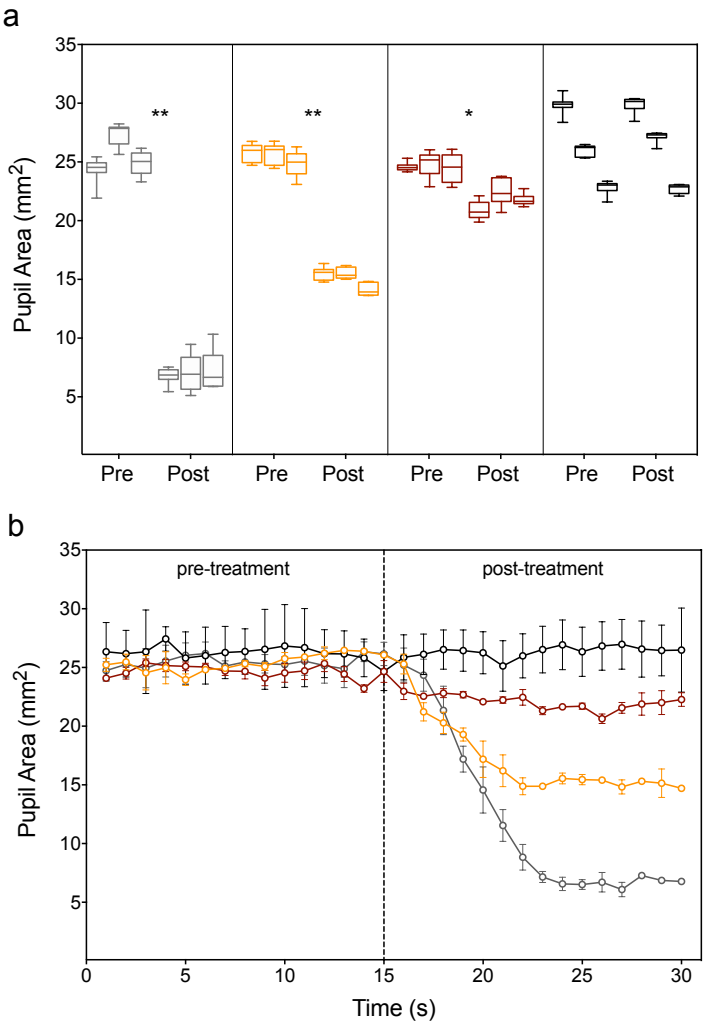

FIGURE 8. Pupil area for the male sea otter right eye during pre-treatment and post-treatment of controlled light exposure for the white broadband condition (grey), 640 nm condition (red), 630 nm condition (orange), and continuous 30-second IR light condition (940 nm, black). (a) Box-and-whisker plots plotted separately for three replicates in each condition that report median, upper and lower quartiles, and upper and lower ranges for pre-treatment (calculated from first 15 seconds) and post-treatment (calculated from last 9 seconds to exclude constriction response). Asterisks indicate that pupil area was significantly smaller post-treatment relative to pre-treatment (one-sided paired t-test); '*' indicates $p<0.01$, '**' indicates $p<0.001$, and '***' indicates $p<0.0001$. (b) Mean ± sem of three replicates is plotted at each second for pre-treatment and post-treatment of all conditions. Controlled light exposure occurred at the 15-second mark, indicated by the vertical dashed line. For two of the three replicates of the 630nm and white broadband conditions, the last three seconds post-treatment did not contain a still image that met image selection criterion, so these three data points represent the measurements from one replicate

SUPPLEMENTARY INFORMATION

SUPPLEMENTARY TABLE 1. Antibodies and lectins used for immunohistochemistry of the sea otter retina

Stain	Host	Target	Concentration	Source
Primary stains				
Cone arrestin		Cone photoreceptors	1:100 1:250 1:1000	
PNA (Bioatinylated peanut agglutinin)	NA	Cone photoreceptors	1:500	Vector Labs, Inc., Burlingame, CA, USA
Secondary stains				
Alexa Fluor 488 --- anti---- IgG		Cone arrestin	1:250	Life technologies, Carlsbad, CA, USA
Alexa Fluor 488 Streptavadin		PNA	1:250	Life technologies, Carlsbad, CA, USA

SUPPLEMENTARY TABLE 2. Summary of measurements and specifications reported in manufacturers' datasheets for LEDs and LED arrays

Light treatment	# LEDs in array	Measured illuminance of array (foot-candles)	Manufacturer	Dominant wavelength (nm)	Typical luminous intensity (mcd)	Viewing angle (deg)
White (broadband)	5	2.4-2.5	Rohm Semiconductor (Kyoto, Japan)	NA	1000	40
Orange (630 nm)	5	1.92	Rohm Semiconductor (Kyoto, Japan)	630	1000	40
Red (640 nm)	5	1.00	Kingbright (City of Industry, CA)	640	900	34

CHAPTER 2

ACTIVE TOUCH IN SEA OTTERS: IN-AIR AND UNDERWATER TEXTURE DISCRIMINATION THRESHOLDS AND BEHAVIORAL STRATEGIES FOR PAWS AND VIBRISSAE

Reproduced/adapted with permission from:

Strobel, S.M., Sills, J.M., Tinker, M.T., and Reichmuth, C.J. 2018. Active touch in sea otters: in-air and underwater texture discrimination thresholds and behavioral strategies for paws and vibrissae. *Journal of Experimental Biology* 221(18): jeb181347. doi:10.1242/jeb.181347.

© 2018. Published by The Company of Biologists Ltd | Journal of Experimental Biology (2018) 221, jeb181347. doi:10.1242/jeb.181347

RESEARCH ARTICLE

Active touch in sea otters: in-air and underwater texture discrimination thresholds and behavioral strategies for paws and vibrissae

Sarah McKay Strobel[1,*], Jillian M. Sills[2], M. Tim Tinker[1] and Colleen J. Reichmuth[2]

ABSTRACT

Sea otters (*Enhydra lutris*) are marine predators that forage on a wide array of cryptic, benthic invertebrates. Observational studies and anatomical investigations of the sea otter somatosensory cortex suggest that touch is an important sense for detecting and capturing prey. Sea otters have two well-developed tactile structures: front paws and facial vibrissae. In this study, we use a two-alternative forced choice paradigm to investigate tactile sensitivity of a sea otter subject's paws and vibrissae, both in air and under water. We corroborate these measurements by testing human subjects with the same experimental paradigm. The sea otter showed good sensitivity with both tactile structures, but better paw sensitivity (Weber fraction, c=0.14) than vibrissal sensitivity (c=0.24). The sea otter's sensitivity was similar in air and under water for paw (c_{air}=0.12, c_{water}=0.15) and for vibrissae (c_{air}=0.24, c_{water}=0.25). Relative to the human subjects we tested, the sea otter achieved similar sensitivity when using her paw and responded approximately 30-fold faster regardless of difficulty level. Relative to non-human mammalian tactile specialists, the sea otter achieved similar or better sensitivity when using either her paw or vibrissae and responded 1.5- to 15-fold faster near threshold. Our findings suggest that sea otters have sensitive, rapid tactile processing capabilities. This functional test of anatomy-based hypotheses provides a mechanistic framework to interpret adaptations and behavioral strategies used by predators to detect and capture cryptic prey in aquatic habitats.

KEY WORDS: Tactile sensitivity, Haptic, Amphibious, Relative difference threshold, Two-alternative forced choice, *Enhydra lutris*

INTRODUCTION

A predator's ability to filter sensory information to capture prey represents a key constraint on diet; however, sensory capabilities and search strategies used by many top predators are poorly understood. Different habitats and prey characteristics often require different sensory modalities for efficient foraging. Large or conspicuous prey in open habitats may be detected visually, whereas small or cryptic prey in terrestrial habitats may be detected via chemoreception or audition. In aquatic habitats, visual cues can be limited at depth, at night or in periods of high turbidity. Although underwater olfaction has been documented for two air-breathing vertebrates in aquatic habitats (Catania, 2006; Catania et al., 2008), such specialized abilities are uncommon. Both passive and active hearing may assist in prey detection, but at close range, taction has emerged as a primary sense among aquatic and semi-aquatic taxa, especially when hunting buried invertebrates or fishes (Dehnhardt and Mauck, 2008). For example, many shorebird species probe the tidally flooded substrate with touch structures at their beak tips (Piersma et al., 1998); star-nosed moles seek prey in subterranean streams using specialized appendages around their nostrils (Catania and Kaas, 1997; Catania and Remple, 2004); and seals, sea lions and walruses detect and pursue prey using their vibrissae while diving (Dehnhardt and Mauck, 2008; Dehnhardt et al., 2001; Kastelein and van Gaalen, 1988; Kastelein et al., 1990; Niesterok et al., 2017).

Sea otters are amphibious mammals that dive <100 m to capture invertebrate prey along the north Pacific coastline (Bodkin et al., 2004; Thometz et al., 2016a). As apex predators in nearshore ecosystems, sea otters consume prey occurring in diverse subtidal and intertidal habitats (Riedman and Estes, 1990) and exert strong direct and indirect effects on ecosystem structure and function (Estes and Duggins, 1995; Estes and Palmisano, 1974; Hughes et al., 2013; Watson and Estes, 2011). Although their prey occur in micro-habitats where visual detection is difficult or impossible, sea otters nonetheless maintain a remarkably high rate of prey capture, consuming over a quarter of their own body mass each day (Costa and Kooyman, 1982). Sea otters hunt at the sea floor, but they return to the surface after each foraging dive to breathe and consume captured prey. Because sea otters rest on their backs at the surface while handling prey, direct observation of prey manipulation and consumption is possible; as a result, they have become a model species for diet composition and foraging behavior studies (Elliott Smith et al., 2015; Estes et al., 2003; Newsome et al., 2015; Thometz et al., 2016a; Tinker et al., 2007, 2008, 2012). Although much is known about their prey handling at the surface, basic cognitive and sensory mechanisms integral to prey search and capture remain unknown.

Behavioral observations and morphological patterns suggest that sea otters rely to some degree on touch during foraging. Telemetry-based field studies reveal that sea otters forage equally day and night, when visual cues may be reduced or absent (Bodkin et al., 2007; Gelatt et al., 2002; Ralls et al., 1995; Tinker et al., 2008). Unique among marine mammals, sea otters have two enhanced, complementary tactile structures that can be controlled with dexterity: flexible paws and a complex array of facial vibrissae (Fig. 1). At the surface, sea otters use their paws to manipulate hard-shelled prey directly and indirectly using tools (Fujii et al., 2015), as well as to regularly groom their fur. Their use of vibrissae at the surface is less clear. Although observations of underwater use of

[1]University of California Santa Cruz, Department of Ecology and Evolutionary Biology, 115 McAllister Way, Santa Cruz, CA 95060, USA. [2]Institute of Marine Sciences, Long Marine Laboratory, 115 McAllister Way, Santa Cruz, CA 95060, USA.

*Author for correspondence (smstrobel@ucsc.edu)

S.M.S., 0000-0002-5259-0589; J.M.S., 0000-0002-3110-4844; M.T.T., 0000-0002-3314-839X; C.J.R., 0000-0003-0981-6842

Received 4 April 2018; Accepted 2 July 2018

List of symbols and abbreviations

2AFC	two-alternative forced choice
AICc	Akaike information criterion corrected for small sample size
c	Weber fraction
CI	credible interval
GLMM	generalized linear mixed model
LOOIC	leave-one-out cross-validation information criterion
MCMC	Markov chain Monte Carlo
MCS	method of constant stimuli
MOL	method of limits
s	test session
S−	incorrect discriminative stimulus; subject's choice of this does not receive reinforcement
x_t	difference between the standard and S− on trial t
α	position of the psychometric curve along the abscissa
β	slope of the psychometric curve
γ	poorest performance expected by chance (0.50)
ΔLOOIC	change in LOOIC from the best-supported model
ΔS	discrimination threshold
ε_s	random effects associated with test session s
λ	lapse rate

vibrissae are sparse, sea otters can use their paws and face to dig into soft substrate in pursuit of burrowing invertebrates (Hines and Loughlin, 1980; Shimek, 1977). In support of these observations, sea otter vibrissae, like those of walruses (Fay, 1982), exhibit evidence of wear – particularly in soft-sediment habitats where infaunal bivalves are hunted (Marshall et al., 2014; M. T. Tinker unpublished observations) – which may result from active functional use or passive incidental contact with abrasive sediment.

Sea otter neural architecture provides additional clues indicating the importance of tactile information. The area of the somatosensory cortex representing paws and vibrissae is disproportionately enlarged compared with terrestrial mustelids (Radinsky, 1968), suggesting that sea otters have good tactile sensitivity with both structures. However, a higher proportion of this enlarged cortical area is dedicated to receiving paw input, which suggests that paws may have greater functional relevance than vibrissae in sea otters. Radinsky (1968) noted the same pattern in other species of invertebrate-eating otters but the opposite pattern in species of fish-eating otters, from which he suggested that the location of enlargement may correspond to mode of prey pursuit and capture – paw-based for invertebrate-eating otters or mouth-based for fish-eating otters.

The gross morphologies of both paws and vibrissae in sea otters seem suited for dexterous touch, consistent with Radinsky's (1968) suggestion. The paws' palmar surfaces are hairless, the digit and palm pads are fused, and the skin has a leathery granular texture (Fig. 1). The neural morphology of sea otter paws has not been described. The structure of the sea otter vibrissal array suggests that substantial blood flow – and thus energetic investment – is directed to these sensory organs to process information in cold, aquatic environments (Marshall et al., 2014). The vibrissae are highly innervated, with a tripartite blood sinus system that more closely resembles aquatic pinnipeds than terrestrial mustelid relatives (Marshall et al., 2014). The vibrissae are smooth, as in otariids (Ginter et al., 2012), some phocids (Berta and Sumich, 1999; Ginter et al., 2012; Marshall et al., 2006), walruses (Berta and Sumich, 1999), water rats (Dehnhardt et al., 1999) and terrestrial mammals (Hyvärinen et al., 2009). Hanke et al. (2013) suggest that smooth vibrissae are advantageous during active touch, i.e. subject-controlled tactile exploration (Gibson, 1962). Active touch is required of benthic foragers, as opposed to mid-water foragers that likely rely on hydrodynamic wake detection. Similar to benthic foragers such as walruses and bearded seals (Fay, 1982; Marshall et al., 2006), the sea otter vibrissal bed is rostrally oriented and comprises microvibrissae and macrovibrissae (Fig. 1).

Despite these behavioral and morphological indications of enhanced tactile sensitivity, fine-scale mechanics of how sea otters use their tactile system to gather information about physical objects or hydrodynamic cues are unknown. Neither absolute nor comparative functional sensitivities of paws and vibrissae have been measured in this species. As sensory perception is inherently probabilistic – influenced by an individual's external environment and internal state – obtaining such data requires controlled conditions with experienced captive subjects trained for psychophysical procedures.

Fig. 1. The right paw and vibrissal region of the sea otter used in the present study. Left panel: sea otter's paw delineated (white dashed lines) into digits (a), upper paw pad (b) and lower paw pad (c). Calipers visible at top of photo; scale bar, 20 mm. Right panel: sea otter's rostrally oriented vibrissal region. Microvibrissae are located medially, and macrovibrissae are located laterally from the midline. The microvibrissae are shorter and more rostrally directed than the macrovibrissae. Scale bar, 20 mm. Photo collection authorized under USFWS research permit MA186914-2. Photo credits: S. M. Strobel and A. Friedlaender.

Here we describe the performance of the sea otter tactile system – paws and vibrissae – in air and under water. To obtain tactile discrimination thresholds (ΔS), we trained and tested an individual sea otter in a behavioral two-alternative forced choice (2AFC) paradigm (Gescheider, 1997) using textured stimuli. To complement these data, we report the sea otter's decision-making strategy, including speed and explorative movement, as well as the effect of testing medium (in air or under water). In addition, we trained and tested four human subjects using their hands in air with the same experimental paradigm to compare the sea otter's abilities with those of a known tactile specialist. These data allowed us to directly compare performance metrics and decision-making strategy between species, assess whether our approach produced comparable results to published studies of humans, and interpret comparisons of the sea otter's performance metrics with published values from marine and terrestrial tactile specialists.

MATERIALS AND METHODS

Testing facility and subject

This study was conducted in Santa Cruz, California, USA, at the University of California Santa Cruz's Long Marine Laboratory and at the California Department of Fish and Wildlife's Marine Wildlife Veterinary Care and Research Center. Testing took place in seawater-filled pools with adjacent haul-out areas. The pools received a continuous supply of fresh seawater from northern Monterey Bay. We monitored water and air temperature at 5-min intervals throughout the study with a temperature logger (TidbiT v2 Temp UTBI-001, Onset Computer Corporation, Bourne, MA, USA), and these remained similar throughout the 2-month testing period (water=15.8±0.4°C, air=15.9±1.2°C).

The subject was a healthy 4-year-old adult female sea otter [*Enhydra lutris* (Linneaus 1758)], identified as 'Selka' (USGS 6511-12R, MBA 595-12). She was trained to participate voluntarily in psychophysical procedures using operant conditioning and positive reinforcement (seafood). The sea otter received approximately 30% of her daily diet during each test session. Her daily diet was established to maintain optimal overall health and was not constrained based on session performance. Animal research was conducted under authorization from the United States Fish and Wildlife Service (research permit MA186914-2) with the approval and oversight of the Institutional Animal Care and Use Committee at the University of California Santa Cruz.

The sea otter was trained and tested to use each tactile structure (i.e. paw or vibrissae) independently in the 2AFC, in air and under water. Daily training occurred over a 17-month period prior to testing to avoid confounding her performance with practice effects and to ensure that she was an expert subject. During training, the sea otter learned to perform the task in the following order: paw in air, paw under water, vibrissae in air, vibrissae under water. Daily testing occurred over a 2-month period post-training; during testing, the sea otter performed the task in the following order: vibrissae in air, vibrissae under water, paw under water, paw in air.

Stimuli

The stimuli comprised a set of acrylic resin plates (Delrin, 20×20×2.6 cm), machined in a pattern of alternating ridges and grooves. Consistent with other published studies of tactile sensitivity (see, e.g. Dehnhardt et al., 1998; Bachteler and Dehnhardt, 1999), we used groove width as the metric of discrimination ability; groove width varied among plates but remained constant within each plate. After machining, stimuli were measured with calipers to confirm sizes and tolerances. The groove widths that defined each stimulus were 5.0, 4.0, 3.6, 3.0, 2.5, 2.4, 2.3, 2.2, 2.1 and 2.0 mm (±0.03 mm average tolerance). Ridge width (2.0 mm, ±0.03 mm average tolerance) and groove depth (5.0 mm, ±0.18 mm average tolerance) were held constant across stimuli. One stimulus per groove width was produced, except for the 2.0 mm stimulus, which served as the predetermined standard for the duration of the experiment. Two of these standard stimuli were produced, each bearing 2.0 mm grooves. As the standard was presented on every trial (simultaneously with one of many potential plates defined as the incorrect stimulus, or S−), the alternating use of two identical standards controlled for any aberrant cues the sea otter might learn after extensive practice with the same plate over hundreds of trials. Consistent with other published studies, stimuli were only presented with grooves vertically oriented; however, we rotated the stimuli 180 deg for each alternating test session to further control for any subtle physical aberrances in the plates.

We used six plates as the S− to the standard for paw testing – ranging from +1.0 mm to +0.1 mm from the standard (3.0, 2.5, 2.4, 2.3, 2.2 and 2.1 mm) – and seven plates as the S− for vibrissal testing – ranging from +1.6 mm to +0.1 mm from the standard (3.6, 3.0, 2.5, 2.4, 2.3, 2.2 and 2.1 mm). We selected these stimuli to span a gradient from easily discriminable to indiscriminable based on threshold estimation during the sea otter's extensive training period.

Test apparatus

The custom-built apparatus comprised an acrylic plastic box (55.5×15×56 cm) with an interchangeable front-facing panel to allow for two differently sized access windows: a narrow one for paw testing and a wide one for vibrissal testing (Fig. 2). The apparatus held two stimuli that fit side-by-side into mounts in the apparatus, one to the sea otter's left and the other to the sea otter's right. The mounts kept the two stimuli separated by 5.2 cm when simultaneously presented to the sea otter. Each stimulus rested against a combined clicker and mechanical switch, which were triggered when the sea otter sufficiently depressed the stimulus from its starting position to indicate her choice. The clicker served to produce an audible, salient sound for the sea otter to associate with the act of making her choice to end each trial. Each session was filmed from inside the apparatus with an overhead-mounted or lateral-mounted high-resolution camera (GoPro Hero3+, 1080, 60 frames s^{-1}) to enable *post hoc* analysis of the sea otter's behavior.

A closed door (which slid vertically into the access window) prevented the sea otter from having visual or tactile access to the stimuli between trials. When closed, the access door activated a mechanical switch mounted to the inside of the apparatus. During trials, when the door slid upwards to open the access window, the sea otter was restricted to using only tactile information. In the paw test, a horizontal slit cut into a neoprene cover for the narrow access window allowed the sea otter to only touch the stimuli with her paws and inhibited her from seeing the stimuli (Fig. 2). In the vibrissal task – during which the wide access window allowed the sea otter to freely approach the stimuli with her face – she was trained to voluntarily wear a neoprene blindfold that did not restrict her mystacial vibrissae (Fig. 2). To prevent the use of paws during the vibrissal task, she was trained to place her paws on a PVC stand attached to the front of the apparatus for the duration of each trial (Fig. 2). On the front face of the apparatus, a square target above the access door marked the fixed location for the sea otter to station (i.e. make firm contact with the target using her nose) prior to each trial (Fig. 2).

Journal of Experimental Biology (2018) 221, jeb181347. doi:10.1242/jeb.181347

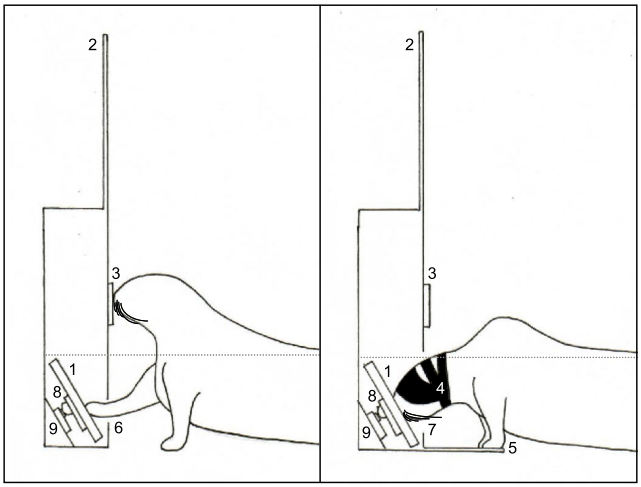

Fig. 2. Schematic drawing of experimental setup. Sea otter interacting with experimental apparatus and left stimulus (1) during paw (left panel) and vibrissal (right panel) testing. A barrier (2) prevented visual cues from the operators. To begin a trial for paw testing, the sea otter positioned her nose on a target (3) on the apparatus front. To begin a trial for vibrissal testing, the blindfolded sea otter (4) positioned her nose on the same target (3) and her paws on a PVC stand extending from the apparatus front (5). The experimenter controlled the sea otter's access to the stimuli via the paw (6) or vibrissal (7) access door. Each stimulus rested against a mechanical clicker (8) that activated an electrical switch (9) when depressed by the sea otter, signifying her choice. The horizontal dotted grey line indicates water height during underwater testing. Illustration credit: S.M.S.

The apparatus rested on a 1-m^2 haul-out platform in the sea otter's pool. We adjusted the height of the haul-out platform and the pool's water level to create the in-air and underwater conditions. For the in-air conditions, the water level was held just below the haul-out platform, such that the sea otter and apparatus were completely in air for each trial. For the underwater conditions, the water level was raised to completely submerge the stimuli, such that the sea otter and apparatus were partially submerged for each trial (Fig. 2). This design allowed the sea otter to retain the same stable standing position on the haul-out platform while performing the task in either medium.

A visual barrier extended vertically from the top of the apparatus to conceal two operators, sitting directly behind the apparatus on the pool deck, from the sea otter. The operators were responsible for opening and closing the access door, as well as removing and replacing the stimuli in the apparatus between trials. In a separate area that was visually and acoustically isolated from the testing enclosure, an experimenter monitored the session on a closed-circuit video system. The experimenter provided instructions to the operators via headphones during each trial. A trainer, who was seated at the side of the pool to the left of the apparatus, provided instructions and primary reinforcement (seafood) to the sea otter during each session. An Advent AV570 speaker (Audiovox Electronics Corporation, Hauppauge, NY, USA) provided conditioned, acoustic feedback to the sea otter and trainer immediately following the sea otter's choice on each trial. This feedback – previously recorded audible cues – comprised either the bridge for a correct response (bell tone) or the delta for an incorrect response (accelerated human verbal 'no').

Experimental procedure

For all conditions, the sea otter participated in a 2AFC procedure to discriminate the standard from the S−. Correct choice of the standard earned the sea otter food reinforcement (one whole, peeled shrimp), while the incorrect choice of the S− was not reinforced. The experimenter used a custom LabVIEW program (National Instruments, Austin, TX, USA) to automate data collection and provide appropriate, instantaneous auditory feedback via the speaker. The experimenter followed a predetermined sequence order generated using a custom MATLAB script (MathWorks, Natick, MA, USA). Stimulus presentation within each session followed a predetermined, pseudorandom, modified Gellermann schedule (Gellermann, 1933) that was counterbalanced to ensure equal probability of (1) the standard appearing on the left and right stimulus positions and (2) the standard appearing in the same or alternative position from the previous trial. The overall session sequence was constrained such that neither stimulus was presented on the same side more than four times consecutively. The operators and the trainer were blind to the sequence order and the trainer was blind to individual trial conditions.

The sea otter was trained using a modified method of limits (MOL), during which the subject faced a single stimulus comparison during a session, and tested using a method of constant stimuli (MCS), during which the subject faced a fixed set of stimulus comparisons during a session (Cornsweet, 1962; Stebbins, 1970). During MOL training, the sea otter was presented with a single stimulus combination (one S− paired with the standard) in multiple trials over successive sessions. The first discrimination the sea otter learned was a smooth S− paired with the standard. The next discrimination was the S− with the largest groove width (5.0 mm) paired with the standard. Trials continued until performance met pre-determined learning criteria, defined as performance ≥75% that differed <7% across two consecutive sessions; the sea otter then continued to the next smallest S− paired with the standard. Training continued with all stimulus combinations in descending order until the sea otter had met learning criteria or reliably failed to meet learning criteria across 10 sessions.

Other than the method of stimulus presentation, the experimental procedure was identical for training and testing. A session began when the sea otter was provided access to the apparatus in the testing pool. The sea otter positioned in the water in front of the trainer, who prompted her to approach the apparatus. The sea otter initiated a trial when she made firm contact with her nose on the target; for the vibrissal conditions, the sea otter also placed her paws on the stand. One to five seconds after the sea otter positioned correctly, the access door was opened, which deactivated the mechanical door switch. The timestamp of this deactivation was automatically

recorded in the LabVIEW program to mark the start of the sea otter's access to the stimuli.

During each trial, the sea otter explored the stimuli with either her paws or her vibrissal region (depending on the test condition) and signified her choice by depressing one plate to activate simultaneously the mechanical switch and clicker located behind the plate. The activation of the stimulus mechanical switch was automatically recorded in the LabVIEW program to mark the end of the trial and trigger the acoustic feedback. After making her choice and receiving feedback, the sea otter removed her paw or face from the apparatus, and the access door was closed. The trainer delivered either primary reinforcement for a correct choice or no primary reinforcement for an incorrect choice; in either case, the trainer then directed the sea otter to a location away from the apparatus to avoid inter-trial cues that might unintentionally indicate the details of the next trial to the sea otter. To prepare the next trial, the operators removed both stimuli simultaneously, rinsed them in fresh water, and replaced the new stimulus combination concurrently in the apparatus according to the experimenter's instructions. Once the next trial was set up, the trainer provided a small food item to reinforce the sea otter's inter-trial behavior and then cued the sea otter to return to the apparatus. Inter-trial intervals generally lasted 25–30 s.

For vibrissal testing, the trainer positioned the blindfold on the sea otter at the beginning of the session. Although the sea otter was free to remove the blindfold between trials, she typically voluntarily wore the blindfold for the duration of the session. The trainer ensured the blindfold's proper positioning following each trial and prior to verbally signaling the sea otter to return to the apparatus for the next trial.

Other than the apparatus's design to restrict the sea otter to use only her paws or only her vibrissal region, the sea otter was unrestrained and free to choose her strategy (e.g. order of exploration of stimuli, duration of exploration, number of touches, manner of touching, paw preference) throughout training and testing.

Following the extensive training period with MOL, the sea otter completed 16 test sessions with MCS. One to two sessions were completed each experimental day. Each session included 28 test trials for paw testing and 24 test trials for vibrissal testing, with warm-up and cool-down phases of six to 10 trials each. The warm-up and cool-down phases were used to maintain stimulus control and assess the sea otter's motivation before and after the test phase, respectively, by presenting an S− that was easily discriminable from the standard. In the test phase of each session, the sea otter was presented with four consecutive blocks of trials. Each S− was paired with the standard once per block of trials (six-trial blocks for vibrissae, seven-trial blocks for paws). For each testing condition, the sea otter completed four sessions, which totaled 16 presentations of each S−.

Analysis and determination of discrimination thresholds

Most previous tactile discrimination studies have used linear interpolation to identify discrimination thresholds from performance data (see, e.g. Dehnhardt and Kaminski, 1995; Dehnhardt et al., 1997; Bachteler and Dehnhardt, 1999; Hille et al., 2001). However, this approach uses only a small portion of the overall data (i.e. the two stimulus levels at which performance is closest to 75%) and does not allow error estimation of the psychometric function or a quantitative comparison of psychometric functions and interpolated thresholds from different experimental conditions.

Given the limitations of the linear interpolation method, we instead used a Bayesian approach to fit a sigmoid psychometric function to the observed performance data, considering each experimental condition separately (Wichmann and Hill, 2001). From the fitted curve, we estimated the sea otter's discrimination threshold (ΔS) – defined as the difference in groove width between the standard and the S− that the subject could reliably detect (i.e. on 75% of presentations). We also estimated the associated 95% credible interval (CI), defined as the range of difference values that includes the true value of ΔS with 95% probability.

Following previous studies (e.g. Wichmann and Hill, 2001), we used a modified two-parameter Weibull function to describe the psychometric curve:

$$\varphi(x_t;\alpha,\beta,\gamma,\lambda,\varepsilon)=\gamma+(1-\gamma-\lambda)\cdot\left(1-\exp\left[-\left(\frac{x_t}{\alpha\cdot\varepsilon_s}\right)^{\beta}\right]\right), \quad (1)$$

where x_t is the difference between the standard and S− in trial t ($0.1<x<1.6$), parameter α determines the position of the curve along the abscissa, and parameter β determines the curve's slope. Parameters γ and λ were used to adjust the function to allow for stimulus-independent errors: γ represents the maximum possible adjustment, which we fixed at 0.5 owing to the 2AFC design (that is, the poorest performance expected by chance), whereas λ represents the lapse rate – the probability of the subject's attention lapsing, resulting in incorrect responses independent of stimulus intensity. Thus $\gamma+(1-\gamma-\lambda)$ results in a deviation of the function from the asymptotic value of 1 and sets the subject's realistic 'best' average performance. Finally, error term ε_s allowed for random effects associated with each test session s, where $\log(\varepsilon_s)$ was drawn from a normal distribution with mean 0 and standard deviation σ.

We used Markov chain Monte Carlo (MCMC) methods to fit Eqn 1 to the observed data (y_t, the subject's response to each trial), which we treated as a binomial variable with possible values 1 (correct response) or 0 (incorrect response). Specifically, for each trial, we assumed y_t was drawn from a Bernoulli distribution with probability $\varphi(x_t;\alpha,\beta,\gamma,\lambda,\varepsilon)$. We set uninformative, uniform priors for parameters α, λ and σ, and used a weakly informed prior for β (given the assumption of an increasing function), drawing from a gamma distribution with parameters shape=1.5 and rate=0.1. After a burn-in of 5000 iterations, we saved 20,000 simulations for computing posterior distributions for all parameters. We examined trace plots and Gelman–Rubin statistics to ensure model convergence (we required a Gelman–Rubin statistic of <1.01 for each parameter), and report means and CIs for all statistics. We calculated the ΔS for each psychometric curve by interpolating the estimated function value along the abscissa at the 75% correct response level, as well as the corresponding upper and lower 95% CIs.

Although our primary research aims were to assess the sea otter's performance using paws and vibrissae, in air and under water, we wanted to determine whether any observed differences in performance between structures or media were biologically relevant. This required a statistical method to compare psychometric functions. Using the same Weibull function and MCMC methods described above, we evaluated multiple models to compare the interpolated ΔS and psychometric functions across tactile structures and testing media, and we used a hierarchical model structure to account for random effects associated with different experimental sessions.

We did not set *a priori* expectations of whether tactile discrimination abilities (and, thus, psychometric curves) would differ between structures (paw versus vibrissae) or within different media (in air versus under water). Accordingly, we evaluated a nested suite of five alternative models, differing in the number of α and β

Table 1. Model comparison results for sea otter performance, including for each model the data grouping, number of α parameters (determines the curve position along the abscissa), number of β parameters (determines the curve slope), leave-one-out information criterion (LOOIC; ±s.e.m.), change in LOOIC from the best-supported model (ΔLOOIC; ±s.e.m.) and *P*-value associated with ΔLOOIC

Model	α	β	LOOIC	ΔLOOIC	*P*-value
Paw (grouped in air and under water), Vibrissae (grouped in air and under water)	**2**	**2**	**345±19.5**	**0**	**0**
Paw (in air and under water separate), Vibrissae (grouped in air and under water)	**3**	**3**	**348±19.9**	**1.73±1.42**	**0.111**
Paw (grouped in air and under water), Vibrissae (in air and under water separate)	3	3	350±19.6	2.67±0.69	0.0000553
Paw (in air and under water separate), Vibrissae (in air and under water separate)	4	4	354±19.9	4.35±1.53	0.00227
Grouped tactile structures [paw (in air and under water) and vibrissae (in air and under water)]	1	1	355±20.3	5.08±2.33	0.0147

The two best-supported models – based on the lowest LOOIC – are in bold; the ΔLOOIC and *P*-value associated with the top-listed model are zero, as each model's ΔLOOIC was calculated relative to this model. A model with $P<0.05$ is significantly more different than expected by chance from the top-listed model.

parameters (Table 1) to determine whether performance differed across testing conditions. In the most saturated model, the α and β parameters varied among all four experimental conditions (paw in air, paw under water, vibrissae in air, vibrissae under water), whereas in the least saturated model all experimental conditions shared a single fitted value of α and β. We then compared model fit to determine whether the data provided adequate support to consider the sea otter's performance as different between tactile structures or media. We used the leave-one-out cross-validation information criterion (LOOIC) to compare models, computing LOOIC and ΔLOOIC for each model (Vehtari et al., 2017). We identified the model with the lowest LOOIC as best supported, but also retained models with ΔLOOIC *P*-values >0.05 (indicating a probability greater than 0.05 that the observed ΔLOOIC was not different from 0).

All model fitting and analyses were conducted using R (https://www.r-project.org/), RStudio (RStudio, Inc., Boston, MA, USA), JAGS (Just Another Gibbs Sampler; Plummer, 2003) and the R packages rjags (http://mcmc-jags.sourceforge.net/) and runjags (Denwood, 2016).

Relative difference thresholds

We calculated the sea otter's relative difference threshold (*c*), or Weber fraction, as the ratio of the discrimination threshold to the standard's groove width ($c=\Delta S/2.0$). We similarly translated 95% CIs around *c* as the ratio of the upper and lower CIs of Δ*S* to the standard groove width. We used the Weber fraction to compare the sea otter's performance with published values for terrestrial and marine tactile specialists performing texture and size discrimination tasks. We were unable to compare the sea otter's performance with results from studies in which the authors either did not use discrete increments to vary the S− from the standard or measure the standard (Carvell and Simons, 1990; Kastelein and van Gaalen, 1988; Kastelein et al., 1990); in these cases, we could not calculate the Weber fraction.

After obtaining the sea otter's Δ*S* for each condition, we used this information to group two S− levels categorically as supra-threshold (the two stimulus levels at which the sea otter's performance was most similar to a perfect 100% mean correct response) and two S− levels categorically as near-threshold (the two stimulus levels at which the sea otter's performance was most similar to 75% mean correct response). The supra-threshold category indicated levels at which correct discrimination was likely easy for the sea otter, and the near-threshold category indicated levels at which correct discrimination was likely difficult for the sea otter. This enabled us to control for the effect of perceived difficulty when assessing the sea otter's behavioral strategy.

Behavioral strategy determination

After the conclusion of testing, a single observer reviewed the GoPro footage for each session and used frame-by-frame analysis (Adobe Premiere Pro CS6, San Jose, CA, USA) to qualitatively and quantitatively describe the sea otter's fine-scale behavioral strategy for making her decision during each trial of the test phase, including type, degree and pattern of exploration. This information was subsequently used to determine whether the sea otter altered her strategy as a function of difficulty.

To describe type of exploration, we examined lateralization in the sea otter's explorative strategy, as well as the sections of the paw (i.e. lower paw pad, upper paw pad or digits) or vibrissal region (i.e. vibrissal-only contact or a combination of vibrissal and facial skin contact) that the sea otter used to explore the stimuli. We used a chi-square test for equality of proportions to assess whether difficulty influenced the sections of the paw or vibrissal region that the sea otter used to explore the stimuli. Additionally, we used R and lme4 (Bates et al., 2015) to perform a generalized linear mixed model (GLMM) analysis that included facial skin contact as a binary categorical fixed effect to assess whether the type of contact with her vibrissal region influenced the odds of the sea otter making a correct choice. We used the outcome of a trial (i.e. correct or incorrect) as a binomial-distributed response variable and included intercepts for session as the random effect. We compared the model containing the fixed effect with a null model that only contained the random effect. We used R and MuMIn (https://CRAN.R-project.org/package=MuMIn) to assign and rank the two models based on AICc (Akaike information criterion corrected for small sample size) scores and calculate the relative importance of the fixed effect.

To describe the degree of exploration, we defined a single touch as unbroken contact of the tactile structure with a stimulus and recorded the number of touches on each stimulus before the sea otter made her choice. For the vibrissal conditions, we defined an additional variable that examined the number of directional movements the sea otter exhibited during a single touch. To describe the pattern of exploration, we recorded the order of stimulus exploration and calculated the number of stimulus comparisons the sea otter used before making her choice. We defined a single comparison as the successive exploration of two stimuli before a choice (as in Hille et al., 2001). Because of the sea otter's typical pattern of exploring only one stimulus before making her choice, comparisons occurred rarely. For example, exploration of the stimulus to the sea otter's right side followed by immediate choice of the stimulus to the sea otter's left side (R–L) was considered an exploration followed by a choice, not a comparison. Exploration of the stimulus to the sea otter's right side followed by an exploration of the stimulus to the sea otter's left side, followed by an immediate choice on the sea otter's right side (R–L–R) was considered one comparison.

Decision times

For each trial in the test phase, we initially calculated response latency as the time difference between the onset of the door's opening (which deactivated the mechanical door switch) and the full

depression of the stimulus (which activated the mechanical stimulus switch). However, this measurement was a poor indicator of decision time, because the sea otter did not always begin exploration of the stimuli immediately after gaining access to them.

To obtain a more accurate and precise measurement of decision time, a single observer reviewed the recorded video footage from each test trial and used frame-by-frame analysis to calculate the time difference (converted from frames s^{-1} to ms) between the sea otter's initial contact with the stimuli and her decision. The frame of the sea otter's initial touch was clearly distinguishable, but the point of decision depended on the sea otter's pattern of exploration. During training, the sea otter exhibited a consistent pattern of exploring the stimulus to her right side first and deciding to either choose that stimulus or move to immediately choose the stimulus to her left side without further exploration. Because this right-side-biased order of exploration created an artificial difference in latency between left and right choices, we defined the decision point in the test phase as follows: (1) for trials in which the sea otter chose the stimulus to her right side after no exploration of the stimulus to her left side, the decision point was the frame in which the sea otter began to depress the right stimulus; (2) for trials in which the sea otter chose a stimulus immediately after exploring the other stimulus, the decision point was the frame in which the sea otter broke physical contact with the stimulus she touched just prior to her choice. For the latter situation, the sea otter never explored the stimulus she chose after leaving the previous stimulus, so she effectively left one stimulus to choose the other. We report decision time as mean±s.e.m.

Our measurements of decision time focused on the time needed for the sea otter to collect and process tactile cues and then initiate a motor action to represent her decision. Thus, we excluded artifacts resulting from apparatus design or psychophysical procedure. This approach is similar to those reported for a texture discrimination task in West Indian manatees (Bauer et al., 2012) and a size discrimination task in harbor seals (Grant et al., 2013); the subjects in these studies used a strategy similar to that of the sea otter. We did not directly compare our measurements with those from tactile discrimination studies that defined decision time more broadly and, consequently, reported longer latencies (Dehnhardt and Dücker, 1996; Hille et al., 2001).

In-air texture discrimination testing with human subjects

Four human subjects used their hands in air to perform the same 2AFC discrimination task as the sea otter. Before training began, each subject received identical written instructions to choose the stimulus with smaller groove widths on each trial using any strategy (e.g. order of stimulus exploration, duration of stimulus exploration, number of touches, one or both hands, hand preference). As with the sea otter, each human was trained using a modified MOL. Upon reaching a performance plateau during training, each human was tested using MCS. During each experimental session, the humans wore a blindfold and headphones that played a broadband masker to restrict their use of visual or acoustic cues. All research with human subjects was conducted indoors (20–25°C) with written informed consent from the participants and with the approval and oversight of the University of California Santa Cruz's Institutional Review Board.

Following the training period with MOL, each subject completed four test sessions with MCS. One to two test sessions were completed each experimental day. Based on threshold estimation from published values and the subjects' training performances, we chose four plates as the S− to the standard for testing, ranging from +0.4 to +0.1 mm from the standard (2.4, 2.3, 2.2 and 2.1 mm). The session sequences were counterbalanced and constrained using the same rules as those for the sea otter. Each test session comprised four warm-up trials, 16 test trials and four cool-down trials. In the test phase of each session, the subject was presented with four consecutive blocks of trials. Each S− was paired with the standard once per block of trials, which totaled 16 presentations of each S− over the test period.

Methods for estimating the sigmoidal function based on the observed performance data (see Eqn 1), difference thresholds, Weber fraction, strategy determination and decision times for each subject were identical to those described for the sea otter, with the exception that we evaluated over a smaller range of stimulus differences ($0.1<x<0.4$). We used the Weber fraction to compare the human subjects' performances with those of the sea otter, as well as with published values for human subjects performing texture and size discrimination tasks.

After obtaining the ΔS for each subject, we used this information to assign one S− level categorically as supra-threshold (the stimulus level at which the subject's performance was most similar to a perfect 100% mean correct response) and one S− level categorically as near-threshold (the stimulus level at which the subject's performance was most similar to 75% mean correct response) for each subject. As with the sea otter, this enabled us to test for the effect of perceived difficulty when assessing the subjects' decision times and behavioral strategies.

Effects of difficulty, structure, testing medium and species on performance

We examined whether difficulty (i.e. supra-threshold or near-threshold), tactile structure (i.e. paw or vibrissae) or testing medium (i.e. in air or under water) influenced the sea otter's explorative strategy or decision time. We used R and lme4 (Bates et al., 2015) to perform GLMM analyses that included difficulty level, tactile structure and testing medium as categorical fixed effects. We used the number of touches as a Poisson-distributed response variable, the number of comparisons before a choice as a Poisson-distributed response variable, and decision time as a log-normal-distributed response variable. We created a set of 12 models for each response variable; in the fully saturated model we allowed for an additive three-way interaction between the fixed effects and included intercepts for session as the random effect. We used R and MuMIn (https://CRAN.R-project.org/package=MuMIn) to assign and rank the models based on AICc scores and calculate the relative importance of each fixed effect.

We similarly examined whether difficulty influenced the human subjects' explorative strategy or decision time, but we used generalized linear model (GLM) analyses in addition to GLMM analyses. We assigned subject as either a random effect (for the GLMM) or as a fixed effect (for the GLM) to assess the contribution of between-subject variation to the observed data.

Additionally, we assessed the effects of species and difficulty on strategy and decision time to assess whether the humans and sea otter performed differently. Because we had multiple human subjects but only one sea otter subject, we nested (1) subject within species and (2) session within subject within species for the random effects; this maintained consistency with the inclusion of random effects in the previous analyses.

RESULTS

Sea otter discrimination thresholds

The sea otter's performance data and psychometric functions for texture discrimination using her paw and vibrissae, in air and under water, suggest differences across structure and possibly

medium (Fig. 3). The thresholds and positions of the psychometric curves along the abscissas indicate that the sea otter showed better, more consistent performance with her paw than her vibrissae and slightly better performance in air than under water for both tactile structures (paw in air: ΔS=0.24 mm, 95% CI=0.16–0.32 mm, Weber fraction=0.12; paw under water: ΔS=0.30 mm, 95% CI=0.22–0.37 mm, Weber fraction=0.15; vibrissae in air: ΔS=0.48 mm, 95% CI=0.38–0.73 mm, Weber fraction=0.24; vibrissae under water: ΔS=0.50 mm, 95% CI=0.37–0.79 mm, Weber fraction=0.25). The discrimination thresholds determined using the Bayesian approach approximated (within 0–10%) those determined with traditional linear interpolation.

We examined the model comparison results to determine whether these differences were significant given expected variation in performance, and thus how to interpret the psychophysical data in a biologically meaningful way. In general, the models used to fit the performance data agree that the sea otter's performance with her paw was superior to that with her vibrissae. The model comparison suggests that performance significantly differed between tactile structures, but not necessarily between in air and under water. Two models were identified as best supported based on LOOIC: (1) the model considering in-air and underwater data together for each structure, and (2) the model considering in-air and underwater data together for vibrissae but separately for paw (Table 1). The model considering data by experimental condition received poor support, as it ranked fourth with a significantly higher LOOIC than the best-supported models (Table 1). We report the estimated means and CIs for each model's parameters (Table S1).

Fitting the psychometric curves to the data grouped by structure, irrespective of medium, indicated that ΔS for paw testing was 0.27 mm (95% CI=0.21–0.32 mm, Weber fraction=0.14), and ΔS for vibrissal testing was 0.47 mm (95% CI=0.40–0.59 mm, Weber fraction=0.24). Again, comparison of the two curves grouped by structure (Fig. 4) showed the sea otter's superior discrimination ability with her paw, evidenced by the left-shifted position of the psychometric curve along the abscissa and the lower calculated ΔS relative to those of her vibrissae.

Sea otter strategy

For both paw and vibrissal testing, the sea otter used a consistent strategy to explore the stimuli. She touched the stimulus presented on her right side first on all trials [100% (416/416)]. She then made her choice based on zero [95.4% (397/416)] to one sequential comparison [4.3% (18/416)]; her maximum of two sequential comparisons occurred only once [0.2% (1/416)]. Thus, the sea otter made her decision to stay (and choose the stimulus on her right) or to shift (leaving the stimulus on her right to immediately choose the stimulus on her left) based on her assessment of the similarity between the initial stimulus and her memory of the standard.

In addition to her strategy of first touching the stimulus on her right, the sea otter showed right-side-biased choice throughout testing. When the standard was presented on her right, she tended to

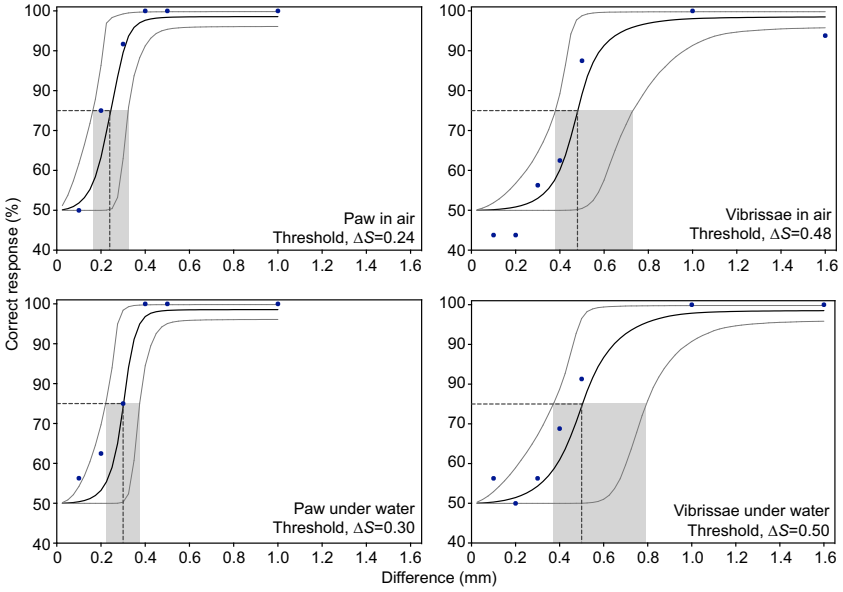

Fig. 3. Psychometric functions for sea otter paw and vibrissal tactile performance in air and under water. Correct response percentages (closed circles) are plotted against the difference between the groove widths of the incorrect stimulus (S−) and standard (2.0 mm) for each of four experimental conditions. Each data point represents the percentage of trials (n=16) for which the sea otter correctly chose the standard instead of the S−. The sea otter completed the same number of trials for each S− for paw and vibrissal testing, but she was presented with fewer S− levels in paw testing. For each experimental condition, we used a modified Weibull function and conducted Markov chain Monte Carlo (MCMC) simulations (n=35,000) to fit the psychometric function (solid black line) and 95% credible intervals (CIs; solid gray lines) to the observed data assuming that each response was generated from a Bernoulli process. Discrimination thresholds (ΔS, vertical dashed line) and 95% CIs (shaded box) at the 75% correct response level were interpolated from the fitted model along the abscissa.

Journal of Experimental Biology

Journal of Experimental Biology (2018) 221, jeb181347. doi:10.1242/jeb.181347

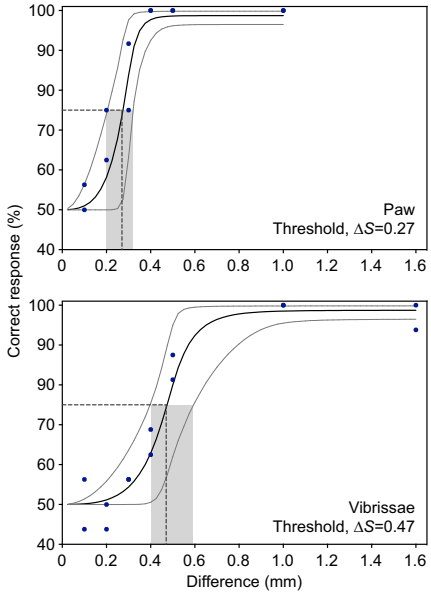

Fig. 4. Psychometric functions for sea otter paw and vibrissal tactile performance, in air and under water combined. Correct response percentages (closed circles) are plotted against the difference between the groove widths of the S− and standard (2.0 mm) for each data grouping: paw and vibrissae. Each data point represents the percentage of trials (n=16 each for in air and under water) for which the sea otter correctly chose the standard instead of the S−. Within a structure, two data points are plotted at each S− level (representing in air and under water separately); however, if the sea otter performed equally well, then the two data points appear to the eye as one. The sea otter completed the same number of trials for each S− for paw and vibrissal testing, but she was presented with fewer S− levels in paw testing. For each data grouping, we used a modified Weibull function and conducted MCMC simulations (n=35,000) to fit the psychometric function (solid black line) and 95% CIs (solid gray lines) to the observed data assuming that each response was generated from a Bernoulli process. Discrimination thresholds (ΔS, vertical dashed line) and 95% CIs (shaded box) at the 75% correct response level were interpolated from the fitted model along the abscissa.

choose correctly regardless of difficulty [supra-threshold: 98.4% (63/64); near-threshold: 89.1% (57/64)]. However, when the standard was presented on her left, she tended to choose correctly on easier trials and dropped to chance level on more difficult trials [supra-threshold: 100% (64/64); near-threshold: 46.9% (30/64)]. This suggests that the sea otter defaulted near threshold to choosing the stimulus she touched first – here, the stimulus presented on her right.

Although the sea otter was allowed to use either or both paws to explore the stimuli prior to making her choice during paw testing in air and under water, she exclusively used her right paw for all trials [100% (192/192)]. Frame-by-frame video analysis showed that she contacted the stimulus with either the entire paw [66.7% (128/192)] or exclusively with the digits (see Fig. 1a) and upper pad (see Fig. 1b) [33.3% (64/192)], but never with exclusively the lower pad (see Fig. 1c). The percentage of trials in which she used exclusively her digits and upper pad instead of her entire paw pad increased with difficulty [P=0.04, X^2_1=4.24; supra-threshold: 25% (16/64); near-threshold: 42.2% (27/64)]. When using her paw, the sea otter contacted the stimulus with only subtle directional movement: she simultaneously flexed her paw, pressing her skin into the stimulus, and made quick successive lateral micro-movements resembling a vibration (Movie 1).

During vibrissal testing in air and under water, the sea otter contacted the stimulus with the midline of her nasal–oral region and did not show lateralized use of her vibrissal bed in any trial [0% (0/224)]. The sea otter did not protract her vibrissae during stimulus exploration, although capable of this controlled motion. Instead, she explored a stimulus by moving her entire head, making light contact with the surface using mystacial microvibrissae and the oral region, and sometimes mystacial macrovibrissae (Movie 1). She made larger explorative movements with her vibrissae compared with her paw, sweeping her head vertically or diagonally across the stimulus. She typically changed direction while retaining light contact with a stimulus with her vibrissae, but not her paw, and as a result explored more surface area of the stimulus and made more directional changes within a single discrete touch. This mode of exploration, the upper limit of video quality and the speed of her exploration (see 'Sea otter decision time', below) made it difficult to determine how contact with oral skin, rhinarium skin and mystacial microvibrissae contributed to her choice. However, we identified a substantial portion of trials in which the sea otter conclusively used vibrissae, without skin contact, to make her decision [48.7% (109/224)]. The percentage of trials with vibrissal-only contact was not influenced by difficulty [P=0.73, X^2_1=0.13; supra-threshold: 56.3% (36/64); near-threshold: 53.1% (34/64)]. Additionally, vibrissal-only contact did not affect the odds of a correct choice, because the model including vibrissal touch as a fixed effect did not differ significantly from the null model.

The sea otter's touch strategy did not differ across experimental conditions, as the best-supported model was the null model, which did not include fixed effects of difficulty, tactile structure or testing medium (Table S2). She made similar numbers of discrete explorative touches with each tactile structure in each medium at each difficulty level, and because the random effect of session accounted for a negligible degree of variance, her touch strategy was consistent across sessions. Difficulty did not influence the alternative movement pattern observed in the vibrissal conditions, in which a single discrete touch comprised multiple directional movements. Testing under water had a slight positive effect on these directional movements; however, this corresponded to an increase of less than one-half touch (Table S3). Results from model selection for the sea otter's comparison strategy similarly indicated that she maintained a consistent, low tendency to compare stimuli for all conditions (Table S2).

Sea otter decision time

The sea otter made decisions quickly with her paw (159.4±4.7 ms) and her vibrissae (346.1±10.0 ms), and for supra-threshold trials (paw: 146.1±6.4 ms; vibrissae: 306.0±18.8 ms) and near-threshold trials (paw: 179.2±9.7 ms; vibrissae: 326.3±16.3 ms) (Fig. 5, left panel). Difficulty, structure and testing medium affected the sea otter's decision time (Table S2). The coefficient estimates obtained from the model selection (Table S2) correspond to decisions that were approximately one-quarter slower when near threshold and approximately two times slower with her vibrissae. Because increased difficulty did not strongly influence the sea otter's touch or comparison strategy, her slower decisions in these conditions can be explained by increased touch duration. Testing medium had a slight effect, corresponding to approximately one-third slower decisions when under water (Table S2).

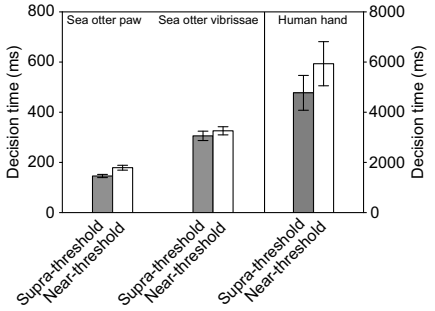

Fig. 5. Decision times for tactile discrimination with sea otter paw, sea otter vibrissae and human hand. Mean±s.e.m. decision times (ms) are plotted for supra-threshold (gray bars) and near-threshold (white bars) trials for paw (in air and under water grouped), vibrissae (in air and under water grouped) and human hands (subjects grouped). The sea otter's data correspond to the left *y*-axis and the humans' data correspond to the right *y*-axis. Note that these differ by one order of magnitude. The sea otter showed quick decision times overall (<400 ms), but quicker decisions with her paw than with her vibrissae and for supra-threshold trials. The human subjects were 15- to 30-fold slower than the sea otter using her vibrissae or paw, respectively. Although the human subjects showed quicker decision times in supra-threshold trials relative to near-threshold trials, similar to the sea otter, this effect was not significant.

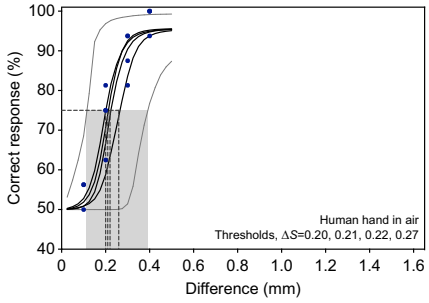

Fig. 6. Psychometric functions for human hand tactile performance in air. Correct response percentages (closed circles) are plotted against the difference between the groove widths of the S− and standard (2.0 mm). Each data point represents the percentage (*n*=16 trials) that each human correctly chose the standard instead of the S−. Four data points are plotted at each S− level (representing performance data from each human separately); however, if the subjects performed equally well, then the two data points appear to the eye as one. Human subjects completed the same number of trials as the sea otter for each S−, but they were presented with fewer S− levels. For each subject, we used a modified Weibull function and conducted MCMC simulations (*n*=35,000) to fit the psychometric function (solid black line) and 95% CIs (solid gray lines) to the observed data assuming that each response was generated from a Bernoulli process. Discrimination thresholds (Δ*S*, vertical dashed line) and 95% CIs (shaded box) at the 75% correct response level were interpolated from the fitted model along the abscissa.

Human discrimination thresholds and strategies

The human subjects primarily used one hand to perform the discrimination task in air. One subject (KC) initially used both hands: the left hand exclusively touching the stimulus on the left and the right hand exclusively touching the stimulus on the right. This strategy differed from the other subjects, and KC showed poor, highly variable performance. To maintain consistency across subjects, we repeated testing with KC, requiring her to use only one hand; subsequent results include only her second round of testing.

Performance data from the four humans generated similar psychometric functions (Fig. 6). Δ*S* for the four subjects were 0.20 mm (95% CI=0.11–0.31 mm, Weber fraction=0.10), 0.21 mm (95% CI=0.12–0.31 mm, Weber fraction=0.11), 0.22 mm (95% CI=0.15–0.35 mm, Weber fraction=0.11) and 0.27 mm (95% CI=0.18–0.39 mm, Weber fraction=0.14). Human performance was comparable to that of the sea otter using her paw (Fig. 7, upper panel). Weber fractions confirm that these human data are within the range of published values (see Fig. 7, lower panel) and, thus, that the experimental paradigm generated comparable results.

Three of the four human subjects exclusively used their right hands [100% (64/64 for each subject)]. Another subject (DS) used both hands on only one trial [0.02% (1/64)], for which she chose incorrectly; other than this trial, DS exclusively used her right hand. All humans primarily used their fingertips for stimuli exploration. Inter-subject differences had a strong effect on strategy metrics, with one subject (KC) consistently increasing discrete touches, comparisons and decision time as difficulty increased relative to the other subjects (Table S4).

Significant differences were apparent between the sea otter and human subjects for strategy and decision time (Table S5). The human subjects gathered information about relative properties of the S− and the standard, instead of remembering absolute properties of the standard like the sea otter. Regardless of difficulty, the human subjects explored the stimuli with almost two times more discrete touches and one-third more stimulus comparisons than the sea otter (Table S5). Notably, the mean decision time of the human subjects was 34-fold slower (Fig. 5, right panel) than the sea otter using her paw and 15-fold slower than the sea otter using her vibrissae (Fig. 5, left panel; see Table S5). Thus, the human subjects took considerably longer to perform the same task with accuracy comparable to that of the sea otter.

DISCUSSION

This study demonstrates sensitive touch in an aquatic top predator. The sea otter learned to discriminate textured stimuli in all four testing conditions in the absence of sensory cues other than taction. She showed more sensitive and rapid abilities with her paw than with her vibrissae, and similar performance in air and under water. The sea otter's performance can be generally compared with those obtained from tactile specialists in texture and size discrimination studies (Fig. 7, lower panel). These include terrestrial animals in air (Dehnhardt et al., 1997; Hille et al., 2001; Lamb, 1983; Morley et al., 1983), amphibious animals in air and under water (Dehnhardt, 1994; Dehnhardt and Dücker, 1996; Dehnhardt et al., 1998), and aquatic animals under water (Bachteler and Dehnhardt, 1999; Bauer et al., 2012).

Temperature can influence mammalian tactile performance, because blood perfusion to peripheral sensory structures – which may be reduced in cold temperatures – is critical for maintaining neural sensitivity. However, the constant and moderate temperatures in this study likely minimized the effects of temperature on measured differences in tactile sensitivity between tactile structures or media.

Psychophysical methods can also influence sensitivity measurements. Fixed-level (e.g. MCS) procedures can overestimate thresholds (and, thus, underestimate sensory ability) relative to adaptive (e.g. MOL) procedures (Kollmeier et al., 1988; Stillman,

Journal of Experimental Biology (2018) 221, jeb181347. doi:10.1242/jeb.181347

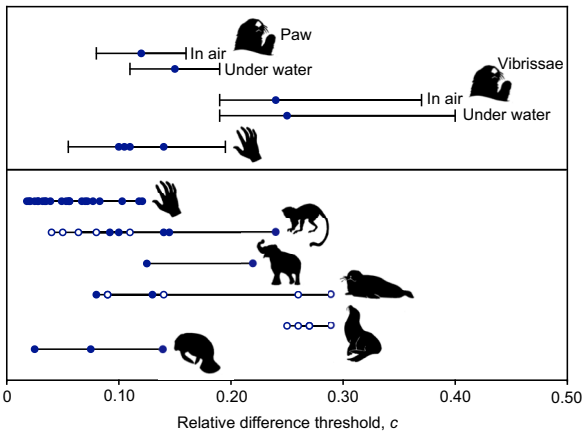

Fig. 7. Tactile sensitivity of sea otter paw and vibrissae compared with terrestrial and aquatic specialists: humans, squirrel monkey, Asian elephant, harbor seal, California sea lion and West Indian manatee. Upper panel (present study): the relative difference threshold (*c*) and 95% CIs of the sea otter paw, sea otter vibrissae and human hands in air. *c* is the ratio of the difference threshold, ΔS, to the standard's groove width ($c=\Delta S/2.0$). Each closed circle represents *c* from a subject (sea otter, *n*=1; human, *n*=4). Lower panel: the relative difference threshold (*c*) of terrestrial tactile specialists [human hands in air (Lamb, 1983; Morley et al., 1983), squirrel monkey hands in air (Hille et al., 2001), elephant trunk in air (Dehnhardt et al., 1997)], amphibious tactile specialists [harbor seal vibrissae under water (Dehnhardt et al., 1998) and California sea lion vibrissae in air (Dehnhardt, 1994; Dehnhardt and Dücker, 1996)] and an aquatic tactile specialist [West Indian manatee vibrissae under water (Bachteler and Dehnhardt, 1999; Bauer et al., 2012)]. *c* is calculated from the standard's groove width or size used in the corresponding study. Each closed circle represents *c* from a subject performing a texture discrimination task (human, *n*=18; squirrel monkey, *n*=4; elephant, *n*=2; harbor seal, *n*=2; manatee, *n*=3). Each open circle represents *c* from a subject performing a size discrimination task (squirrel monkey, *n*=6; harbor seal, *n*=6; California sea lion, *n*=5). If subjects showed equal *c*, then the data points appear to the eye as one, even though they are plotted separately. For studies in which subjects performed the same discrimination task with multiple sets of standards (Dehnhardt, 1994; Dehnhardt and Kaminski, 1995; Hille et al., 2001; Lamb, 1983; Morley et al., 1983), the reported sample size reflects the discrimination tasks – plotted separately – even if the subject was the same. Illustration credit: K. Finch.

1989; Taylor et al., 1983). We found preliminary support for this methodological artifact with the sea otter: thresholds calculated via linear interpolation (see, e.g. Dehnhardt et al., 1998) during MOL training were slightly lower than calculated thresholds during MCS testing. Because the thresholds from other studies were obtained with MOL (Bachteler and Dehnhardt, 1999; Dehnhardt et al., 1997, 1998; Hille et al., 2001), the sea otter's slightly elevated thresholds relative to these species may reflect methodological differences, not true differences in tactile sensitivity.

We base our comparisons in this study on the stable, repeatable performance of a highly trained individual. Other studies describe small inter-subject differences in threshold measurements and attribute these to differences in strategy (see, e.g. Bauer et al., 2012; Dehnhardt and Kaminski, 1995; Dehnhardt et al., 1997). We report similar findings for the human subjects tested in this study. Although we certainly expect to find variation in sea otter tactile sensitivity at the population level, assessing this variation requires research focused on collecting lower resolution data than those we report here.

The sensitive sea otter tactile system likely enables high foraging efficiency for processing hard-shelled prey at the water's surface and for hunting visually cryptic prey in low light conditions under water (Bodkin et al., 2004, 2007; Estes et al., 2003). Additionally, the quick exploration and decision-making demonstrated by the sea otter in this study are consistent with energy-rate-maximizing behavior documented for wild foraging sea otters (Ostfeld, 1982; Thometz et al., 2016a). Thometz et al. (2016a) report that sea otters spend half of their 46–72 s foraging dives traveling to and from prey patches; thus, search time equates to 23–36 s for each foraging dive (Thometz et al., 2016a). In this short time frame, a sea otter must find and capture prey to offset substantial energetic costs of foraging (Yeates et al., 2007), high baseline metabolic demands (Costa and Kooyman, 1982) and additional energetic costs of reproduction, such as providing for a pup (Thometz et al., 2016a,b).

The few documented descriptions of underwater foraging behavior in this species suggest the importance of paws and vibrissae for capture of prey (Hines and Loughlin, 1980; Shimek, 1977), which take shelter infaunally or in high-refuge habitats to avoid detection (Lowry and Pearse, 1973; Raimondi et al., 2015). These prey can show active defense to avoid capture if detected by predators, such as burrowing deeper into the sediment or affixing more tightly to the substrate (e.g. Watanabe, 1983). The combination of sensitive tactile structures in sea otters likely enables quick and accurate abilities to detect prey and interpret whether that prey is worth pursuing. Paws may be especially critical to reach into crevices that a sea otter vibrissal complex is too large to exploit.

Translating these experimental results into predictions of sea otter tactile space is difficult, as artificial stimuli differ from typical prey texture and shape. Sedimentation, vegetation and relief likely make prey discrimination more difficult than in our controlled experimental setting. Notably, however, the thresholds measured in this study correspond to discrimination of objects that differ by the width of standard mechanical pencil lead or less (≤0.5 mm). Prey differ from their micro-habitats by more than this amount, in both size and texture. Additionally, the size difference between prey at which biomass increases is larger than this amount. Thus, both discrimination of prey identity and size should be within tactile discrimination range of foraging sea otters.

The specialized tactile sensitivity in sea otters and the increased paw sensitivity relative to vibrissal sensitivity – both measured behaviorally in this study – coincide with predictions based on brain (Radinsky, 1968) and vibrissal morphology (Marshall et al., 2014). In addition, the measured difference in sensitivity between tactile structures agrees with behavioral observations: wild sea otters use their paws to manipulate and eat prey items at the water's surface, and captive sea otters preferentially use their paws to grasp food and objects (S.M.S., unpublished observations). This pattern is consistent with the sea otter's different decision time between tactile structures: she made quicker decisions with her paw than with her vibrissae. This may result from differences in mechanoreceptor structure, innervation and distribution, or simply from the sea otter's ability to move her paw across the stimuli with more coordination than her entire head.

We can also consider fine-scale aspects of behavioral performance – speed of decision-making and explorative strategy – in the context of patterns demonstrated by other known tactile specialists. These are important when considering the link between structure and function in the sea otter tactile system and interpreting observed foraging patterns in this species.

Decision time and the speed–accuracy trade-off

The sea otter's supra-threshold decision times for either paw or vibrissal discrimination were comparable to those for auditory signal detection in phocids (Sills et al., 2014, 2015), visual discrimination in humans (Kirchner and Thorpe, 2006) and size discrimination in harbor seals (Grant et al., 2013). However, the sea otter's near-threshold decision times were 1.5- to 3-fold faster (Kirchner and Thorpe, 2006; Sills et al., 2014, 2015). At the extreme, the sea otter performed at least 15-fold faster than manatees in a comparable texture discrimination task across all tested levels (Bauer et al., 2012). This means that the sea otter achieved similar accuracy more quickly than these other species when using either her paw or her vibrissae near threshold, and more quickly than the manatees for the task in general.

Even when directly comparing the sea otter with the human subjects in this study, the sea otter maintained quicker decisions with her paw or her vibrissae than the human subjects with their fingertips. Notably, the sea otter's slowest decision time with her paw (500 ms) was still faster than the quickest decision time for humans (767 ms).

Unlike the sea otter, the human subjects typically compared the stimuli before making a choice. Because we did not restrict the trial length for either species, their similar reported sensitivities do not control for obvious differences in stimulus exploration. If the human subjects were restricted to the same explorative time chosen by the sea otter, we would expect a substantial decrease in performance. Lamb (1983) reported a 60% decrease in mean performance when human subjects were restricted to 300 ms stimulus contact time, similar to or greater than the sea otter's mean contact time in this study, instead of 1200 ms. This restricted time is still faster than the human subjects' mean contact times in this study. We found support for the influence of explorative time on sensitivity measurements, because the human subject with the slowest mean decision time (KC; 13,572 ms) had the lowest calculated threshold (i.e. better sensitivity), and the human subject with the fastest mean decision time (JY; 1007 ms) had the highest calculated threshold (i.e. poorer sensitivity).

Sensory perception is a trade-off between speed and accuracy (see, e.g. Fitts, 1966; Wickelgren, 1977). Star-nosed moles represent the mammalian threshold for processing tactile information, making decisions to attack prey in 25 ms, but they must correct erroneous directional movements one-third of the time (Catania and Remple, 2005). In psychophysical tests, improved accuracy with increased explorative time or successive comparisons has been demonstrated in harbor seals performing size discriminations (Dehnhardt and Kaminski, 1995) and humans performing texture discriminations (Sinclair and Burton, 1991). As difficulty increases, subjects require longer decision times (Bachteler and Dehnhardt, 1999; Bauer et al., 2012; Dehnhardt and Dücker, 1996); however, the presence or intensity of this response can vary by individual even on the same task (Dehnhardt and Kaminski, 1995; Hille et al., 2001).

Explorative strategy

In this study, the sea otter consistently employed a quick and decisive strategy, in which she relied on memory of the standard's absolute properties instead of relative properties of the standard and S−. This strategy reduced the 2AFC discrimination paradigm into a less-sensitive go/no-go procedure. This tendency has been documented in harbor seals (Dehnhardt and Kaminski, 1995; Grant et al., 2013), manatees (Bachteler and Dehnhardt, 1999; Bauer et al., 2012) and squirrel monkeys (Hille et al., 2001) on similar tactile discrimination tasks.

The sea otter's propensity to contact the stimuli with her shorter, rostrally oriented microvibrissae instead of her longer macrovibrissae is similar to vibrissal use in pinnipeds during the identification stage of tactile discrimination tasks (Dehnhardt, 1990, 1994; Grant et al., 2013; Kastelein and van Gaalen, 1988). However, the sea otter's lack of lateral movements differed from other species. Lateral movements have been reported as optimal for feeling texture (Lederman and Klatzky, 1990, 1993; Morley et al., 1983) and were used frequently by the humans in this study and by squirrel monkeys, manatees and rats performing texture discrimination in other studies (Bachteler and Dehnhardt, 1999; Carvell and Simons, 1990; Hille et al., 2001). The explorative strategy used by the sea otter in this study provides an interesting case study; however, because inter-individual differences in strategy have been documented in other species, further generalizations should be avoided.

Future directions

This study highlights how a behavioral approach can address questions about tactile cues relevant for prey capture in the wild. For example, this study focused on active touch, yet sea otters may use hydrodynamic information while foraging for burrowed invertebrates, similar to harbor seals' ability to detect simulated benthic flatfish breathing currents (Niesterok et al., 2017). Although sea otter vibrissae seem morphologically adapted to active touch rather than passive touch required for hydrodynamic detection, this may not preclude sea otters from detecting water currents emitted by prey as a byproduct of respiration. Further behavioral experiments should assess whether sea otter hydrodynamic detection thresholds fall within these typical flow rates.

With respect to temperature, sea otters must retain sensory function in cold habitats – sea surface temperatures reach −3°C in their Alaskan range (NOAA National Data Buoy Center, https://www.ndbc.noaa.gov/). Similar to other marine mammals (Hyvärinen, 1989; Hyvärinen et al., 2009; Ling, 1966; Marshall et al., 2006; McGovern et al., 2015), sea otter vibrissae have an elongated upper cavernous sinus, which may serve as thermal protection (Marshall et al., 2014) to retain heat in these peripheral sensory structures (Dehnhardt et al., 1998, 2003; Erdsack et al., 2014).

We are currently investigating thermal adaptations in sea otter paws, and we predict that substantial blood flow is directed to the mechanoreceptors. Notably, thermographic images of wild otters collected in California and Alaska show considerable heat loss from both the vibrissal pads and the paws in air. Investigations of neural and thermoregulatory structures in sea otter paws will assist in interpreting structure–function relationships in this species and in other otter species that differ in diet preferences and primary mode of prey capture. This research is presently ongoing in our laboratory.

Conclusions

This behavioral study describes how a sea otter interacts with textured stimuli using touch. Our results indicate that sea otter paws and vibrissae can be used to discern the fine details of textured surfaces. Tactile sensitivity is generally comparable to that of terrestrial and marine specialists, including humans performing the same experimental task. Paws showed heightened sensitivity relative to vibrissae, but each structure showed similar performance whether in air or under water.

Our interpretations of the sea otter's sensitivity measurements are likely conservative when considering her consistent tendency to choose without comparing stimuli and different psychophysical methods used to evaluate other tactile specialists. Thus, these results may underestimate the true capabilities of the sea otter tactile system relative to other species. Additionally, determining the extent to which these abilities may be derived in sea otters is difficult given the present lack of information about tactile sensitivity in species not traditionally viewed as tactile specialists, as well as the need to consider other stimuli that are important to aquatic animals.

The significance of this research lies beyond the measurement and comparison of sensory thresholds. Our findings improve the understanding of sensory biology in sea otters and build a mechanistic framework to interpret observed behavior in wild sea otters – such as dive patterns and activity expenditure – especially during foraging for visually cryptic prey species and in low light periods. More broadly, this study contributes to our knowledge of sensory ecology and foraging behavior in air-breathing aquatic vertebrates, including the importance of touch for these top predators.

Acknowledgements

We thank Andrew Johnson, Dr Michael Murray and Karl Mayer at Monterey Bay Aquarium for providing the sea otter and logistical support; Laird Henkel at the Marine Wildlife Veterinary Care and Research Center; and Dr Terrie Williams, Traci Kendall and Beau Richter at the Marine Mammal Physiology Project for providing pool access. We are indebted to the staff and volunteers, past and present, at the Cognition and Sensory Systems Lab; in particular, we thank McKenna Eagan, Michelle Hartwick, Emma Levy, Jake Linsky, Jenna Lofstrom, Colleen Marcus, Ross Nichols, Kirby Parnell, Brandi Ruscher-Hill, Andrew Rouse, K. C. Scofield, Holly Sorenson, Mariah Tengler, Connor Whalen and Jamie Yamashita. Additionally, we thank Steve Weiss for construction of the stimuli and apparatus, Dr Ryan Sills for stimulus calibration, and Drs Gordon Bauer, Guido Dehnhardt and Wolf Hanke for advice on experimental design. Drs Gordon Bauer, Jim Estes, Pete Raimondi, Bruce Lyon and two anonymous reviewers contributed thoughtful comments to the manuscript.

Competing interests

The authors declare no competing or financial interests.

Author contributions

Conceptualization: S.M.S., C.J.R.; Methodology: S.M.S., J.M.S., C.J.R.; Software: S.M.S., M.T.T.; Validation: S.M.S., C.J.R.; Formal analysis: S.M.S., M.T.T.; Investigation: S.M.S., J.M.S., C.J.R.; Data curation: S.M.S.; Writing - original draft: S.M.S.; Writing - review & editing: S.M.S., J.M.S., M.T.T., C.J.R.; Visualization: S.M.S.; Supervision: C.J.R.; Project administration: S.M.S., C.J.R.; Funding acquisition: S.M.S., C.J.R.

Funding

This work was supported by the National Science Foundation Graduate Research Fellowship Program under grant no. NSF DGE 1339067. Research costs were supported in part by the Monterey Bay Aquarium's Conservation Program, as well as small grants from the Friends of Long Marine Lab, the Dr Earl H. Myers and Ethel M. Myers Oceanographic and Marine Biology Trust, and the Ecology and Evolutionary Biology Department at the University of California, Santa Cruz.

Supplementary information

Supplementary information available online at
http://jeb.biologists.org/lookup/doi/10.1242/jeb.181347.supplemental

References

Bachteler, D. and Dehnhardt, G. (1999). Active touch performance in the Antillean manatee: evidence for a functional differentiation of facial tactile hairs. *Zoology* **102**, 61-69.

Bates, D., Mächler, M., Bolker, B. and Walker, S. (2015). Fitting linear mixed-effects models using lme4. *J. Stat. Softw.* **67**, 1-48.

Bauer, G. B., Gaspard, J. C., III, Colbert, D. E., Leach, J. B., Stamper, S. A., Mann, D. and Reep, R. (2012). Tactile discrimination of textures by Florida manatees (*Trichechus manatus latirostris*). *Mar. Mammal Sci.* **28**, E456-E471.

Berta, A. and Sumich, J. L. (1999). Integumentary, sensory, and urinary systems. In *Marine Mammals: Evolutionary Biology*, pp. 130-172. San Diego, CA: Academic Press.

Bodkin, J. L., Esslinger, G. G. and Monson, D. H. (2004). Foraging depths of sea otters and implications to coastal marine communities. *Mar. Mammal Sci.* **20**, 305-321.

Bodkin, J. L., Monson, D. H. and Esslinger, G. G. (2007). Activity budgets derived from time-depth recorders in a diving mammal. *J. Wildl. Manage.* **71**, 2034-2044.

Carvell, G. E. and Simons, D. J. (1990). Biometric analyses of vibrissal tactile discrimination in the rat. *J. Neurosci.* **10**, 2638-2648.

Catania, K. C. (2006). Underwater "sniffing" by semi-aquatic mammals. *Nature* **444**, 1024-1025.

Catania, K. C. and Kaas, J. H. (1997). Somatosensory fovea in the star-nosed mole: behavioral use of the star in relation to innervation patterns and cortical representation. *J. Comp. Neurol.* **387**, 215-233.

Catania, K. C. and Remple, F. E. (2004). Tactile foveation in the star-nosed mole. *Brain. Behav. Evol.* **63**, 1-12.

Catania, K. C. and Remple, F. E. (2005). Asymptotic prey profitability drives star-nosed moles to the foraging speed limit. *Nature* **433**, 519-522.

Catania, K. C., Hare, J. F. and Campbell, K. L. (2008). Water shrews detect movement, shape, and smell to find prey underwater. *Proc. Natl. Acad. Sci. U. S. A.* **105**, 571-576.

Cornsweet, T. N. (1962). The staircase-method in psychophysics. *Am. J. Psychol.* **75**, 485-491.

Costa, D. P. and Kooyman, G. L. (1982). Oxygen consumption, thermoregulation, and the effect of fur oiling and washing on the sea otter, *Enhydra lutris*. *Can. J. Zool.* **60**, 2761-2767.

Dehnhardt, G. (1990). Preliminary results from psychopysical studies on the tactile sensitivity in marine mammals. In *Sensory Abilities of Cetaceans* (ed. J. A. Thomas and R. A. Kastelein), pp. 435-446. New York: Plenum Press.

Dehnhardt, G. (1994). Tactile size discrimination by a California sea lion (*Zalophus californianus*) using its mystacial vibrissae. *J. Comp. Physiol. A* **175**, 791-800.

Dehnhardt, G. and Dücker, G. (1996). Tactual discrimination of size and shape by a California sea lion (*Zalophus californianus*). *Anim. Learn. Behav.* **24**, 366-374.

Dehnhardt, G. and Kaminski, A. (1995). Sensitivity of the mystacial vibrissae of harbour seals (*Phoca vitulina*) for size differences of actively touched objects. *J. Exp. Biol.* **198**, 2317-2323.

Dehnhardt, G. and Mauck, B. (2008). Mechanoreception in secondarily aquatic vertebrates. In *Sensory Evolution on the Threshold: Adaptations in Secondarily Adapted Vertebrates* (ed. J. G. M. Thewissen and S. Nummela), pp. 295-314. Berkeley, CA: University of California Press.

Dehnhardt, G., Friese, C. and Sachser, N. (1997). Sensitivity of the trunk of Asian elephants for texture differences of actively touched objects. *Z. Saugetierkd.* **62**, 37-39.

Dehnhardt, G., Mauck, B. and Hyvärinen, H. (1998). Ambient temperature does not affect the tactile sensitivity of mystacial vibrissae in harbour seals. *J. Exp. Biol.* **201**, 3023-3029.

Dehnhardt, G., Hyvärinen, H., Palviainen, A. and Klauer, G. (1999). Structure and innervation of the vibrissal follicle-sinus complex in the Australian water rat, *Hydromys chrysogaster*. *J. Comp. Neurol.* **411**, 550-562.

Dehnhardt, G., Hanke, W. and Bleckmann, H. (2001). Hydrodynamic trail-following in harbor seals (*Phoca vitulina*). *Science* **293**, 102-104.

Dehnhardt, G., Mauck, B. and Hyvärinen, H. (2003). The functional significance of the vibrissal system of marine mammals. In *The Merkel Cell* (ed. K. I. Baumann, Z. Halata and I. Moll), pp. 127-135. Berlin, Heidelberg: Springer.

Denwood, M. J. (2016). runjags: an R package providing interface utilities, model templates, parallel computing methods and additional distributions for MCMC models in JAGS. *J. Stat. Softw.* **71**, 1-25.
Elliott Smith, E. A., Newsome, S. D., Estes, J. A. and Tinker, M. T. (2015). The cost of reproduction: differential resource specialization in female and male California sea otters. *Oecologia* **178**, 17-29.
Erdsack, N., Dehnhardt, G. and Hanke, W. (2014). Thermoregulation of the vibrissal system in harbor seals (*Phoca vitulina*) and Cape fur seals (*Arctocephalus pusillus pusillus*). *J. Exp. Mar. Biol. Ecol.* **452**, 111-118.
Estes, J. A. and Duggins, D. O. (1995). Sea otters and kelp forests in Alaska: generality and variation in a community ecological paradigm. *Ecol. Monogr.* **65**, 75-100.
Estes, J. A. and Palmisano, J. F. (1974). Sea otters: their role in structuring nearshore communities. *Science* **185**, 1058-1060.
Estes, J. A., Riedman, M. L., Staedler, M. M., Tinker, M. T. and Lyon, B. E. (2003). Individual variation in prey selection by sea otters: patterns, causes and implications. *J. Anim. Ecol.* **72**, 144-155.
Fay, F. H. (1982). *Ecology and Biology of the Pacific Walrus, Odobenus rosmarus divergens*. North American Fauna, no. 74 Washington, DC: US Fish and Wildlife Service.
Fitts, P. M. (1966). Cognitive aspects of information processing: III. Set for speed versus accuracy. *J. Exp. Psychol.* **71**, 849-857.
Fujii, J. A., Ralls, K. and Tinker, M. T. (2015). Ecological drivers of variation in tool-use frequency across sea otter populations. *Behav. Ecol.* **26**, 519-526.
Gelatt, T. S., Siniff, D. B. and Estes, J. A. (2002). Activity patterns and time budgets of the declining sea otter population at Amchitka Island, Alaska. *J. Wildl. Manage.* **66**, 29-39.
Gellermann, L. W. (1933). Chance orders of alternating stimuli in visual discrimination experiments. *J. Genet. Psychol.* **42**, 206-208.
Gescheider, G. A. (1997). *Psychophysics: the Fundamentals*, 3rd edn. Mahwah, NJ: Lawrence Erlbaum Associates.
Gibson, J. J. (1962). Observations on active touch. *Psychol. Rev.* **69**, 477-491.
Ginter, C. C., DeWitt, T. J., Fish, F. E. and Marshall, C. D. (2012). Fused traditional and geometric morphometrics demonstrate pinniped whisker diversity. *PLoS ONE* **7**, 1-10.
Grant, R., Wieskotten, S., Wengst, N., Prescott, T. and Dehnhardt, G. (2013). Vibrissal touch sensing in the harbor seal (*Phoca vitulina*): How do seals judge size? *J. Comp. Physiol. A* **199**, 521-533.
Hanke, W., Wieskotten, S., Marshall, C. and Dehnhardt, G. (2013). Hydrodynamic perception in true seals (Phocidae) and eared seals (Otariidae). *J. Comp. Physiol. A* **199**, 421-440.
Hille, P., Becker-Carus, C., Dücker, G. and Dehnhardt, G. (2001). Haptic discrimination of size and texture in squirrel monkeys (*Saimiri sciureus*). *Somatosens. Mot. Res.* **18**, 50-61.
Hines, A. H. and Loughlin, T. R. (1980). Observations of sea otters digging for clams at Monterey Harbor, California. *Fish. Bull.* **78**, 159-163.
Hughes, B. B., Eby, R., Van Dyke, E., Tinker, M. T., Marks, C. I., Johnson, K. S. and Wasson, K. (2013). Recovery of a top predator mediates negative eutrophic effects on seagrass. *Proc. Natl. Acad. Sci. USA* **110**, 15313-15318.
Hyvärinen, H. (1989). Diving in darkness: whiskers as sense organs of the ringed seal (*Phoca hispida saimensis*). *J. Zool.* **218**, 663-678.
Hyvärinen, H., Palviainen, A., Strandberg, U. and Holopainen, I. J. (2009). Aquatic environment and differentiation of vibrissae: comparison of sinus hair systems of ringed seal, otter and pole cat. *Brain. Behav. Evol.* **74**, 268-279.
Kastelein, R. and van Gaalen, M. (1988). The sensitivity of the vibrissae of a Pacific walrus (*Odobenus rosmarus divergens*) Part 1. *Aquat. Mamm.* **14**, 123-133.
Kastelein, R., Stevens, S. and Mosterd, P. (1990). The tactile sensitivity of the mystacial vibrissae of a Pacific walrus (*Odobenus rosmarus divergens*). Part 2: Masking. *Aquat. Mamm.* **16**, 78-87.
Kirchner, H. and Thorpe, S. J. (2006). Ultra-rapid object detection with saccadic eye movements: visual processing speed revisited. *Vision Res.* **46**, 1762-1776.
Kollmeier, B., Gilkey, R. H. and Sieben, U. K. (1988). Adaptive staircase techniques in psychoacoustics: A comparison of human data and a mathematical model. *J. Acoust. Soc. Am.* **83**, 1852-1862.
Lamb, G. D. (1983). Tactile discrimination of textured surfaces: psychophysical performance measurements in humans. *J. Physiol.* **338**, 551-565.
Lederman, S. J. and Klatzky, R. L. (1990). Haptic classification of common objects: knowledge-driven exploration. *Cogn. Psychol.* **22**, 421-459.
Lederman, S. J. and Klatzky, R. L. (1993). Extracting object properties through haptic exploration. *Acta Psychol.* **84**, 29-40.
Ling, J. K. (1966). The skin and hair of the southern elephant seal, *Mirounga leonina* (Linn.) I. The facial vibrissae. *Aust. J. Zool.* **14**, 855-866.
Lowry, L. F. and Pearse, J. S. (1973). Abalones and sea urchins in an area inhabited by sea otters. *Mar. Biol.* **23**, 213-219.
Marshall, C. D., Amin, H., Kovacs, K. M. and Lydersen, C. (2006). Microstructure and innervation of the mystacial vibrissal follicle-sinus complex in bearded seals, *Erignathus barbatus* (Pinnipedia: Phocidae). *Anat. Rec. Part A* **288A**, 13-25.
Marshall, C. D., Rozas, K., Kot, B. and Gill, V. A. (2014). Innervation patterns of sea otter (*Enhydra lutris*) mystacial follicle-sinus complexes. *Front. Neuroanat.* **8**, 1-8.
McGovern, K. A., Marshall, D. and Davis, R. W. (2015). Are vibrissae viable sensory structures for prey capture in northern elephant seals, *Mirounga angustirostris*? *Anat. Rec.* **298**, 750-760.
Morley, J. W., Goodwin, A. W. and Darian-Smith, I. (1983). Tactile discrimination of gratings. *Exp. Brain Res.* **49**, 291-299.
Newsome, S. D., Tinker, M. T., Gill, V. A., Hoyt, Z. N., Doroff, A., Nichol, L. and Bodkin, J. L. (2015). The interaction of intraspecific competition and habitat on individual diet specialization: a near range-wide examination of sea otters. *Oecologia* **178**, 45-59.
Niesterok, B., Krüger, Y., Wieskotten, S., Dehnhardt, G. and Hanke, W. (2017). Hydrodynamic detection and localization of artificial flatfish breathing currents by harbour seals (*Phoca vitulina*). *J. Exp. Biol.* **220**, 174-185.
Ostfeld, R. S. (1982). Foraging strategies and prey switching in the California sea otter. *Oecologia* **53**, 170-178.
Piersma, T., van Aelst, R., Kurk, K., Berkhoudt, H. and Maas, L. R. M. (1998). A new pressure sensory mechanism for prey detection in birds: the use of principles of seabed dynamics? *Proc. R. Soc. B Biol. Sci.* **265**, 1377-1383.
Plummer, M. (2003). JAGS: A program for analysis of Bayesian graphical models using Gibbs sampling. Proceedings of the 3rd International Workshop on Distributed Statistical Computing (DSC 2003), Technische Universität Wien, Vienna, Austria, 1-8.
Radinsky, L. B. (1968). Evolution of somatic sensory specialization in otter brains. *J. Comp. Neurol.* **134**, 495-506.
Raimondi, P., Jurgens, L. J. and Tinker, M. T. (2015). Evaluating potential conservation conflicts between two listed species: Sea otters and black abalone. *Ecology* **96**, 3102-3108.
Ralls, K., Hatfield, B. B. and Siniff, D. B. (1995). Foraging patterns of California sea otters as indicated by telemetry. *Can. J. Zool.* **73**, 523-531.
Riedman, M. L. and Estes, J. A. (1990). The sea otter (*Enhydra lutris*): behavior, ecology and natural history. *US Fish and Wildlife Service Biological Report* **90**, 1-126.
Shimek, S. (1977). The underwater foraging habits of the sea otter, *Enhydra lutris*. *Calif. Fish Game* **63**, 120-122.
Sills, J. M., Southall, B. L. and Reichmuth, C. (2014). Amphibious hearing in spotted seals (*Phoca largha*): underwater audiograms, aerial audiograms and critical ratio measurements. *J. Exp. Biol.* **217**, 726-734.
Sills, J. M., Southall, B. L. and Reichmuth, C. (2015). Amphibious hearing in ringed seals (*Pusa hispida*): underwater audiograms, aerial audiograms and critical ratio measurements. *J. Exp. Biol.* **218**, 2250-2259.
Sinclair, R. J. and Burton, H. (1991). Tactile discrimination of gratings: psychophysical and neural correlates in human and monkey. *Somatosens. Mot. Res. Res.* **8**, 241-248.
Stebbins, W. C. (1970). Principles of animal psychophysics. In *Animal Psychophysics: The Design and Conduct of Sensory Experiments* (ed. W. C. Stebbins), pp. 1-19. New York, NY: Appleton-Century Crofts.
Stillman, J. A. (1989). A comparison of three adaptive psychophysical procedures using inexperienced listeners. *Percept. Psychophys.* **46**, 345-350.
Taylor, M. M., Forbes, S. M. and Creelman, C. D. (1983). PEST reduces bias in forced choice psychophysics. *J. Acoust. Soc. Am.* **74**, 1367-1374.
Thometz, N. M., Staedler, M. M., Tomoleoni, J. A., Bodkin, J. L., Bentall, G. B. and Tinker, M. T. (2016a). Trade-offs between energy maximization and parental care in a central place forager, the sea otter. *Behav. Ecol.* **27**, 1552-1566.
Thometz, N. M., Kendall, T. L., Richter, B. P. and Williams, T. M. (2016b). The high cost of reproduction in sea otters necessitates unique physiological adaptations. *J. Exp. Biol.* **219**, 2260-2264.
Tinker, M. T., Costa, D. P., Estes, J. A. and Wieringa, N. (2007). Individual dietary specialization and dive behaviour in the California sea otter: using archival time–depth data to detect alternative foraging strategies. *Deep. Res. II* **54**, 330-342.
Tinker, M. T., Bentall, G. and Estes, J. A. (2008). Food limitation leads to behavioral diversification and dietary specialization in sea otters. *Proc. Natl. Acad. Sci. USA* **105**, 560-565.
Tinker, M. T., Guimarães, P. R., Novak, M., Marquitti, F. M. D., Bodkin, J. L., Staedler, M., Bentall, G. and Estes, J. A. (2012). Structure and mechanism of diet specialisation: testing models of individual variation in resource use with sea otters. *Ecol. Lett.* **15**, 475-483.
Vehtari, A., Gelman, A. and Gabry, J. (2017). Practical Bayesian model evaluation using leave-one-out cross-validation and WAIC. *Stat. Comput.* **27**, 1413-1432.
Watanabe, J. M. (1983). Anti-predator defenses of three kelp forest gastropods: contrasting adaptations of closely-related prey species. *J. Exp. Mar. Biol. Ecol.* **71**, 257-270.
Watson, J. and Estes, J. A. (2011). Stability, resilience, and phase shifts in rocky subtidal communities along the west coast of Vancouver Island, Canada. *Ecol. Monogr.* **81**, 215-239.
Wichmann, F. A. and Hill, N. J. (2001). The psychometric function: I. Fitting, sampling, and goodness of fit. *Percept. Psychophys.* **63**, 1293-1313.
Wickelgren, W. A. (1977). Speed-accuracy tradeoff and information processing dynamics. *Acta Psychol.* **41**, 67-85.
Yeates, L. C., Williams, T. M. and Fink, T. L. (2007). Diving and foraging energetics of the smallest marine mammal, the sea otter (*Enhydra lutris*). *J. Exp. Biol.* **210**, 1960-1970.

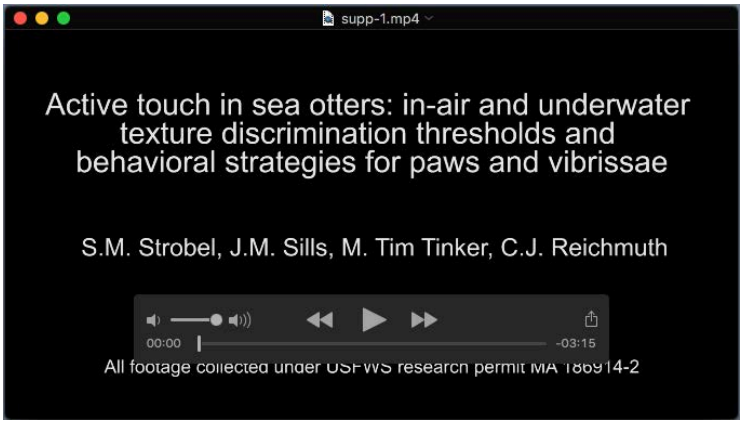

Movie 1. Sea otter's behavioral strategy for paw and vibrissal texture discrimination in air and under water. Video footage of the sea otter interacting with stimulus combinations. For each experimental condition, two trials are shown at full speed and ¼-speed. The sea otter chooses correctly each trial. These trials are representative of her tendencies to explore the right stimulus first and not compare stimuli before making a choice. Video collection authorized under USFWS research permit MA186914-2.

Link to Movie 1: http://movie.biologists.com/video/10.1242/jeb.181347/video-1

Table S1. Means and 95% credible intervals for parameter estimates of Bayesian models.

Model	Parameter	Mean(s)	CI(s)
Paw (grouped air and water)	α_{paw}	***0.29***	***0.23 - 0.34***
Vibrissae (grouped air and water)	$\alpha_{vibrissae}$	***0.51***	***0.42 - 0.63***
	β_{paw}	***7.50***	***1.35 - 20.63***
	$\beta_{vibrissae}$	***6.29***	***1.46 - 14.44***
	λ	***0.013***	***0.00047 - 0.030***
	σ	***0.097***	***0.000078 - 0.23***
Paw (air and water separate)	$\alpha_{paw,\ air}$	***0.26***	***0.19 - 0.34***
Vibrissae (grouped air and water)	$\alpha_{paw,\ water}$	***0.31***	***0.24 - 0.38***
	$\alpha_{vibrissae}$	***0.51***	***0.42 - 0.63***
	$\beta_{paw,\ air}$	***8.07***	***0.82 - 24.1***
	$\beta_{paw,\ water}$	***13.05***	***1.29 - 34.1***
	$\beta_{vibrissae}$	***6.29***	***1.39 - 14.47***
	λ	***0.014***	***0.0003 - 0.032***
	σ	***0.102***	***0.00066 - 0.24***
Paw (grouped air and water)	α_{paw}	0.29	0.23 - 0.34
Vibrissae (air and water separate)	$\alpha_{vibrissae,\ air}$	0.52	0.37 - 0.73
	$\alpha_{vibrissae,\ water}$	0.55	0.39 - 0.78
	β_{paw}	7.63	1.40 - 21.08
	$\beta_{vibrissae,\ air}$	10.09	0.83 - 27.72
	$\beta_{vibrissae,\ water}$	7.53	0.92 - 21.72
	λ	0.013	0.0002 - 0.031
	σ	0.11	0.00032 - 0.25

Paw (air and water separate)	$\alpha_{paw,\ air}$	0.26	0.18 - 0.33
Vibrissae (air and water separate)	$\alpha_{paw,\ water}$	0.31	0.24 - 0.39
	$\alpha_{vibrissae,\ air}$	0.53	0.39 - 0.74
	$\alpha_{vibrissae,\ water}$	0.56	0.39 - 0.79
	$\beta_{paw,\ air}$	8.26	0.98 - 24.94
	$\beta_{paw,\ water}$	13.21	1.13 - 34.12
	$\beta_{vibrissae,\ air}$	10.23	0.87 - 28.04
	$\beta_{vibrissae,\ water}$	7.71	0.81 - 22.43
	λ	0.014	0.00022 - 0.033
	σ	0.12	0.00048 - 0.27
Grouped tactile structures [paw (in air and under water) and vibrissae (in air and under water)]	α	0.39	0.31 - 0.47
	β	4.89	1.88 - 9.27
	λ	0.015	0.00044 - 0.035
	σ	0.31	0.11 - 0.54

The two best-supported models are in bolded italics.

Table S2. Results from GLMM model selection for sea otter strategy: number of discrete exploratory touches, number of stimulus comparisons, and decision time (ms).

Model No.	Intercept	Str_v	Med_{uw}	Str_v x Med_{uw}	$Diff_{nt}$	$Diff_{nt}$ x Str_v	$Diff_{nt}$ x Med_{uw}	AICc	ΔAICc	AIC weight
Number of discrete exploratory touches										
1	***1.05***	***n.i.***	***n.i.***	***n.i.***	***n.i.***	***n.i.***	***n.i.***	***534.23***	***0.00***	***0.78***
2	1.06	0.96	0.96	1.14	n.i.	n.i.	n.i.	540.06	5.83	0.04
3	1.02	1.08	n.i.	n.i.	1.05	0.90	n.i.	540.20	5.97	0.04
4	1.03	1.03	1.02	n.i.	0.99	n.i.	n.i.	540.35	6.12	0.04
5	1.03	n.i.	1.05	n.i.	1.02	n.i.	0.96	540.35	6.12	0.04
6	1.07	0.96	0.96	1.14	0.99	n.i.	n.i.	542.15	7.92	0.01
7	1.004	1.08	1.02	n.i.	1.05	0.90	n.i.	542.27	8.04	0.01
8	1.02	1.02	1.05	n.i.	1.02	n.i.	0.96	542.42	8.19	0.01
9	1.04	1.01	0.96	1.14	1.05	0.90	n.i.	544.08	9.85	0.01
10	1.05	0.96	0.98	1.14	1.02	n.i.	0.96	544.23	10.00	0.01
11	0.99	1.08	1.05	n.i.	1.07	0.90	0.96	544.35	10.12	0.00
12	1.03	1.01	0.98	1.14	1.07	0.90	0.96	546.19	11.96	0.00
Importance		**0.18**	**0.18**	**0.07**	**0.17**	**0.07**	**0.06**			
Number of stimulus comparisons										
1	0.06	0.25	0.25	28	n.i.	n.i.	n.i.	107.4	0.00	0.21
2	0.04	n.i.	n.i.	n.i.	n.i.	n.i.	n.i.	107.6	0.18	0.19
3	0.03	0.94	0.25	28	4.00	0.08	n.i.	107.6	0.19	0.19
4	0.03	~1	~0	7.17e8	3.00	0	4.78e7	108.6	1.20	0.12
5	0.01	6.19	n.i.	n.i.	4.00	0.08	n.i.	109.3	1.85	0.08
6	0.07	0.25	0.25	28	0.86	n.i.	n.i.	109.4	2.02	0.08
7	0.05	0.25	0.39	28	1.50	n.i.	0.4	110.9	3.50	0.04
8	0.01	5.81	1.55	n.i.	4.00	0.08	n.i.	111.0	3.56	0.04
9	0.02	n.i.	2.58	n.i.	1.50	n.i.	0.4	112.6	5.16	0.02
10	0.03	1.55	1.55	n.i.	0.86	n.i.	n.i.	112.8	5.41	0.01
11	0.01	5.58	2.09	n.i.	5.50	0.09	0.55	112.9	5.46	0.01
12	0.02	1.55	2.42	n.i.	1.50	n.i.	0.4	114.3	6.88	0.01
Importance		**0.79**	**0.72**	**0.64**	**0.59**	**0.44**	**0.19**			
Decision time										

1	130.5	1.22	1.95	1.37	0.83	n.i.	n.i.	3127.7	0.00	0.22
2	121.5	1.38	2.13	1.37	0.83	0.85	n.i.	3128.3	0.64	0.16
3	139.2	1.09	1.95	1.23	n.i.	n.i.	n.i.	3128.6	0.89	0.14
4	137.9	1.22	1.82	1.25	0.83	n.i.	1.13	3129.0	1.31	0.12
5	130.1	1.23	2.12	1.24	n.i.	0.86	n.i.	3129.3	1.63	0.10
6	128.3	1.36	2.00	1.26	0.83	0.86	1.11	3130.0	2.21	0.07
7	146.9	1.09	1.82	1.13	n.i.	n.i.	1.12	3130.0	2.26	0.07
8	152.9	n.i.	1.82	1.13	n.i.	n.i.	1.13	3130.3	2.62	0.06
9	137.3	1.23	1.98	1.13	n.i.	0.86	1.12	3130.7	2.99	0.05
10	146.1	1.23	2.09	n.i.	n.i.	0.87	n.i.	3142.7	15.0	1.21e-04
11	184.7	1.23	n.i.	1.33	0.81	n.i.	n.i.	3295.7	168.1	7.18e-38
12	224.0	n.i.	n.i.	n.i.	n.i.	n.i.	n.i.	3297.0	169.3	3.85e-38
Importance		**0.94**	**1.0**	**1.0**	**0.58**	**0.38**	**0.37**			

Fixed ($Diff_{nt}$ = difficulty, near-threshold; Str_{v} = tactile structure, vibrissae; Med_{uw} = testing medium, under water) and interactive effects between the fixed effects were systematically removed to create the suite of models. Models are ranked according to the corrected Akaike information criterion (AICc). The AIC weight of each model and the relative importance of each variable (*i.e.*, the summed AIC weights of each model in which the variable is included) are listed as proportions. All model coefficients have been exponentiated for ease of interpretation. The intercept, therefore, represents the number of touches, stimulus comparisons, or decision time (ms) under the default values of the fixed effects (structure = paw, medium = in air, difficulty = supra-threshold). Other coefficients represent multipliers relative to the default values; "n.i." indicates that the variable was not included in the model. Note that because the expected values are so close to 0, it is possible for the multipliers to be very large or very small. The best supported model for number of discrete exploratory touches, the null model, is bolded and italicized.

Table S3. Results from GLMM model selection for sea otter strategy using her vibrissae: directional explorative touches.

Model No.	Intercept	Med_{uw}	$Diff_{nt}$	$Diff_{nt}$ x Med_{uw}	AICc	ΔAICc	AIC weight
1	1.60	1.40	n.i.	n.i.	373.90	0.00	0.48
2	1.66	1.40	0.93	n.i.	375.71	1.80	0.20
3	1.90	n.i.	n.i.	n.i.	376.13	2.23	0.16
4	1.56	1.56	1.06	0.80	377.11	3.21	0.10
5	1.97	n.i.	0.93	n.i.	377.90	4.00	0.07
Importance		**0.78**	**0.36**	**0.10**			

Fixed ($Diff_{nt}$ = difficulty, near-threshold; Med_{uw} = testing medium, under water) and interactive effects between the fixed effects were systematically removed to create the suite of models. Models are ranked according to the corrected Akaike information criterion (AICc). The AIC weight of each model and the relative importance of each variable (*i.e.*, the summed AIC weights of each model in which the variable is included) are listed as proportions. All model coefficients have been exponentiated for ease of interpretation. The intercept, therefore, represents the number of directional touches under the default values of the fixed effects (medium = in air, difficulty = supra-threshold). Other coefficients represent multipliers relative to the default values; "n.i." indicates that the variable was not included in the model.

Table S4. Results from GLMM and GLM model comparison for human strategy: number of discrete exploratory touches, number of stimulus comparisons, and decision time (ms).

Model No.	Model Type	Intercept	$Diff_{nt}$	$Subj_{DS}$	$Subj_{JY}$	$Subj_{KC}$	$Diff_{nt}$ x $Subj_{DS}$	$Diff_{nt}$ x $Subj_{JY}$	$Diff_{nt}$ x $Subj_{KC}$	AICc	ΔAICc	AIC weight
Number of discrete exploratory touches												
1	***GLM***	***2.33***	***1.18***	***0.74***	***0.77***	***1.74***	***n.i.***	***n.i.***	***n.i.***	***428.97***	***0.00***	***0.87***
2	GLM	2.5	1.03	0.70	0.80	1.45	1.12	0.91	1.40	433.17	4.20	0.11
3	GLMM	2.33	1.18	n.i.	n.i.	n.i.	n.i.	n.i.	n.i.	437.79	8.82	0.11
4	GLMM	2.53	n.i.	n.i.	n.i.	n.i.	n.i.	n.i.	n.i.	437.97	9.00	0.0097
5	GLMM	2.39	1.12	n.i.	n.i.	n.i.	n.i.	n.i.	n.i.	442.41	13.43	0.0011
6	GLM	2.47	1.18	n.i.	n.i.	n.i.	n.i.	n.i.	n.i.	468.52	39.55	2.25e-09
Importance			**0.99**		**0.98**			**0.11**				
Number of stimulus comparisons												
1	***GLM***	***0.77***	***1.36***	***0.83***	***1.03***	***3.41***	***n.i.***	***n.i.***	***n.i.***	***366.91***	***0.00***	***0.90***
2	GLM	0.81	1.23	0.77	1.23	2.92	1.14	0.71	1.30	371.44	4.54	0.09
3	GLMM	1.01	1.36	n.i.	n.i.	n.i.	n.i.	n.i.	n.i.	376.73	9.83	0.007
4	GLMM	1.19	n.i.	n.i.	n.i.	n.i.	n.i.	n.i.	n.i.	378.96	12.05	0.002
5	GLMM	1.06	1.24	n.i.	n.i.	n.i.	n.i.	n.i.	n.i.	382.04	15.14	0.0005
6	GLM	1.20	1.36	n.i.	n.i.	n.i.	n.i.	n.i.	n.i.	432.62	65.71	4.83e-15
Importance			**1.0**		**0.99**			**0.09**				
Decision time												
1	***GLM***	***2391.6***	***1.38***	***1.27***	***0.33***	***4.85***	***n.i.***	***n.i.***	***n.i.***	***2480.3***	***0.00***	***0.86***
2	GLM	2668.3	1.17	1.60	0.36	4.20	0.66	0.88	1.25	2483.9	3.64	0.14
3	GLMM	2857.3	1.38	n.i.	n.i.	n.i.	n.i.	n.i.	n.i.	2560.6	80.3	3.14e-18
4	GLMM	3471.9	n.i.	n.i.	n.i.	n.i.	n.i.	n.i.	n.i.	2570.6	90.3	2.09e-20
5	GLM	4776.6	1.24	n.i.	n.i.	n.i.	n.i.	n.i.	n.i.	2608.5	128.2	1.25e-28

6	GLMM	3319.7	1.08	n.i.	n.i.	n.i.	n.i.	n.i.	n.i.	2628.4	148.1	6.01e-33
Importance			**1.0**		**1.0**			**0.14**				

The fixed effects ($Diff_{nt}$ = difficulty, near-threshold, $Subj_{DS}$ = subject (DS); $Subj_{JY}$ = subject (JY); $Subj_{KC}$ = subject (KC)) were systematically removed to create the suite of models. Models are ranked according to the corrected Akaike information criterion (AICc). The AIC weight of each model and the relative importance of each variable (*i.e.*, the summed AIC weights of each model in which the variable is included) are listed as proportions. All model coefficients have been exponentiated for ease of interpretation. The intercept, therefore, represents the number of touches, number of stimulus comparisons, or decision time (ms) under the default values of the fixed effects (difficulty = supra-threshold, subject = CM). Other coefficients represent multipliers relative to the default values; "n.i." indicates that the variable was not included in the model. Model 3 and Model 5 differed with respect to the random effect—in Model 3, subject was included as a random effect, without an interaction with difficulty; in Model #3, the slope and intercept of each subject's response to difficulty was allowed to vary. The best-supported model for each response variable is in bolded italics.

Table S5. Results from GLMM and LMM model comparisons for sea otter and human: discrete exploratory touches, number of stimulus comparisons, and decision time (ms).

Model No.	Intercept	$Species_{so}$	$Diff_{nt}$	$Diff_{nt}$ x $Species_{so}$	AICc	ΔAICc	AIC weight
Number of discrete exploratory touches (GLMM)							
1	2.54	0.41	n.i.	n.i.	975.46	0.00	0.49
2	2.43	0.41	1.09	n.i.	976.32	0.86	0.32
3	2.34	0.45	1.18	0.84	977.29	1.83	0.20
4	1.61	n.i.	n.i.	n.i.	1031.16	55.70	3.93e-13
5	1.54	n.i.	1.09	n.i.	1032.00	56.50	2.58e-13
Importance		**1.0**	**0.51**	**0.20**			
Number of stimulus comparisons (GLMM)							
1	1.03	1.32	0.04	n.i.	487.68	0.00	0.52
2	1.01	1.36	0.05	0.63	489.09	1.41	0.26
3	1.20	n.i.	0.04	n.i.	489.38	1.70	0.22
4	0.18	1.32	n.i.	n.i.	549.52	61.84	1.94e-14
5	0.21	n.i.	n.i.	n.i.	551.24	63.56	8.21e-15
Importance		**0.78**	**1.0**	**0.26**			
Decision time (LMM)							
1	***2891.33***	***1.35***	***0.0006***	***98.37***	***7439.8***	***0.00***	***0.97***
2	2795.32	1.41	0.066	n.i.	7447.0	7.23	0.026
3	3431.33	n.i.	0.065	n.i.	7487.6	47.82	4.03e-11
4	720.11	1.39	n.i.	n.i.	7529.8	89.97	2.84e-20
5	876.76	n.i.	n.i.	n.i.	7569.3	129.46	7.51e-29
Importance		**1.0**	**1.0**	**0.97**			

The fixed effects ($Diff_{nt}$ = difficulty, near-threshold; $Species_{so}$, sea otter) and interactive effects between the fixed effects were systematically removed to create the suite of models. Models are ranked according to the corrected Akaike information criterion (AICc). The AIC weight of each model and the relative importance of each variable (*i.e.*, the summed AIC weights of each model in which the variable is included) are listed as proportions. All model coefficients have been exponentiated for ease of interpretation. The intercept, therefore, represents the number of touches, stimulus comparisons, or the decision time (ms) under the default values of the fixed effects (species = human, difficulty = supra-threshold). Other coefficients represent multipliers relative to the default values; "n.i." indicates that the variable was not included in the model. Note that because the expected value for sea otter is much smaller than that for human, the multipliers can be very large or very small. The best supported model for decision time, the saturated model, is bolded and italicized.

CHAPTER 3

ANATOMICAL PERSPECTIVE ON THE SENSE OF TOUCH IN SEA OTTERS: MECHANORECEPTORS AND STRUCTURAL FEATURES OF GLABROUS SKIN

ABSTRACT

Sea otters (*Enhydra lutris*) are touch specialists that demonstrate rapid and accurate sensitivity using their front paws and facial vibrissae. Previous anatomical investigations of underlying neural organization in the sea otter vibrissal bed and somatosensory cortex coincide with recently measured abilities, but no studies have described sensory receptors in the paws or other regions of glabrous skin. In this study, we use a histological approach to assess the presence, density, and distribution of mechanoreceptors in the glabrous (*i.e.*, hairless) skin of sea otter paws, nose (*i.e.*, rhinarium), lips and flipper digits. We complement this approach with standard electron microscopy to describe skin surface texture and its effect on the transduction of mechanical stimuli. Our results confirm the presence of Merkel cells and Pacinian corpuscles, but not Meissner corpuscles, in all sea otter glabrous skin. The paws showed the highest density of Merkel cells and Pacinian corpuscles. Within the paw, relative densities of both mechanoreceptor types were highest in the distal metacarpal pad and digits, which suggests that this area serves as a tactile fovea for sea otters. In addition to an increased receptor density, the paw displayed the thickest epidermis. Rete ridges (epidermal projections into the dermis) and dermal papillae (dermal projections into the epidermis) were developed across all glabrous skin structures. These quantitative and qualitative descriptions of neural organization and physical features coincide with observations of tactile exploratory behavior in captive and wild sea otters. Our findings, when combined with previous anatomical and behavioral

results, contribute to a holistic understanding of how aquatic predators can use the sense of touch to detect and capture visually cryptic prey.

INTRODUCTION

As the interface between an organism and the external environment, sensory systems mediate appropriate behavior. Across taxa, evolutionary processes have tuned neural systems to function efficiently within common tradeoffs. Interspecific variation in foraging ecologies (Brenowitz 1980; Martin 2007) and predation risk (Guillemain, Martin, & Fritz, 2002) are often reflected in associated peripheral and central nervous structures. Even within a single species and a single sensory modality, variation in density or type of neural organization can directly correspond to variation in sensory perception. For example, the retinas of raptors have two distinct areas of acute vision, or visual foveas, which cooperate to allow for acuity during prey pursuit over a long distance and binocular vision for prey capture over a short distance (Tucker 2000a, b; Tucker et al. 2000). The star-nosed mole has acute tactile perception with its nose appendages (*i.e.*, rays), but a single ray serves as the tactile fovea; this ray boasts the highest innervation density and neural allocation in the somatosensory cortex, and the mole preferentially uses it to explore objects with touch (Catania and Kaas 1997).

Sea otters (*Enhydra lutris*) provide an interesting case to examine the links between structure and function for the sense of touch given their prey resources, energetic requirements, and constant heat loss to the aquatic environment. Recent measurements of sensory ability (Strobel et al. 2018) support the long-held suspicion that touch is a specialized sense in these coastal, amphibious mammals (see, *e.g.*, Radinsky 1968a; Kenyon 1969; Riedman and Estes 1990). As shallow divers

distributed along the eastern Pacific, sea otters forage under water for visually cryptic, sessile, hard-shelled benthic invertebrates. Relative to other diving predators, unsuccessful foraging is especially costly for sea otters, since they have one of the highest mass-specific metabolic rates among mammals (Costa and Kooyman 1982), spatial separation between prey capture at depth and consumption at the surface (*e.g.*, Kenyon 1969; Bodkin et al. 2004), and a minimal mammalian dive response (Yeates et al. 2007). Maintenance of peripheral blood flow while diving likely preserves neural function in peripheral sensory organs but expends substantial energy through heat loss across repeated foraging dives.

Sea otters have highly dense fur that conserves heat during in-air activities at the water's surface and provides an effective barrier between skin and seawater while foraging (Williams et al. 1992; Kuhn et al. 2010). However, sea otters have retained regions of glabrous skin, including the nose, lips, ears, and volar surfaces of the forefeet (*i.e.*, paws) and the hindfeet (*i.e.*, flippers). The appearance and surface area of glabrous skin seems reduced for the flippers but highly derived for the paws. The elongated webbed flippers are covered in fur, except at the distal ends, where a single ventral volar pad and a non-retractable dorsal claw occurs for each toe (Pocock 1928; Kenyon 1969). In contrast, the entire palmar surface of each paw is fused, with creased delineations between five digit pads (somewhat reduced between the third and fourth digits), two metacarpal pads, and an ulnar carpal pad (Pocock 1928) (Fig. 1a). Sea otters can move their digits independently even within the fused palmar pads, and they clearly use their paws to dexterously open hard-shelled prey, manipulate

tools, explore objects in their environment, and groom their fur. The claws on sea otter paws are semi-retractable and reduced relative to terrestrial carnivores (Kenyon 1969), in a similar pattern as other amphibious tactile-oriented mammals (Hamrick 2001). They tend to keep their claws relaxed during object exploration and extend them primarily during object manipulation (pers. obs.).

Behavioral measurements of paw and whisker touch sensitivity in sea otters (Strobel et al. 2018) support general predictions based on neural organization in the somatosensory cortex that both touch structures are specialized (Radinsky 1968b). However, sensitivity may differ across the palmar paw, since sea otters preferentially use the upper palmar paw (digits and distal metacarpal pad) to make discrete, rapid touch explorations of texture. Additionally, the extent to which the adjacent glabrous nose and lips contribute to measured whisker sensitivity has not been explicitly tested (Strobel et al. 2018). As the first point of contact between an animal and an approaching stimulus, facial skin, including the nose, lips, and eyelids, can show high innervation and abundant sensory receptors in terrestrial mammals (Montagna et al. 1975; Halata and Munger 1983; Munger and Halata 1983; Abrahams et al. 1987; Halata 1990), even in species that have sensitive whiskers (Silverman et al. 1986; Halata 1990). Although sea otters show differential use of their glabrous skin structures, and the surface anatomies of these structures vary substantially, no studies have examined the underlying sensory architecture in their glabrous skin and its influence on touch ability.

Mechanoreceptors, which range from free nerve endings to highly specialized encapsulated neurons, mediate the wide variety of tactile sensations experienced by mammals. Mechanoreceptors can be highly specialized or more generalized in terms of their response to different types and intensities of mechanical stimuli. Mechanoreceptor types are differentially distributed across the body's skin, and variation in density of each type corresponds with variation in tactile perception (Johansson and Vallbo 1979; Andres and v Düring 1990; Paré et al. 2002). In addition to mechanoreceptor density, skin surface texture and the topography of the epidermal-dermal interface may influence tactile perception by mediating grip strength, transduction of mechanical stimuli, and mechanical properties of the skin (Cartmill 1979; Cauna 1985; Halata 1990; Hamrick 2001). Properties of the external environment can also directly or indirectly affect mechanoreceptor function. Cold ambient temperatures lead to reduced tactile sensitivity in humans (Bolanowski and Verrillo 1982; Verrillo and Bolanowski 1986; Gescheider et al. 1997), which may result from negative effects of temperature on the action potential, signal amplification or transmission, and localized blood flow.

Our previous behavioral approach determined that paw and vibrissal active touch abilities are specialized in sea otters (Strobel et al. 2018). The current study directly complements this behavioral approach to determine how form supports function and contributes to sea otters' efficient foraging behavior. We use histology and standard electron microscopy to assess structural and neural features of the peripheral touch system across four glabrous skin structures in sea otters—nose, lips,

and palmar surfaces of the paws and flippers—with tissues obtained from post-mortem animals. We first determine which mammalian cutaneous mechanoreceptors are represented in sea otters, including an assessment of Merkel cells, Meissner corpuscles, and Pacinian corpuscles. Merkel cells are slowly adapting type-I receptors that have high spatial resolution and detect subtle skin deformations resulting from sustained light touch, such as points, edges and curvature (Iggo and Muir 1969; Johnson 2001). Meissner corpuscles are rapidly adapting touch receptors with poor spatial resolution but high sensitivity for low-frequency vibration and motion perception, which are essential for grip control of objects (Johnson 2001). Pacinian corpuscles are rapidly adapting pressure receptors with poor spatial resolution but extreme sensitivity to high-frequency vibrations, which is essential for indirectly perceiving vibrations transmitted through a tool to the skin (Bell et al. 1994; Johnson 2001). After identification and abundance counts for each mechanoreceptor type, we compare morphology and regional variation in density to that described for other terrestrial and amphibious mammals. We explore the relationship between touch anatomy and touch ability to identify regions of specialized tactile acuity. We further speculate on the function of skin texture and thickness for sensitivity and robustness, and the thermoregulatory implications of increased neural and circulatory investment. Our findings contribute to the fields of sensory biology and foraging ecology by broadening current understanding of how tactile perception mediates predator-prey interactions in an aquatic environment.

MATERIALS AND METHODS

Subjects and Tissue Collection

We obtained tissues from wild adult sea otters humanely euthanized in a clinical setting due to non-neurological health issues (n=3; two males, one female). Tissue collection occurred within 20 minutes of death. For each specimen, we excised the left and right paws at the radiocarpal joint, the rhinarium, the lips, and the left and right second or third flipper digit at the metatarsophalangeal joint and place them in sealed containers on ice. Within 3 h, we removed the integumentary tissue from each structure, including the epidermis, dermis, and subcutaneous tissues superior to the flexor tendons. We further segmented the integumentary tissue from each paw into eight regions of interest (ROIs): five digit pads, two metacarpal pads, and carpal pad, following the natural creases in the pad. We immersed each ROI upon removal in 10% neutral buffered formalin. Collection and use of vertebrate samples were conducted under authorization from the United States Fish and Wildlife Service (Letters of Authorization: 08EVEN00-2016-B-0187 and 08EVEN00-2017-B-0045) with the approval and oversight of the Institutional Animal Care and Use Committee at the University of California Santa Cruz and the Research Oversight Committee at Monterey Bay Aquarium.

Tissue Preparation and Imaging

After fixation, we trimmed 1-2 representative tissues from each ROI along the sagittal plane to fit into standard histology cassettes (2.5 cm x 3 cm). At the

Veterinary Histology Lab at University of California Davis, tissues were embedded in paraffin and cut in 5μm slices in the sagittal plane using a rotary microtome; slices were mounted on glass slides and stained using routine protocols with haematoxylin and eosin (H&E). We obtained two-dimensional images for each tissue at 10x magnification using a Zeiss AxioImager Z2 widefield microscope equipped with a Zeiss AxioCam 506 color camera (Carl Zeiss Microscopy GmbH, Jena, Germany). We stitched the resulting 100+ tiles using Zeiss Zen Pro software to form one composite image per tissue. This composite image was stored as a .czi file to retain tissue scaling and metadata.

In preparation for imaging with standard electron microscopy we sampled a 1x1x1cm section from the remaining digit, rhinarium, lips, and flipper of one otter after four months of fixation in 10% neutral buffered formalin. We washed the samples in 1xPBS and then dehydrated them in a graded ethanol series (30%, 50%, 70%, 80%, 90%, 95%, 100%). We transferred the samples from 100% ethanol into a critical point dryer to replace the ethanol with supercritical-fluid carbon dioxide. Following critical point drying, we mounted the samples, sputter-coated them with gold, and tile-imaged each tissue at 25x or 40x magnification in a FEI Quanta 3D scanning electron microscope. We stitched the tiles to form one composite image per sample.

Tissue Area Measurement

We used a custom macro and manual tracing in Fiji (Schindelin et al. 2012) to calculate total area for each H&E-stained tissue. We first converted the composite

image of the tissue to a grayscale 8-bit image, then used thresholding to assign each pixel into the binary categories of "tissue" or "background." We visually compared the thresholded image to the full-color image to manually adjust our pixel cut-off value. To exclude small pieces of low-quality tissue, we manually traced a contour area around the tissue and summed the area of all traced particles larger than 100 mm. Small holes or tears were present in many tissues as a result of histological processing or natural skin morphologies (*e.g.*, the nostril in the rhinarium). To avoid overestimating surface area for these tissues, we reversed the assignment of "tissue" and "background" in the thresholded image, used the same manually-traced contour area around the tissue, and summed the area of all traced particles smaller than 0.2 mm. We continued to visually compare the thresholded image to the full-color image, and we adjusted the upper size limit of traced particles, as needed, to more accurately reflect the maximum hole size in the tissue. We used a custom R Script to calculate total tissue area as the difference between the summed tissue area and the summed hole area.

In addition to total tissue area, we calculated relevant tissue area for each mechanoreceptor type. Since Merkel cells only occur in the stratum basale of the epidermis, we considered this layer as the relevant tissue. We manually traced a contour line in Fiji along the stratum basale-dermis juncture for each tissue to calculate its curvilinear length. Since Meissner corpuscles and Pacinian corpuscles do not occur in the epidermis, we considered the dermis as the relevant tissue. Since the epidermis had a higher contrast difference with the background than the dermis due to

staining intensities, and thus was easier to threshold accurately, we calculated dermis surface area as the difference of total tissue area and epidermal area. To calculate epidermis area, we followed the same thresholding method described for the total tissue area to assign the epidermis as "tissue" and the rest of the tissue as "background," visually comparing the thresholded image to the full-color image to manually adjust our pixel cut-off value. To exclude small pieces of low-quality tissue and areas of the dermis assigned incorrectly as "tissue," we manually traced a contour area around the epidermis and summed the area of all traced particles larger than a minimum cutoff set manually when examining each tissue. For tissues with epidermal holes or tears, we calculated and subtracted the area of these using the same methods described for the total tissue area.

Mechanoreceptor Morphology and Distribution

A single observer scanned slowly through the tiled image for each tissue to census three mechanoreceptor types that were reliably identifiable based on morphology and staining patterns (Merkel 1875; Halata 1990; Bell et al. 1994; Young et al. 2014): Merkel cells, Meissner corpuscles, and Pacinian corpuscles. However, since we were unable to find any structures resembling typical Meissner corpuscles, the following details apply only to Merkel cells and Pacinian corpuscles.

We report the size of mechanoreceptors as area (mean ± sem) for a subset of Merkel cells (n=967, 38.3%), as well as area and longitudinal length for a subset of Pacinian corpuscles (n=121, 30.6%). We calculated area using the polygon tracing

and oval tools in Zen Pro to trace the outline of the external capsule for each mechanoreceptor type. We calculated longitudinal length by using the straight line tracing tool in Zen Pro to trace the longest axis of the Pacinian corpuscle.

In addition to mechanoreceptor type, we noted if the mechanoreceptor occurred alone or within a cluster (≥2 mechanoreceptors). If within a cluster, we noted the total number of the same mechanoreceptor type associated with the cluster. We also recorded if the mechanoreceptor was closely associated with a rete ridge, a dermal papillae, or neither. We determined the proximal-distal orientation of each tissue of the paw digits *post-hoc* and virtually segmented it into quadrants (distal, distal-medial, proximal-medial, and proximal) to link the position of each mechanoreceptor to its position in a living sea otter at a finer detail than we sampled.

Statistical Analyses

We assessed if density of each mechanoreceptor type varied across structures, within structure, between left and right sides, and along the proximal-distal axis of the digits using GLMM analysis and *post-hoc* custom contrasts. We also assessed if thickness of the epidermis and five skin layers varied across structures, within structure, and between left and right sides. We used R and lme4 (Bates et al. 2015) to perform GLMM analyses that included either structure, section, side, or proximal-distal location as the categorical fixed effect and individual sea otter as the random effect. For all models we included a fixed intercept but random regression coefficients for the fixed effect within sea otter as a random effect. For the side and

proximal-distal models assessed within the paw we nested section within sea otter as the random effect, and for the proximal-distal model assessed within the flipper digit pads we nested slice within sea otter as the random effect to account for our subsampling of each tissue.

For each mechanoreceptor type we used presence and mechanoreceptor proportion as binomial-distributed response variables and density as a Gamma-distributed response variable. For each skin layer and the sum of the skin layers for the epidermis, we used thickness as a Gamma-distributed response variable. We excluded zero data from the density models. To calculate a density for each tissue and mechanoreceptor type we summed counts for each identified mechanoreceptor and divided by the relevant tissue area. To calculate proportion for each quadrant and mechanoreceptor type along the proximal-distal axis in each tissue, we divided the mechanoreceptor count in the quadrant by the total mechanoreceptor count of that type in the tissue.

We used R and multcomp (Hothorn et al. 2008) to test a series of *post-hoc* hypotheses using custom contrasts with equal weighting to compare presence (Supp. Table 1), density (Supp. Table 2), and proportion (Supp. Table 3) for each mechanoreceptor type and to compare thickness for the epidermis and each skin layer separately across structure and section. We did not use custom contrasts for the side model, since we could assess the binary fixed effect within the GLMM. If we received convergence warnings on a model, we used allFit in the lme4 package to assess if model fit differed significantly with different optimizers. If log-likelihoods

for each optimizer were within thousandths of a decimal point, we determined that the optimizer did not influence parameter estimates. To control the family-wise Type 1 error rate given multiple contrasts we used a reversed sequential Bonferroni procedure, which firsts tests the largest p-value within a family of tests at the significance level (Hochberg 1988). If not significant, we tested the next largest p-value within the family at the significance level for that test divided by 2. If not significant, we tested the next largest p-value within the family at the significance level for that test divided by 3, and so on. When the first significant test was reached, we considered all tests with p-values less than that critical value as significant.

RESULTS

Gross Description of Structures and Sections

Although we considered the paw pad as a glabrous skin structure, we did find hair distributed in predictable patterns. Short guard hairs are sparsely distributed at the base of the digit pads and extend into the crease to the upper palm pad (Fig. 1a,b). Longer guard hairs are distributed across the lower half of the lower palm pad and extend into the crease to the carpal pad (Fig. 1a). In the paw, the glabrous surface extends distally past the claws and wraps the distal tips to cover the dorsal side of the distal digits (Fig. 1c). In the flipper this pattern is reversed: the claw extends distally past the glabrous surface, which is entirely volar and separated from the claw with a small margin of hair (Fig. 1d).

During tissue preparation, differences in skin thickness were apparent across structures. The paw sections' thick integuments quickly dulled the scalpel blades and were the most difficult to remove cleanly due to substantial connective tissue to the adjacent sections and the underlying musculature and bones. Measurements of skin layer thickness in H&E stained tissues corresponded with gross differences observed during tissue preparation. The flipper, rhinarium, and paw displayed the five typical mammalian glabrous skin layers (stratum corneum, stratum lucidum, stratum granulosum, stratum spinosum, stratum basale), but the lips lacked the stratum lucidum (Fig. 2). Absolute epidermal thickness was highest in the paw, but thickness of each layer remained proportional across the structures with five epidermal layers (*i.e.*, the paw, flipper, and rhinarium; Fig. 2). Tissues often tore at the hypodermis boundary during histological processing, so we could not reliably quantify how dermal thickness differed across structures.

Epidermal surface texture varied greatly within and across structures (Fig. 3). The paw showed surface texture variation along the proximal-distal axis (Fig. 1a, 3a). The carpal pad comprised consistently sized pegs arranged in transverse ridges along the diagonal axis, which were separated by shallow grooves (Fig. 1a). The palm pads showed short, narrow pegs separated by wide, shallow valleys with no discernable ridge pattern (Fig. 1a). The digits showed dense packing of tall, wide, molariform pegs separated by deep, narrow valleys with no discernable ridge pattern; peg size varied and sometimes one peg contained additional pegged projections (Fig. 1a, 1b, 3a). The surface texture of the paw was consistent with the underlying epidermis

structure, in which well-developed, tightly packed intermediate and limiting ridges resulted in deep, narrow rete ridges and dermal papillae (Fig. 3a).

Flipper pad surface texture was similar to the carpal pad (Fig. 1d, 3b), but at high magnifications, additional microridges were apparent on the surface of the pegs. Surface texture in the flipper was consistent with the underlying epidermis structure, in which well-developed intermediate and limiting ridges formed narrow, shallow rete ridges and wide dermal papillae (Fig. 3b). Rhinarium surface texture comprised relatively smooth skin with slight creasing around its perimeter and the dorsally-oriented nostrils, short, wide, flattened pegs with minimal spacing in the inferior half, and taller, more rounded pegs at a lower density in the superior half (Fig. 3c). Unlike the flipper and paw digit pads, surface texture in the rhinarium was not directly reflected in the underlying epidermis structure. Intermediate ridges, but not limiting ridges, were well developed and formed narrow, wide rete ridges with narrow dermal papillae (Fig. 3c). Lip surface texture comprised smooth skin organized in ridges at a similar height to the skin around the rhinarium's perimeter and nostrils (Fig. 3d), and similar microridges as the flipper digit pad were apparent at high magnifications. Similar to the rhinarium, the smooth surface texture in the lips was not directly reflected in the underlying epidermis structure. Intermediate and limiting ridges were well-developed but formed narrow, shallow rete pegs and dermal papillae (Fig. 3d).

The hair that occurred along the boundaries of structures and paw sections showed typical morphology for guard hair: each hair shaft was surrounded by an internal root sheath, an external root sheath, a glassy membrane, and a perifollicular

connective tissue sheath (Fig. 4). Regardless of structure, each hair follicle was associated with two lobulated sebaceous glands (Fig. 4a), one on either side, and an apocrine sweat gland. Apocrine sweat glands were found in all glabrous skin structures, but only in association with pilosebaceous units. Eccrine sweat glands occurred throughout the dermis of the paw and flipper, but not in the rhinarium or lips. In both the paw and flipper, eccrine sweat glands were inversely associated with pilosebaceous-apocrine units.

Variation in dermal innervation and circulatory structures was apparent across glabrous skin structures during initial observations. Gross dermal innervation appeared substantially higher in the digits, upper palm, and carpal pad of the paw than in the flipper, lips, or rhinarium. We noted similar relative increase of higher circulatory investment in these paw areas, especially in the superficial dermis, which included dense aggregations of arteriovenous anastomoses, capillaries, and glomus bodies.

Gross Description of Mechanoreceptor Types and Distribution

We confirmed the presence of Merkel cells and Pacinian corpuscles based on morphology in sea otter glabrous skin, but we failed to find structures resembling typical Meissner corpuscles. The sea otter Merkel cell showed a characteristic oval shape with a large nucleus and pale-staining cytoplasm (Fig. 5). Merkel cells were located in the basal epidermis, primarily associated with the base of rete pegs (93.6%, 2184/2333 cells) and rarely associated with dermal papillae (0.002%, 5/2333).

Occasionally they were not associated clearly with either rete pegs or dermal papillae (0.06%, 144/2333). We typically found a close spatial association between Merkel cells in the stratum basale and discoid nerve terminals innervated with myelinated afferent nerve fibers in the shallow dermis (Fig. 5b). Merkel cells were occasionally found alone (Fig. 5a), but they were primarily found in clusters (79.4%, Fig. 5b). These clusters ranged in size (7.1 ± 0.28 cells/cluster, range: 2-32). Clusters comprised cells that were either clumped across multiple cell layers of the stratum basale or spread out in line along a single cell layer of the stratum basale (Fig. 5a). Whether clustered or unclustered, the size of individual Merkel cells remained consistent (113.26 ± 1.11 μm^2). Merkel cells tended to be oriented with their long axis parallel to the epidermis and dermis, consistent with descriptions in the literature (Iggo and Andres 1982), although this orientation changed to perpendicular when following the curvature of the basal epidermis along lateral portions of rete pegs. When hair occurred in the glabrous skin, we did not find evidence of Merkel cells associated with the hair follicle.

The sea otter Pacinian corpuscle showed the characteristic morphology described in other mammals: an inner unmyelinated neurite surrounded by concentric nonneuronal lamellae (Fig. 5). Pacinian corpuscles were found both in the shallow dermis and deep in the tissue at the boundary between the dermis and hypodermis. Pacinian corpuscles were often associated with dermal papillae (48.2%, 174/361). Occasionally, they were associated with rete pegs (21.6%, 78/361), or not clearly associated with either rete pegs or dermal papillae (29.9%, 108/361). Pacinian

corpuscles were primarily found unclustered (61.3%, Fig. 5b); when found together, cluster size was low (2.6 ± 0.11 corpuscles/cluster, range: 1-8, Fig. 5b). The sizes of Pacinian corpuscles varied more than Merkel cells, but this variation remained within the same order of relative magnitude (area: 0.0375 ± 0.00512 mm^2, longitudinal length: 0.368 ± 0.0324 mm). Pacinian corpuscles were sometimes oriented perpendicular and parallel to the epidermis.

Our identification and subsequent counts of both mechanoreceptor types were conservative, since we only counted cells or corpuscles that we could confidently identify based on morphology. We found many unmyelinated afferent nerve fibers surrounded by lamellae that resembled the inner core of Pacinian corpuscles. These structures either occurred as a single unit or as a cluster of distinct neurites, each surrounded by lamellae but connected within a single encapsulation that resembled the outer core of a Pacinian corpuscle. We also found structures identical to this description, except they lacked a central unmyelinated afferent nerve fiber. All of these unidentified neural structures tended to be concentrated in the shallow dermis and, similar to overall innervation patterns, showed a qualitatively higher density in the digits, upper palm, and carpal pad of the paw than in the flipper, lips, or rhinarium. We suspect that they comprise free nerve endings, extreme distal ends of Pacinian corpuscles, and encapsulated nerve endings of other mechanical or thermal receptors. These nerve fibers often traced a path from the deep dermis up to the basal epidermis, at which point they continued up either side of the rete peg into the dermal

papillae. All identified mechanoreceptors and unidentified neural structures were closely associated with arteriovenous anastomoses and capillaries (Fig. 5).

Variation in Mechanoreceptor Presence and Density

Merkel cells were present in the majority of tissues for all structures (Fig. 6a). Pacinian corpuscles were present in at least one tissue across all structures; the proportion of tissues with at least one Pacinian corpuscle varied across and within structures from (16.7-100%, Fig. 6b), but this variation was not statistically significant (Supp. Table 1). In contrast to minimal presence-absence patterns, density varied substantially and significantly across structures for both Merkel cells and Pacinian corpuscles (Fig. 7, Supp. Tables 2-3). Merkel density in the paw was significantly higher than in any of the other glabrous skin structures (Fig. 7a). Pacinian density in the paw was significantly higher than in the flipper pad and rhinarium (Fig. 7b). Pacinian corpuscle density was also higher in the paw relative to lips, but since positive density was only found in one replicate, we had low statistical power for this contrast (Fig. 7b). The random effect of sea otter explained 23.7% of the total unexplained variance for Merkel cell density and 14.8% of the total unexplained variance for Pacinian corpuscle density (Supp. Table 3), which suggests that identifying additional predictor variables may improve overall fit of the models to the observed data.

We found no significant effects of laterality (*e.g.*, left or right sides) for presence or non-zero density of Merkel cells or Pacinian corpuscles in the paw or

flipper digit pad (Supp. Tables 4-5). Given the lack of lateral effect for these structures we did not control for left or right side in further analyses of variation in density.

Density varied across sections of the paw pad, with the digits and upper palm showing significantly higher densities for both mechanoreceptor types (Fig. 8, Supp. Table 6). The four longest digits (2, 3, 4, and 5) showed especially high densities, about two-thirds more than other sections in the paw pad. The random effect of sea otter explained 70.9% of the total unexplained variance for Merkel cell density and 60.6% of the total unexplained variance for Pacinian corpuscle density (Supp. Table 6), which suggests that the predictor variables contributed an relatively good fit of the models to the observed data. The distal portions of the five digits showed a significantly higher proportional density for both Merkel cells and Pacinian corpuscles relative to the proximal portions of the digits (Fig. 10, Supp. Tables 7-8). In contrast, proportional density did not significantly vary along the proximal-distal axis in the metacarpal pads, carpal pad, or flipper digit pads (Fig. 10, Supp. Tables 7).

DISCUSSION

The results from this anatomical study complement our behavioral assessment of active touch to enable a more complete understanding of the sense of touch in a semi-aquatic top predator. Densities of Merkel cells and Pacinian corpuscles were greater in the paw than in other glabrous skin areas, which suggests that paws are the primary touch structures in sea otters. Within the paw pad, densities of both

mechanoreceptors increased along the proximo-distal axis, with highest densities in the upper metacarpal pad and the longest four digits. The proximo-distal pattern of increasing mechanoreceptor densities was apparent within the digits and metacarpal pad but absent in the lower metacarpal pad and carpal pad. These results suggest that the distal paw, especially the distal digits, functions as a tactile fovea in sea otters, both for spatial resolution and detection of high-frequency vibrations transmitted to the skin from objects held in the paw (Johnson and Hsiao 1992; Johnson 2001). These areas not only coincide with the behavioral strategy used by a sea otter in controlled measures of texture discrimination (Strobel et al. 2018), but also with the behavior of captive and wild sea otters during tactile exploration, object manipulation, prey handling, and tool-use (Hall and Schaller 1964; Fujii et al. 2015).

The morphologies of Pacinian corpuscles and Merkel cells in sea otters were consistent with those described for other mammals (Merkel 1875; Halata 1990; Bell et al. 1994; Young et al. 2014) and the unnamed Merkel-cell-like structures previously noted in the flipper digit pads of sea otters (Williams et al. 1992). Although the association between Merkel cells and the basal layer of rete pegs was consistent with the typical mammalian pattern, small Pacinian corpuscles occurred frequently in the shallow dermis of sea otters and showed a topographic relation to the epidermis. A similar pattern has been reported for the trunk tip of Asian elephants (Rasmussen and Munger 1996), but the authors note that this is unusual relative to descriptions for marsupials and placental mammals, including humans and primates (Halata 1990). We did not find definitive Meissner corpuscles in sea otter glabrous

skin. This result is not particularly surprising, since Meissner corpuscles have primarily been reported in the palms, footsoles, lips, and oral mucosae of primates, some rodents, marsupials, and elephants (Winkelmann 1964; Ide 1977; Munger and Ide 1988; Tachibana and Fujiwara 1991; Hoffmann et al. 2004; Weissengruber et al. 2006; Verendeev et al. 2015). However, we did find substantial encapsulated and unencapsulated neural structures distributed in the shallow dermis of the paw relative to other glabrous skin areas. These structures resembled Pacinian corpuscles and "Meissner-like" structures described in the trunks of African and Asian elephants (Rasmussen and Munger 1996; Hoffmann et al. 2004) and the footpads of cats and mice (Bolanowski and Pawson 2003; Gonzalez-Martinez et al. 2004), as well as a heterogenous grouping of "simple corpuscles" described in the footpads of raccoons (Munger and Pubols 1972; Rice and Rasmusson 2000) and squirrels (Brenowitz 1980). Consistent with conclusions in these studies, we suspect that the unclassified neural structures in sea otters contribute to tactile sensitivity due to their proximity to the epidermis and close association with rete pegs and dermal papillae. Overall, the combination of dense Merkel cells, shallowly distributed Pacinian corpuscles, and unclassified neural tissue may explain the sensitive touch measured in sea otters (Strobel et al. 2018) despite the absence of defined Meissner corpuscles.

Mechanoreceptor Density and Distribution

Direct comparison of absolute mechanoreceptor densities between the sea otters in this study and species in other studies is difficult and questionably

informative given methodological differences, but we offer a comparison of relative densities and patterns. The proximo-distal increase of mechanoreceptor density in the sea otter paw is qualitatively similar to patterns observed in the hands of humans and non-human primates (Johansson and Vallbo 1979; Kumamoto et al. 1993a; Stark et al. 1998; Paré et al. 2002), the forefeet of cats (Kumamoto et al. 1993b) and the Asian elephant trunk (Rasmussen and Munger 1996). However, Pacinian corpuscles are more evenly distributed across the hand in humans (Johansson and Vallbo 1979), which may relate to the different ways in which sea otters and humans grasp objects. Proximo-distal patterns were less apparent in the graviportal feet of African elephants and the dexterous paws of tree squirrels (Brenowitz 1980; Bouley et al. 2007), which likely reflects the different ways in which sea otters and these species use their extremities to detect tactile cues.

Sea otters show minimal densities of Merkel cells, Pacinian corpuscles, or Meissner-like corpuscles in the rhinarium and lips relative to other species (Halata and Munger 1983; Lacour et al. 1991), which coincide with observations of wild and captive sea otters' tendency to explore objects with the paws first, rarely approaching objects for exploration face first. Nose trauma often results from mating in females and intrasexual aggression in males in the southern sea otter population (Staedler and Riedman 1993). Although nose wounds can contribute substantially as a cause of death in this population (Estes et al. 2003; Kreuder et al. 2003; Chinn et al. 2016), little evidence so far suggests that this is a result of reduced foraging success due to reduced rhinarium skin sensitivity, as would be expected if tactile perception via the

rhinarium were critical for prey detection or capture. Additionally, in controlled measurements of vibrissal tactile sensitivity, a trained sea otter was capable of accurate and quick perception even when her nose and lips did not contact the stimuli (Strobel et al. 2018). These combined observations of sea otter behavior do not discount that the rhinarium and lips process tactile cues, but they do suggest that these structures contribute minimally to specialized touch abilities in sea otters.

Epidermal thickness, texture, and the aquatic environment

In all vertebrates, the epidermis serves as a barrier against abrasions and regulates heat and water flux. The presence of the typical five mammalian skin layers in the paw, flipper pad, and rhinarium in this study is consistent with previous descriptions of sea otter haired skin (Kenyon 1969), but we measured a substantially thicker epidermis that ranged from four to 260 times higher than haired skin. The thickness of epidermal layers in sea otters remained proportional across structures in this study, but the epidermis was absolutely thicker in the upper metacarpal and digit pads relative to other glabrous skin areas. Given the abrasive benthic foraging habitat of sea otters and the extensive anti-predator defenses of their hard-shelled invertebrate prey, this localized superkeratinization may be a defense mechanism to minimize damage to their sensitive paws while capturing and handling prey (Rothman and Lorincz 1963). Superkeratinization is common for locomotory skin in other terrestrial and amphibious mammals footpads, but it has also been reported for the anterior facial skin of the walrus, another amphibious benthic feeder (Fay 1982).

In other mammals epidermal thickness can be negatively correlated with touch specialization (Catania 2000), but this is clearly not a pattern in sea otters (Strobel et al. 2018). Determining whether increased neural investment in the paw is necessary to maintain sensitivity despite increased epidermal thickness, or if increased epidermal thickness is necessary to maintain the sensitivity of the paws given abrasive foraging habitat may be possible, albeit highly difficult, to tease apart in controlled longitudinal captive studies.

Our findings of well-developed rete pegs and dermal papillae in all glabrous skin areas differ from those described for sea otter haired skin (Kenyon 1969). Deep rete pegs may have multiple functions in sea otters. Deep rete pegs can strengthen the epidermal-dermal interface, which may protect the skin from tearing under high shearing forces. Additionally, deep rete pegs and their associated dermal papillae enable neural structures and blood flow to be closer to the skin surface, which likely improves tactile perception. When skin surface texture closely resembles that of the underlying dermis-epidermis interface, as in the sea otter paw, localization and transmission of mechanical stimuli to mechanoreceptors may be improved (Cauna 1985; Hamrick 2001).

Although this study did not focus on assessing thermoregulatory properties of glabrous skin, we did observe qualitative variation across structures that may relate to heat flux in sea otters. We noted a thick subcutaneous fat layer in the paw that was not present in other glabrous skin during tissue preparation and a qualitatively higher circulatory investment across the paw pad, including arteriovenous anastomoses,

capillaries, and glomus bodies. These features likely improve heat retention and vasoconstriction efficiency, respectively, via countercurrent heat exchange (Rothman and Lorincz 1963). However, it is unclear how these features function together to maintain neural function in the paw across thermal gradients. A qualitatively decreased circulatory investment in the glabrous skin of the flipper digit pads, lips, and rhinarium of sea otters may relate to their decreased neural investment and/or suggest that these structures play a minimal role in radiative heat flux.

Both eccrine and apocrine sweat glands were present in sea otter glabrous skin. We noted eccrine sweat glands only in the paw and flipper pads, in which they were distinctly confined to areas where hair did not occur. In human skin eccrine sweat glands dissipate heat, but in the volar pads of terrestrial mammals they primarily improve frictional gripping and tactile sensitivity by moistening the skin (Adams and Hunter 1969; Adelman et al. 1975; Meyer et al. 1990; Meyer and Tsukise 1995; Stumpf et al. 2004). It seems unlikely that sea otters would need to increase skin hydration given their aquatic habitat, so determining whether these eccrine sweat glands are vestigial or functional requires a comparative approach across terrestrial and semiaquatic mustelids. The association of apocrine glands with pilosebaceous units in glabrous skin is consistent with previous reports for sea otter haired skin (Kenyon 1969; Kuhn et al. 2010). In many mammals these glands odorous secretions effective in chemical communication (Mykytowycz 1972), but given that sea otters are not known for territorial scent-marking, the oily secretions from these glands are more likely to serve as waterproofing for the guard hairs.

Future Directions

This study used a sampling design that allowed us to make intraspecific comparisons, but a more intensive serial sectioning approach would allow quantification of absolute mechanoreceptor density and innervation density. These data for adult sea otters would substantially help to place their degree of tactile specialization in a comparative context.

The tradeoff between retention of neural function in the periphery and heat in the core is especially interesting to examine in sea otters, given their high metabolism, amphibious lifestyle, and North Pacific distribution in areas of year-round cold water. Further analyses could examine capillary density and glandular structure in sea otters. In North America sea otters are distinctly split between a subarctic subspecies (*Enhydra lutris kenyoni*) and a temperate subspecies (*Enhydra lutris nereis*), and a comparison between these populations may improve understanding of how different climates drive differential selection in mammalian tactile form and function. Quantifying variation in guard hair density on the palmar pads of the paw (pers. obs.) within and between populations could inform how this variation affects sensitivity to mechanical stimuli and temperature tolerance.

Mechanoreceptor distribution and density has been documented to change as mammals age. Preliminary examinations of the glabrous skin from deceased sea otter fetuses and living young sea otter pups reveal marked difference from our observed distribution of Pacinian corpuscles and skin surface texture (pers. obs.). Since assessing touch ability for fetuses and young pups in controlled settings is impossible

or impractical, investigating the ontogenetic component from an anatomical perspective may help predict how changes in neural organization result in developmental changes in sea otter pup foraging ability.

Conclusions

This study assessed tactile sensitivity in sea otters using a histological approach to describe the morphology, density, and distribution of neural structures in four glabrous skin structures. We confirmed the presence of two common mammalian mechanoreceptors—Merkel cells and Pacinian corpuscles—using morphometric characteristics and failed to confirm the presence of Meissner corpuscles. Variation in relative densities across the paw pad, flipper pad, lips, and rhinarium suggest that the paw is the primary tactile sense organ for sea otters. An increased relative density of mechanoreceptors in the distal paw suggest that this area serves as a tactile fovea and coincides with fine-scale observations of sea otter behavior during object exploration and manipulation. Combined with our previous work on sea otter touch abilities using psychophysical methods, the results from this study support the general conclusion that sea otter paws function as sensitive receptors that can efficiently detect and capture visually cryptic prey, as well as dexterously handle tools and captured prey.

ACKNOWLEDGMENTS

We thank Melissa Miller, Laird Henkel, Francesca Batac, Erin Dodd, and Colleen Young and Angie Reed at California Department of Fish and Wildlife's Marine Wildlife Veterinary Care and Research Center, who first brought our attention to Pacinian corpuscles and provided facilities and resources for sample preparation. We thank Andy Johnson, Michael Murray, Erin Lenihan, and Marissa Young at Monterey Bay Aquarium for sample collection and Lilian Carswell at US Fish and Wildlife Service for assistance with federal authorizations for this research. Many individuals provided advice and offered expertise throughout the long development of this project, including Alan Shabel, Alex Ehrenberg, and Shawn Shirazi at University of California Berkeley; Verena Affolter, Becky Griffey, and Amber Villarreal at Veterinary Histology Lab at University of California Davis, Richard Luong at IDEXX, and Frank Rice at Integrated Tissue Dynamics. Ben Abrams at the Microscopy Center at University of California Santa Cruz was an invaluable source of microscopy support, and Tom Yuzvinsky at the W.M. Keck Center for Nanoscale Optofluidics at University of California Santa Cruz performed the standard electron microscopy. Juliette Linossier and Sarah Santich assisted with histological sample preparation. Tim Tinker, Pete Raimondi, Bruce Lyon, James Estes, and Rita Mehta in the Ecology and Evolutionary Biology Department at University of California Santa Cruz contributed to the interpretation of this research. This work was supported by the Department of Education Graduate Assistance in Areas of National Need Fellowship P200A150100 and the Sea Otter Foundation and Trust.

REFERENCES

Abrahams VC, Hodgins M, Downey D (1987) Morphology, distribution, and density of sensory receptors in the glabrous skin of the cat rhinarium. J Morphol 191:109–114

Adams T, Hunter WS (1969) Modification of skin mechanical by eccrine sweat gland activity properties. J Appl Physiol 26:417–419

Adelman S, Taylor CR, Heglund NC (1975) Sweating on paws and palms: what is its function? Am J Physiol 229:1400–1402

Andres KH, v Düring M (1990) Comparative and functional aspects of the histological organization of cutaneous receptors in vertebrates. In: Zenker W, Neuhuber WL (eds) The Primary afferent neuron: a survey of recent morpho-functional aspects. Plenum Press, New York, NY, pp 1–17

Bates D, Maechler M, Bolker B, Walker S (2015) Fitting linear mixed-effects models using lme4. J Stat Softw 67:1–48

Bell J, Bolanowski S, Holmes MH (1994) The structure and function of Pacinian corpuscles: A review. Prog Neurobiol 42:79–128

Bodkin JL, Esslinger GG, Monson DH (2004) Foraging depths of sea otters and implications to coastal marine communities. Mar Mammal Sci 20:305–321

Bolanowski SJ, Pawson L (2003) Organization of Meissner corpuscles in the glabrous skin of monkey and cat. Somatosens Mot Res 20:223–231 . doi: 10.1080/08990220310001622915

Bolanowski SJ, Verrillo RT (1982) Temperature and criterion effects in a somatosensory subsystem: a neurophysiological and psychophysical study. J Neurophysiol 48:836–855

Bouley DM, Alarcón CN, Hildebrandt T, O'Connell-Rodwell CE (2007) The distribution, density and three-dimensional histomorphology of Pacinian corpuscles in the foot of the Asian elephant (Elephas maximus) and their potential role in seismic communication. J Anat 211:428–435 . doi: 10.1111/j.1469-7580.2007.00792.x

Brenowitz GL (1980) Cutaneous mechanoreceptor distribution and its relationship to behavioral specializations in squirrels. Brain Behav Evol 17:432–453 . doi: 10.1159/000121813

Cartmill M (1979) The volar skin of primates: its frictional characteristics and their functional signif icance. Am J Phys Anthropol 50:497–510

Catania KC, Kaas JH (1997) Somatosensory fovea in the star-nosed mole: Behavioral use of the star in relation to innervation patterns and cortical representation. J Comp Neurol 387:215–233 . doi: 10.1002/(SICI)1096-9861(19971020)387:2<215::AID-CNE4>3.0.CO;2-3

Cauna N (1985) Nature and functions of the papillary ridges of the digital skin. Anat Rec 119:449–468

Chinn SM, Miller MA, Tinker MT, et al (2016) The high cost of motherhood: end-lactation syndrome in southern sea otters (Enhydra lutris nereis) on the central California coast, USA. J Wildl Dis 52:307–318 . doi: 10.7589/2015-06-158

Costa DP, Kooyman GL (1982) Oxygen consumption, thermoregulation, and the effect of fur oiling and washing on the sea otter, Enhydra lutris. Can J Zool 60:2761–2767 . doi: 10.1139/z82-354

Estes JA, Hatfield BB, Ralls K, Ames J (2003) Causes of mortality in California sea otters during periods of population growth and decline. Mar Mammal Sci 19:198–216

Fay FH (1982) Ecology and biology of the Pacific walrus, Odobenus rosmarus divergens, North Amer. U.S. Fish and Wildlife Service, Washington, D.C.

Fujii JA, Ralls K, Tinker MT (2015) Ecological drivers of variation in tool-use frequency across sea otter populations. Behav Ecol 26:519–526 . doi: 10.1093/beheco/aru220

Gescheider GA, Thorpe JM, Goodarz J, Bolanowski SJ (1997) The effects of skin temperature on the detection and discrimination of tactile stimulation. Somatosens Mot Res 14:181–188 . doi: 10.1080/08990229771042

Gonzalez-Martinez T, Germana GP, Monjil DF, et al (2004) Absence of Meissner corpuscles in the digital pads of mice lacking functional TrkB. Brain Res 1002:120–128 . doi: 10.1016/j.brainres.2004.01.003

Guillemain M, Martin GR, Fritz H (2002) Feeding methods, visual fields and vigilance in dabbling ducks (Anatidae). Funct Ecol 16:522–529

Halata Z (1990) Sensory innervation of the hairless and hairy skin in mammals including humans. In: Zenker W, Neuhuber WL (eds) The Primary afferent neuron: a survey of recent morpho-functional aspects. Plenum Press, New York,

NY, pp 19–34

Halata Z, Munger BL (1983) The sensory innervation of primate facial skin. II. Vermilion border and mucosa of lip. Brain Res Rev 5:81–107

Hall KRL, Schaller GB (1964) Tool-using behavior of the California sea otter. J Mammal 45:287–298

Hamrick MW (2001) Morphological diversity in digital skin microstructure of didelphid marsupials. J Anat 198:683–688 . doi: 10.1017/S0021878201007750

Hochberg Y (1988) A sharper Bonferroni procedure for multiple tests of significance. Biometrika 75:800–802

Hoffmann JN, Montag AG, Dominy NJ (2004) Meissner corpuscles and somatosensory acuity: The prehensile appendages of primates and elephants. Anat Rec - Part A Discov Mol Cell Evol Biol 281:1138–1147 . doi: 10.1002/ar.a.20119

Hothorn T, Bretz F, Westfall P (2008) Simultaneous Inference in General Parametric Models. Biometrical J 50:346–363

Ide C (1977) Development of meissner corpuscle of mouse toe pad. Anat Rec 188:49–67

Iggo A, Andres KH (1982) Morphology of cutaneous receptors. Ann Rev Neurosci 5:1–31

Iggo A, Muir AR (1969) The structure and function of a slowly adapting touch corpuscle in hairy skin. J Physio 200:763–796

Johansson RS, Vallbo AB (1979) Tactile sensibility in the human hand: relative and absolute densities of four types of mechanoreceptive units in glabrous skin. J Physiol 286:283–300

Johnson KO (2001) The roles and functions of cutaneous mechanoreceptors. Curr Opin Neurobiol 11:455–461 . doi: 10.1016/S0959-4388(00)00234-8

Johnson KO, Hsiao SS (1992) Neural mechanisms of tactual forma and texture perception. Annu Rev Neurosci 15:227–50

Kenyon K (1969) The sea otter in the eastern Pacific ocean. Washington, D.C.

Kreuder C, Miller MA, Jessup DA, et al (2003) Patterns of mortality in southern sea otters (Enhydra lutris nereis) from 1998-2001. J Wildl Dis 39:495–509

Kuhn RA, Ansorge H, Godynicki S, Meyer W (2010) Hair density in the Eurasian otter Lutra lutra and the Sea otter Enhydra lutris. Acta Theriol (Warsz) 55:211–222 . doi: 10.4098/j.at.0001-7051.014.2009

Kumamoto K, Senuma H, Ebara S, Matsuura T (1993a) Distribution of pacinian corpuscles in the hand of the monkey, Macaca fuscata. J Anat 183:149–154

Kumamoto K, Takei M, Kinoshita M, et al (1993b) Distribution of pacinian corpuscles in the cat forefoot. J Anat 182:23–28

Lacour JP, Dubois D, Pisani A, Ortonne JP (1991) Anatomical mapping of Merkel cells in normal human adult epidermis. Br J Dermatol 125:535–542 . doi: 10.1111/j.1365-2133.1991.tb14790.x

Martin GR (2007) Visual fields and their functions in birds. J Ornithol 148:S547–S562 . doi: 10.1007/s10336-007-0213-6

Merkel F (1875) Tastzellen und Tastkörperchen bei den Hausthieren und beim Menschen. Arch für mikroskopische Anat 636–654

Meyer W, Bartels TI, Tsukise A, Neurand K (1990) Histochemical aspects of stratum corneum function in the feline foot pad. Arch Dermatol Res Res 281:541–543

Meyer W, Tsukise A (1995) Lectin histochemistry of snout skin and foot pads in the wolf and domesticated dog (Mammalia: Canidae). Ann Anat 177:39–49 . doi: 10.1016/S0940-9602(11)80129-9

Montagna W, Roman NA, Macpherson E (1975) Comparative study of the innervation of the facial disc of selected mammals. J Invest Dermatol 65:458–465 . doi: 10.1111/1523-1747.ep12608197

Munger BL, Halata Z (1983) The sensory innervation of primate facial skin. I. Hairy Skin. Brain Res Rev 5:45–80

Munger BL, Ide C (1988) The structure of cutaneous sensory receptors. Arch Histol Cytol 51:1–34

Munger BL, Pubols LM (1972) The sensorineural organization of the digital skin of the raccoon. Brain Behav Evol 5:367–393

Mykytowycz R (1972) The behavioural role of the mammalian skin glands. Naturwissenschaften 59:133–139

Paré M, Smith AM, Rice FL (2002) Distribution and terminal arborizations of cutaneous mechanoreceptors in the glabrous finger pads of the monkey. J Comp Neurol 445:347–359 . doi: 10.1002/cne.10196

Pocock RI (1928) Some external characters of the sea-otter (Enhydra lutris). Proc Zool Soc London 98:983–991

Radinsky LB (1968a) Evolution of somatic sensory specialization in otter brains. J Comp Neurol 134:495–506 . doi: 10.1002/cne.901340408

Radinsky LB (1968b) Evolution of somatic sensory specialization in otter brains. J Comp Neurol 134:495–506 . doi: 10.1002/cne.901340408

Rasmussen LEL, Munger BL (1996) The sensorineural specializations of the trunk tip (finger) of the Asian elephant, Elephas maximus. Anat Rec 246:127–134

Rice FL, Rasmusson DD (2000) Innervation of the digit on the forepaw of the raccoon. J Comp Neurol 417:467–490 . doi: 10.1002/(SICI)1096-9861(20000221)417:4<467::AID-CNE6>3.0.CO;2-Q

Riedman ML, Estes JA (1990) The sea otter (Enhydra lutris): behavior, ecology, and natural history. Biol Rep 90:1–136

Rothman S, Lorincz AL (1963) Defense mechanisms of the skin. Annu Rev Med 14:215–242

Schindelin J, Arganda-Carreras I, Frise E, et al (2012) Fiji: An open-source platform for biological-image analysis. Nat Methods 9:676–682. doi: 10.1038/nmeth.2019

Silverman RT, Munger BL, Halata Z (1986) The Sensory Innervation of the Rat Rhinarium. Anat Rec 210–225

Staedler M, Riedman M (1993) Fatal mating injuries in female sea otters (Enhydra lutris nereis). Mammalia 57:135–139

Stark B, Carlstedt T, Hallin RG, Risling M (1998) Distribution of human Pacinian corpuscles in the hand: A cadaver study. J Hand Surg (British Eur Vol 23B:370–372

Strobel SM, Sills JM, Tinker MT, Reichmuth CJ (2018) Active touch in sea otters: in-air and underwater texture discrimination thresholds and behavioral strategies for paws and vibrissae. J Exp Biol 221:1–14

Stumpf P, Künzle H, Welsch U (2004) Cutaneous eccrine glands of the foot pads of the small Madagascan tenrec (Echinops telfairi, Insectivora, Tenrecidae): skin glands in a primitive mammal. Cell Tissue Res 315:59–70 . doi: 10.1007/s00441-003-0815-0

Tachibana T, Fujiwara N (1991) Mechanoreceptors of the hard palate of the mongolian gerbil include special junctions between epithelia and Meissner lamellar cells: A comparison with other rodents. Anat Rec 231:396–403

Tucker VA (2000a) Gliding flight: drag and torque of a hawk and a falcon with straight and turned heads, an a lower value for the parasite drag coefficient. J Exp Biol 203:3733–3744

Tucker VA (2000b) The deep fovea, sideways vision and spiral flight paths in raptors. J Exp Biol 203:3745–3754

Tucker VA, Tucker AE, Akers K, Enderson JH (2000) Curved flight paths and sideways vision in peregrine falcons (Falco peregrinus). J Exp Biol 203:3755–3763

Verendeev A, Thomas C, Mcfarlin SC, et al (2015) Comparative analysis of meissner's corpuscles in the fingertips of primates. J Anat 227:72–80 . doi: 10.1111/joa.12327

Verrillo RT, Bolanowski SJ (1986) The effects of skin temperature on the psychophysical responses to vibration on glabrous and hairy skin. J Acoust Soc Am 80:528–32 . doi: 10.1121/1.394047

Weissengruber GE, Egger GF, Hutchinson JR, et al (2006) The structure of the cushions in the feet of African elephants (Loxodonta africana). J Anat 209:781–792 . doi: 10.1111/j.1469-7580.2006.00648.x

Williams TD, Allen DD, Groff JM, Glass RL (1992) An analysis of California sea otter (Enhydra lutris) pelage and integument. Mar Mammal Sci 8:1–18

Winkelmann RK (1964) Nerve endings of the North American opossum (Didelphis virginia): A comparison with nerve endings of primates. Am J Phys Anthropol 22:253–258

Yeates LC, Williams TM, Fink TL (2007) Diving and foraging energetics of the smallest marine mammal, the sea otter (Enhydra lutris). J Exp Biol 210:1960–1970 . doi: 10.1242/jeb.02767

Young B, O'Dowd G, Woodford P (2014) Wheater's Functional Histology: A text and colour atlas, 6th edn. Elsevier Churchill Livingstone, Philadelphia, PA

FIGURES

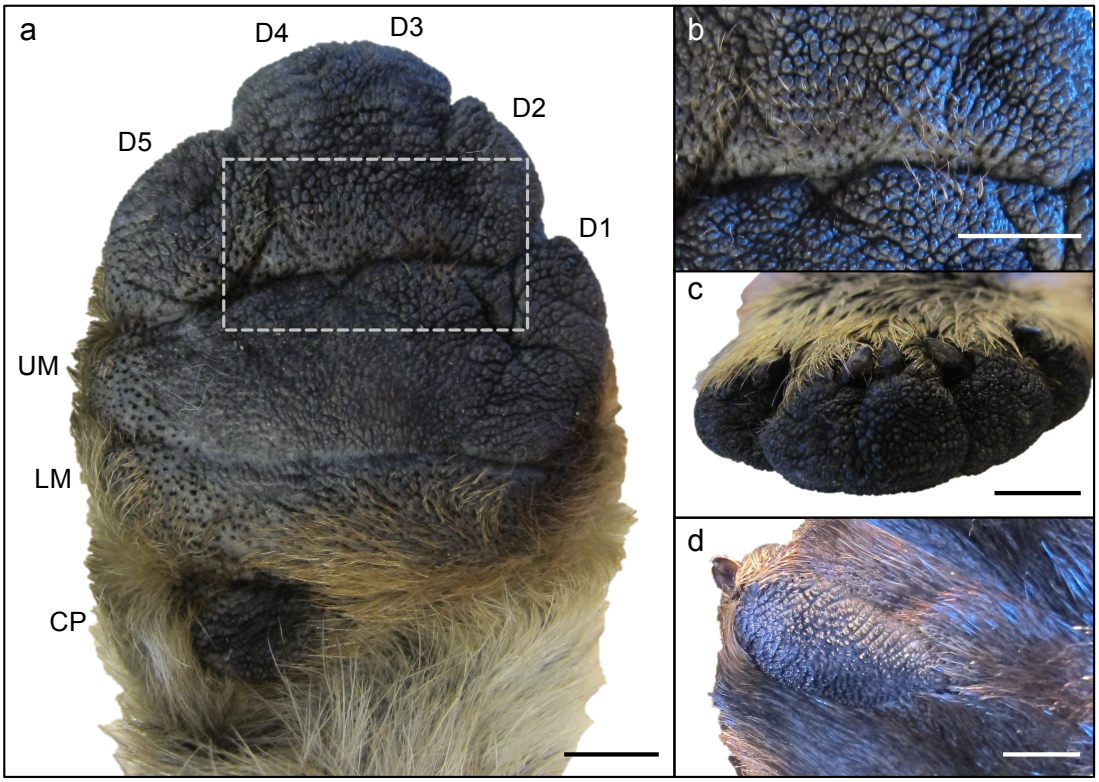

FIGURE 1. Sea otter right paw (a-c) and third digit pad of the right flipper (d); scale bars = 1 cm. (a) The paw comprises a fused palmar surface with eight sections delineated by creasing: ulnar carpal pad (CP), lower metacarpal pad (LM), upper metacarpal pad (UM), and five digits (D1-D5). Hair and hair follicles are distributed across the lower metacarpal pad and in the digit-palmar interface, represented by the boxed area in (a) and the corresponding close-up image in (b). (c) Glabrous skin extends over the digit tips to the base of the semi-retractable claws. Note that the pads of digits 3 and 4 are delineated clearly here, but not on the palmar surface (a). In contrast, a band of hair separates the base of the claw from the digit pad in the flipper (d). The surface texture represented in (a-c) varies along the proximo-distal axis and from that in the digit pad of the flipper (d). Ridges transversed both the carpal and flipper digit pads (a,d). In the paw, skin was pegged and no ridge pattern was discernable in the metacarpal pads and digit pads. The pegs increased in density and height along the proximo-distal axis (a,b).

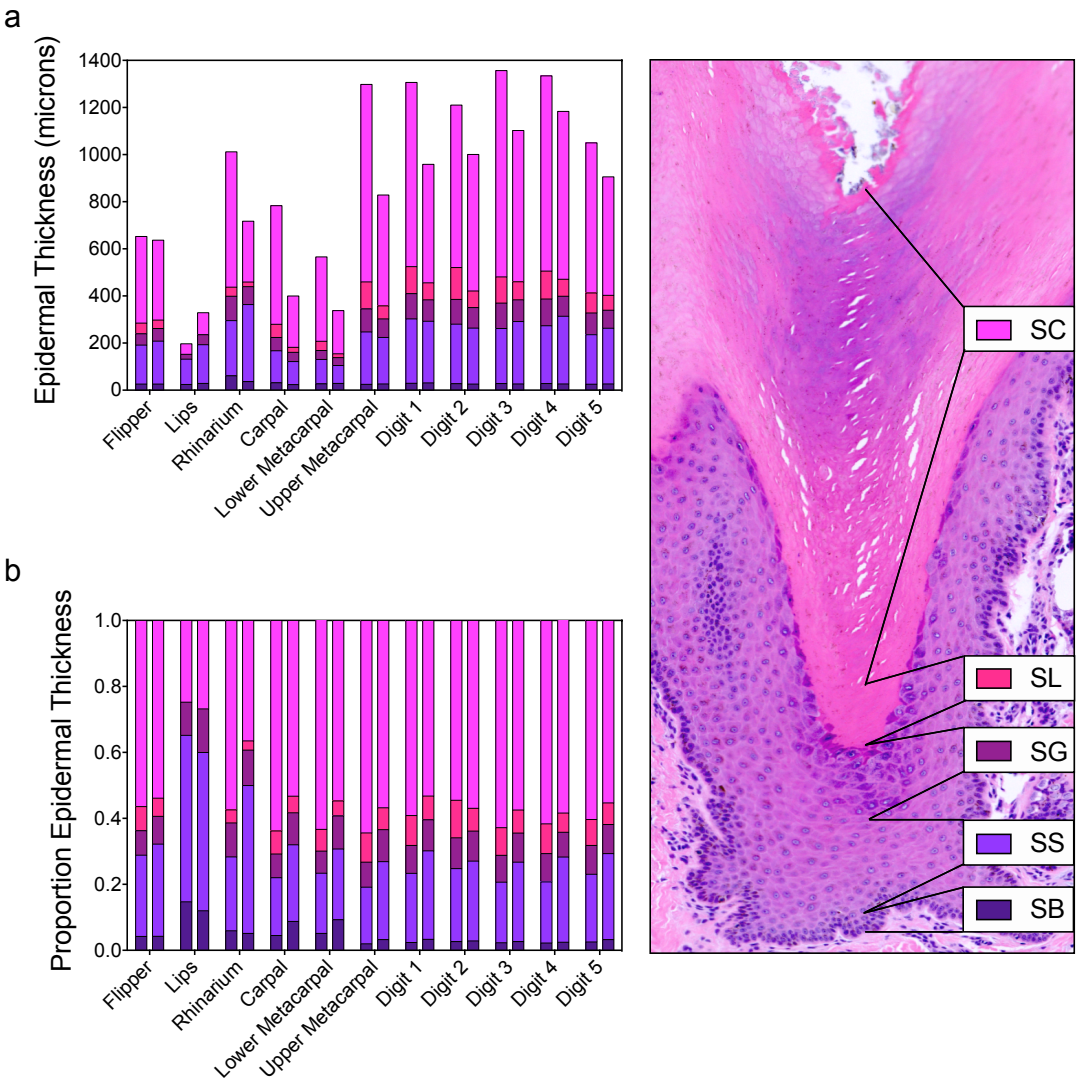

FIGURE 2. Epidermal thickness and proportional thickness of each epidermal layer determined in H&E-stained glabrous skin: stratum corneum (SC), stratum lucidum (SL), stratum granulosum (SG), stratum spinosum (SS), and stratum basale (SB). All layers were present in the flipper, rhinarium, and paw pads, but the stratum lucidum was not apparent in the lips (a,b). The epidermis was thickest in the upper metacarpal and five digits of the paw pad (a), but layer thicknesses were proportional across the flipper, rhinarium, and paw pads (b).

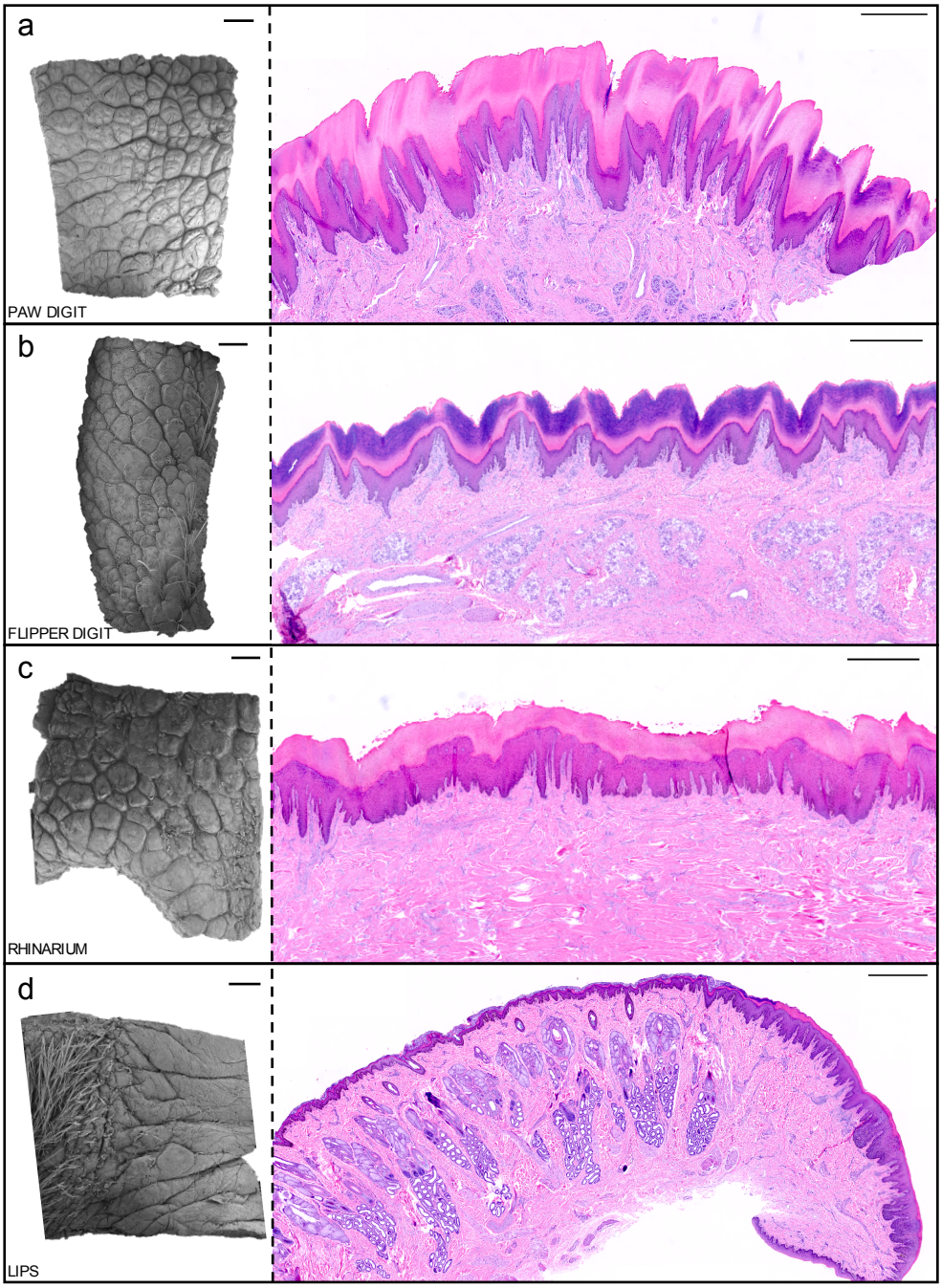

FIGURE 3. Sea otter skin samples from glabrous skin structures—(a) digit 3 of right paw, (b) digit 3 of right flipper, (c) right superior rhinarium, (d) right superior lips—imaged with standard electron microscopy (left panel) and H&E stained and imaged with light microscopy (right panel); scale bars = 1 mm for both image types. Surface texture varied across all structures. (a) In the paw digit pad, tall, narrow, and rounded pegs were densely packed with no discernable ridge pattern. Pegs were often

molariform and contained additional pegged projections. This surface texture was reflected in the underlying epidermis structure (right panel), in which well-developed intermediate and limiting ridges were tightly packed, resulting in deep, narrow rete ridges and dermal papillae. (b) In the flipper digit pad, wide, flat pegs were densely packed and organized in diagonal transverse ridges. This surface texture was reflected in the underlying epidermis structure (right panel), in which well-developed intermediate and limiting ridges formed narrow, shallow rete ridges and wide dermal papillae. (c) In the rhinarium, wide pegs transitioned from short and flat around the nostril perimeter to taller and more rounded in the superior. This surface texture was not directly reflected in the underlying epidermis structure (right panel), in which well-developed intermediate ridges, but not limiting ridges, resulted in narrow and wide rete ridges and narrow dermal papillae. (d) In the lips, smooth skin was organized in ridges perpendicular to the hair boundary, with some shallow transverse creases. The lip ridges were similar in height to the pegs around the nostril perimeter of the rhinarium. This surface texture was not directly reflected in the underlying epidermis structure (right panel), in which well-developed intermediate and limiting ridges resulted in narrow, shallow rete pegs and dermal papillae.

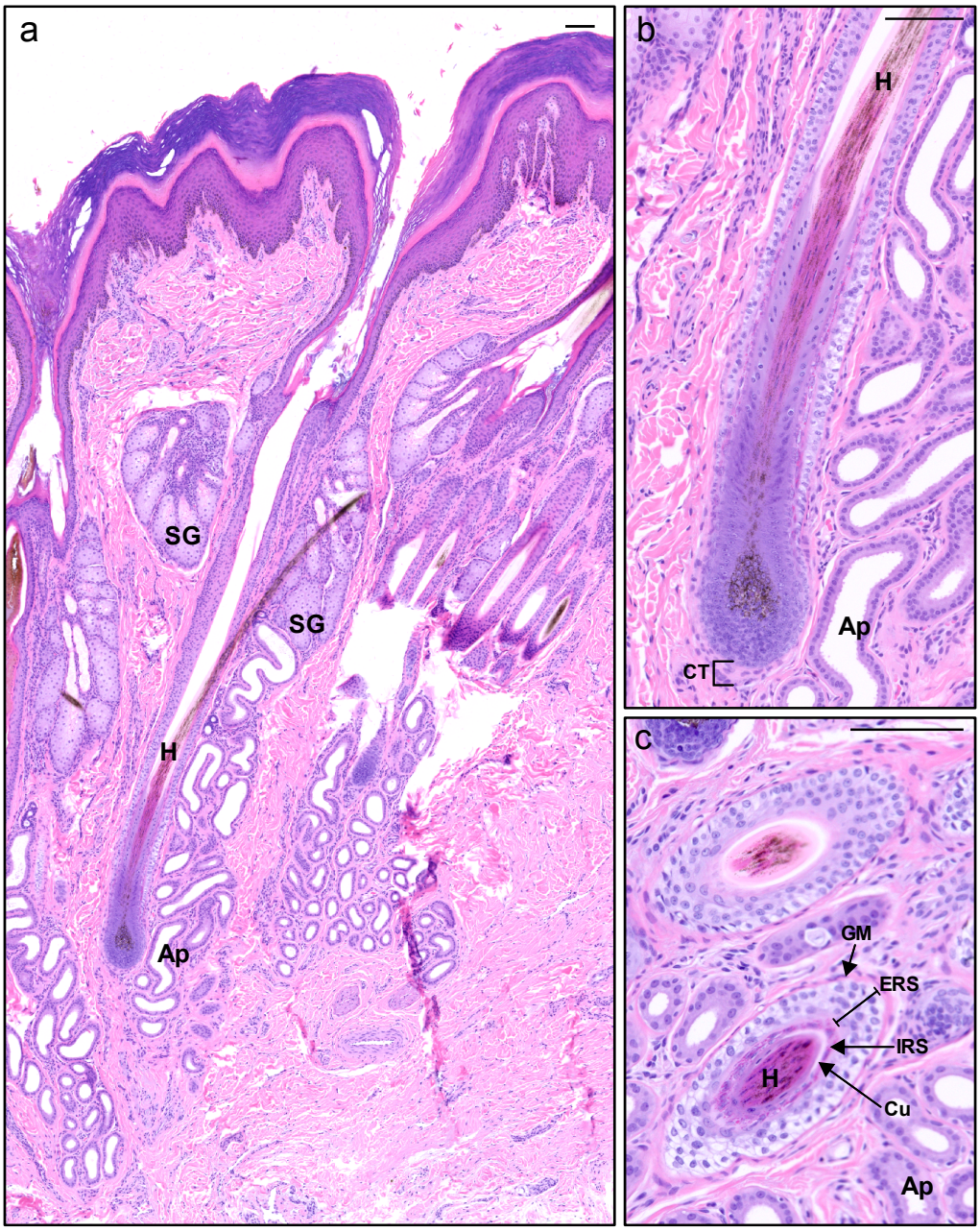

FIGURE 4. Guard hair shaft (H) within hair follicle from H&E-stained glabrous skin: sectioned longitudinally from digit 1 of right paw (a,b) and in cross-section from digit 3 of left flipper (c); scale bars = 100µm. Each hair follicle is associated with two lobulated sebaceous glands (SG) and an apocrine sweat gland (Ap), whose duct empties into the hair follicle. A connective tissue sheath (CT) surrounds the glassy membrane (GM) of the external root sheath (ERS). Moving inwards, the internal root sheath (IRS) surrounds the pale-staining cuticle layer (Cu) that encompasses the hair shaft (H).

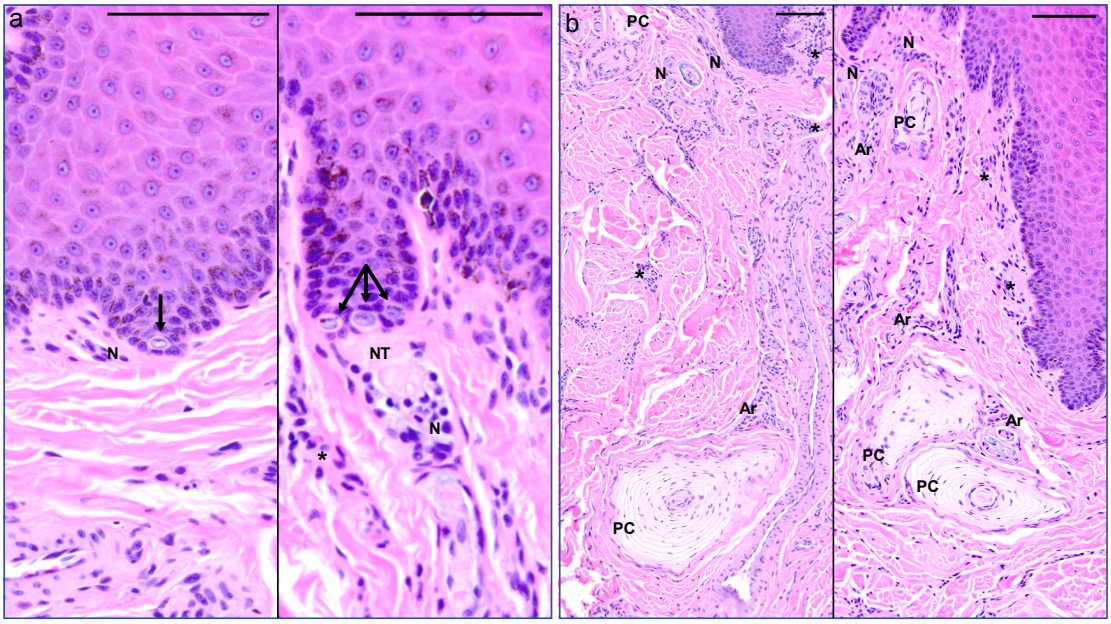

FIGURE 5. H&E-stained tissues from paw digit pad that demonstrate morphology and distribution of Merkel cells (a, arrows) and Pacinian corpuscles (b, PC); scale bars = 100µm. Arteriovenous anastomoses (Ar), capillaries (*), and large myelinated sensory nerves (N), were closely associated with both mechanoreceptor types and extended superficially to the epidermis. (a) Merkel cells (arrows) were distributed along the stratum basale as either solitary cells (left panel) or a cluster (right panel). Often afferent nerve fibers leading to the discoid nerve terminal (right panel, NT) were apparent in the shallow dermis in close association with the Merkel cells. (b) Pacinian corpuscles (PC) were distributed in the deep and shallow dermis as either solitary cells (left panel) or a cluster (right panel).

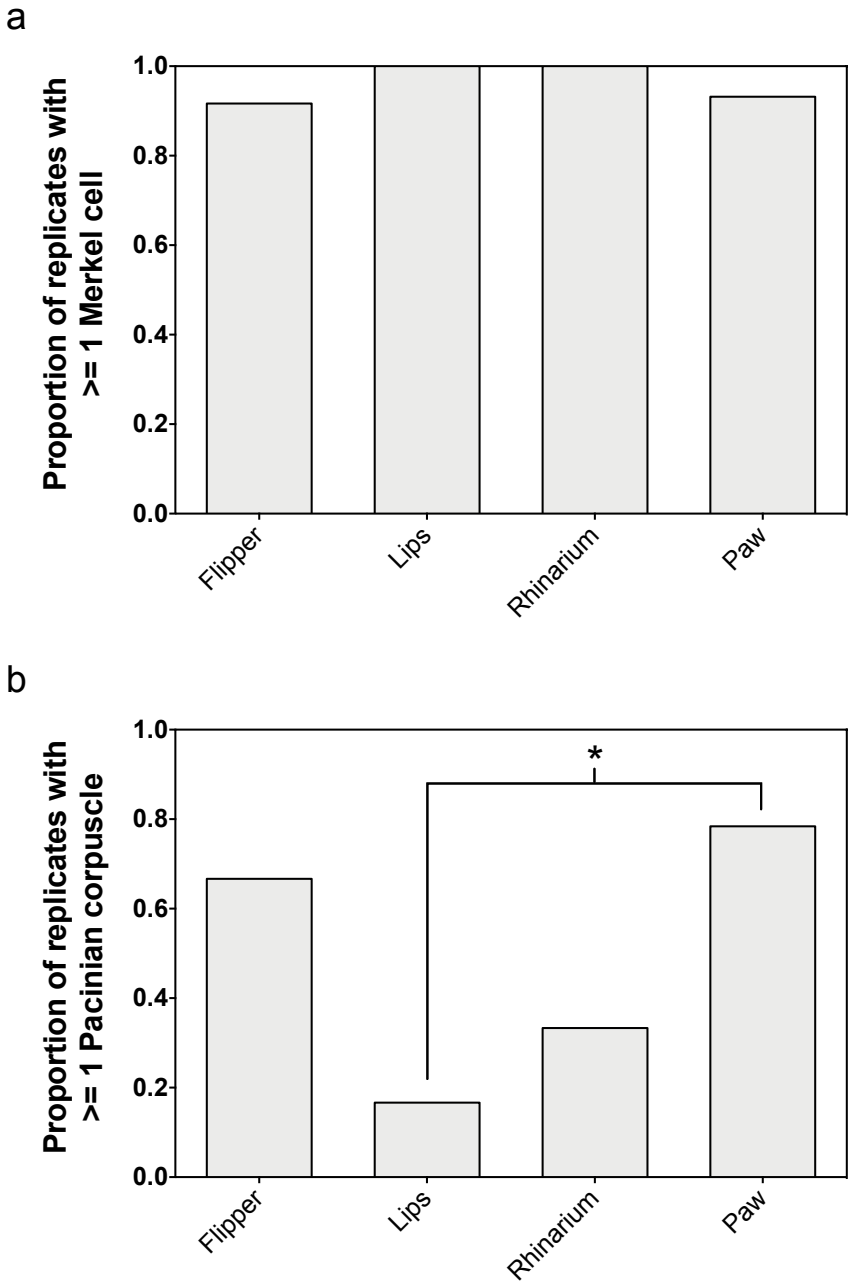

FIGURE 6. Proportion of replicates of each glabrous skin structure summed across sea otters ($n_{flipper}$: 12, n_{lips}: 6, $n_{rhinarium}$: 3, n_{paw}: 88) with positive Merkel cell presence (a) and positive Pacinian corpuscle presence (b). Each mechanoreceptor type was present in at least one replicate from each glabrous skin structure. (a) No significant differences for Merkel cell presence were found across structures. Although Pacinian corpuscles were found in a higher proportion of replicates for the paw pads relative to other glabrous skin structures, this pattern was only significant (*, $p<0.1$) when contrasting the paw to the lips (b).

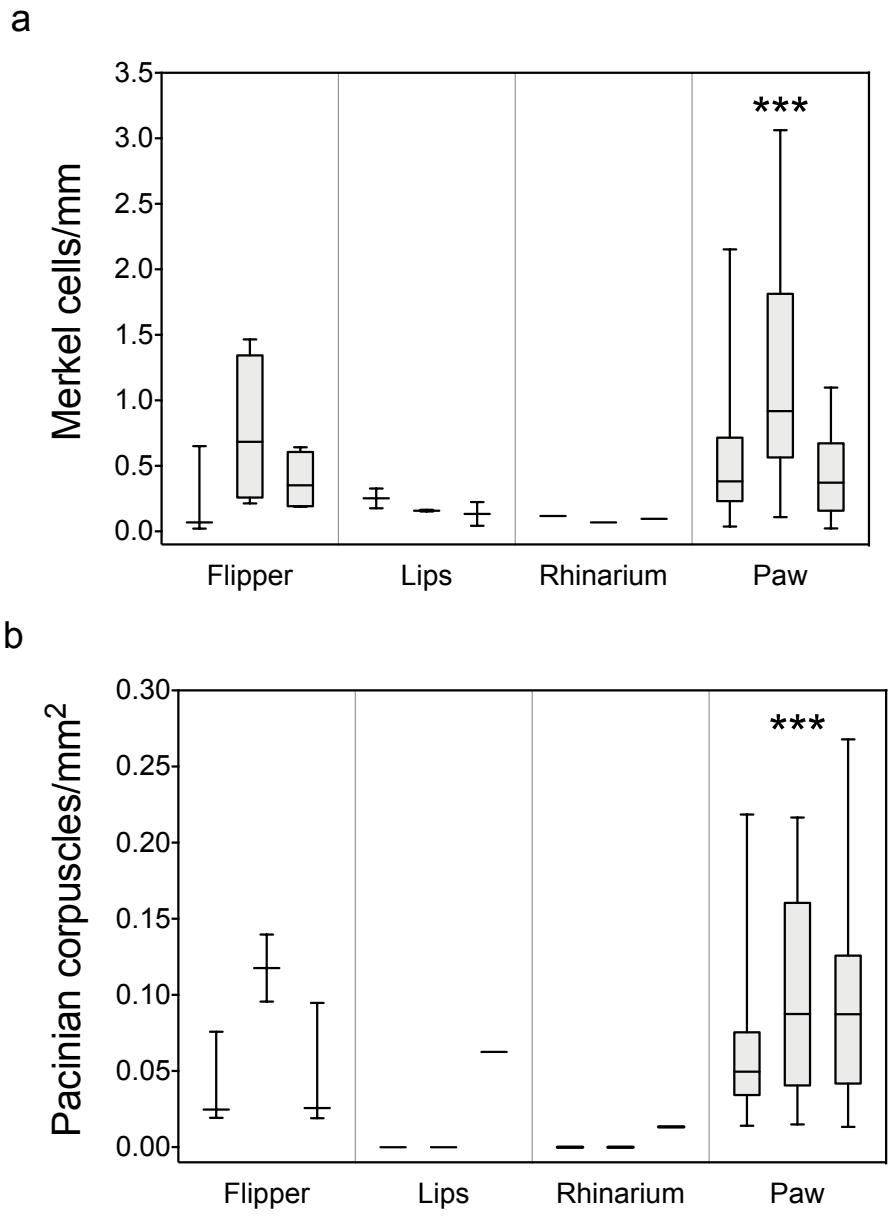

FIGURE 7. Absolute densities of mechanoreceptors across glabrous skin structures with positive density, plotted separately across sea otters. Despite variability in the paw and across sea otters, Merkel cells per mm (a) and Pacinian corpuscles per mm^2 (b) were significantly higher in the paw than in all other structures (***, $p<0.001$).

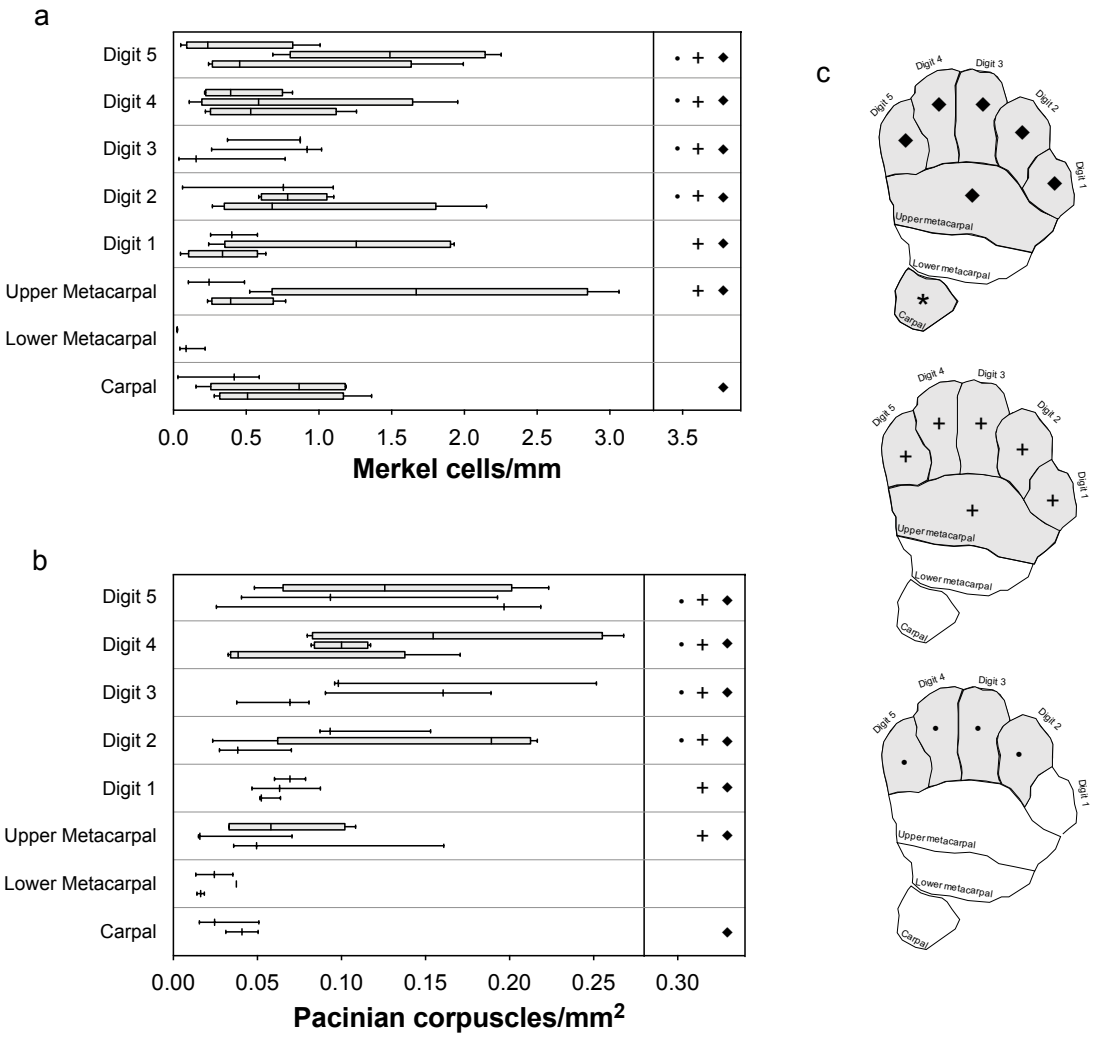

FIGURE 8. Absolute densities of mechanoreceptors across paw pads with positive density, plotted separately across sea otters. Despite variability across sea otters, Merkel cells per mm (a) and Pacinian corpuscles per mm^2 (b) increased significantly along the proximo-distal axis when tested across three contrasts (c). Contrasts, represented by shaded and unshaded regions, are illustrated for the right paw (c), but analyses correspond to combined densities from left and right paws. The density of each mechanoreceptor type was significantly higher in the carpal pad, upper metacarpal pad, and digits when contrasted to the lower metacarpal pad (◆, $p<0.05$), significantly higher in the upper metacarpal pad and digits when contrasted to the lower metacarpal pad (+, $p<0.1$), and significantly higher in digits 2 through 4 when contrasted to the other paw pads (·, $p<0.05$ for Merkel cell density and $p<001$ for Pacinian corpuscle density).

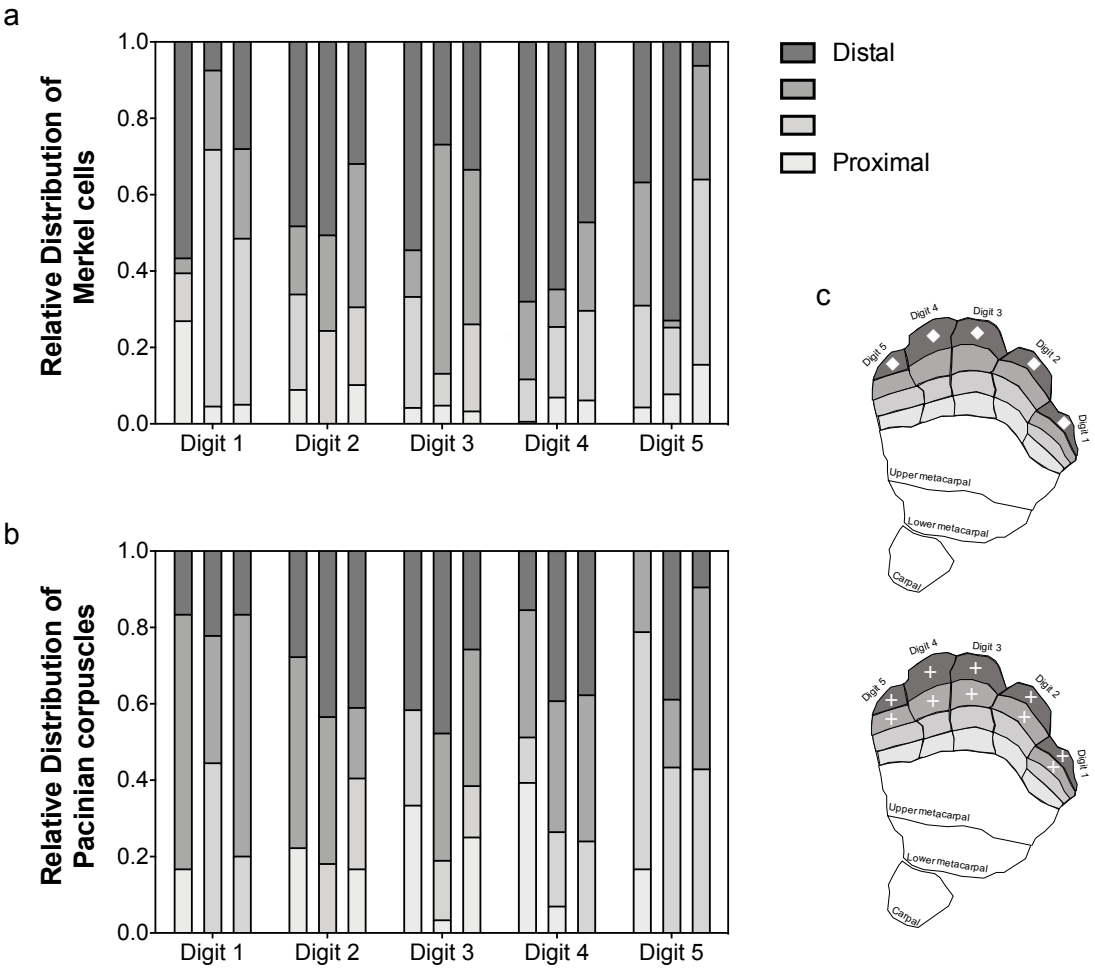

FIGURE 9. Proportional densities of mechanoreceptors across proximal-distal quadrants of paw digit pads (light gray to dark gray shaded regions), plotted separately for individual sea otters. Despite variability across sea otters, relative Merkel cell density (a) and relative Pacinian corpuscle density (b) increased significantly along the proximo-distal axis when tested across two contrasts (c). Contrasts, represented by presence and absence of symbols (◆ and +), are illustrated for the right paw (c), but analyses correspond to combined relative densities from left and right paws. The relative density of each mechanoreceptor type was significantly higher in the most distal digit quadrant when contrasted to the other digit quadrants (◆, $p<0.01$ for Merkel cell relative density and $p<0.05$ for Pacinian corpuscle relative density), and significantly higher in the distal half of the digits when contrasted to the proximal half of the digits (+, $p<0.01$ for Merkel cell relative density and $p<0.001$ for Pacinian corpuscle relative density).

SUPPLEMENTARY INFORMATION

SUPPLEMENTARY TABLE 1. Design of and results from *post-hoc* custom contrasts from GLMM model: presence of Merkel cells (Mk) and Pacinian corpuscles (PC) across and within glabrous skin structures.

Type	Contrast	Estimate	Std. Error	p-value	Adjusted Sig.
Mk	Paw >= Other Structures	-12.046	4333.706	0.876	>0.1/2, n.s.
	Paw >= Lips	-16.970	7568.064	0.876	>0.1/3, n.s.
	Paw >= Rhinarium	-16.981	10732.449	0.875	>0.1/4, n.s.
	Paw >= Flipper	-2.555	2.547	0.996	>0.1, n.s.
	Digits >= Non-digits in paw	23.784	8319.122	0.758	>0.1/2, n.s.
	Upper paw >= Lower paw	20.565	7172.908	0.758	>0.1/3, n.s.
	Digits 2-5 >= Other sections in paw	9.329	10529.779	0.759	>0.1, n.s.
	Other sections in paw >= Lower palm	19.204	6044.466	0.758	>0.1/4, n.s.
PC	Paw >= Other Structures	8.412	124.666	0.8531	>0.1/2, n.s.
	Paw >= Lips	3.376	1.841	0.0968	>0.1/4, n.s.
	Paw >= Rhinarium	22.161	377.760	0.8561	>0.1/3, n.s.
	Paw >= Flipper	-0.0664	1.263	0.8895	>0.1, n.s.
	Digits >= Non-digits in paw	9.103	153.245	0.478	>0.1/2, n.s.
	Upper paw >= Lower paw	8.121	122.597	0.475	>0.1/4, n.s.
	Digits 2-5 >= Other sections in paw	10.648	191.553	0.480	>0.1, n.s.
	Other sections in paw >= Lower palm	6.771	108.806	0.477	>0.1/3, n.s.

The estimate and standard error of the mean difference between contrasts and significance of the difference is reported. ">=" indicates "is greater than" and a one-sided test with significance level $p<0.1$. Adjusted significance represents the significance level based on a reversed sequential Bonferroni procedure to control family-wise Type 1 error. Shading separates each family of test. In this procedure the largest p-value is tested at the significance level, the next largest at half the significance value, the next largest at one-third the significance value, and so on. If a significant value is reached, we reject all other tests with p-values smaller than that value. Significant contrasts and associated adjusted significance levels are bolded.

SUPPLEMENTARY TABLE 2. Design of and results from *post-hoc* custom contrasts from GLMM model: non-zero density of Merkel cells (Mk) and Pacinian corpuscles (PC) across and within glabrous skin structures.

Type	Contrast	Estimate	Std. Error	p-value	Adjusted Sig.
Mk	**Paw >= Other Structures**	1.4374	0.2972	<0.001	**sig.**
	Paw >= Lips	1.2526	0.4203	0.00428	**sig.**
	Paw >= Rhinarium	1.9215	0.5782	0.00134	**sig.**
	Paw >= Flipper	1.1708	0.5366	0.048	**<0.1, sig.**
	Digits >= Non-digits in paw	0.6567	0.3859	0.0917	**<0.1, sig.**
	Upper paw >= Lower paw	1.0241	0.5271	0.0563	**sig.**
	Digits 2-5 >= Other sections in paw	0.8251	0.3770	0.0328	**sig.**
	Other sections in paw >= Lower palm	2.0306	0.9405	0.0354	**sig.**
PC	**Paw >= Other Structures**	1.811	0.331	<0.001	**sig.**
	Paw >= Lips	0.352	0.708	0.6747	>0.1, n.s.
	Paw >= Rhinarium	1.898	0.708	0.0129	**<0.1/2, sig.**
	Paw >= Flipper	3.226	0.0147	<0.001	**sig.**
	Digits >= Non-digits in paw	0.4352	0.2670	0.1481	>0.1, n.s.
	Upper paw >= Lower paw	0.6800	0.3369	0.0675	>0.1/2, n.s.
	Digits 2-5 >= Other sections in paw	1.6495	0.2367	<0.001	**sig.**
	Other sections in paw >= Lower palm	0.7684	0.2968	0.016	**<0.1/3, sig.**

The estimate and standard error of the mean difference between contrasts and significance of the difference is reported. ">=" indicates "is greater than" and a one-sided test with significance level $p<0.1$. Adjusted significance represents the significance level based on a reversed sequential Bonferroni procedure to control family-wise Type 1 error. Shading separates each family of test. In this procedure the largest p-value is tested at the significance level, the next largest at half the significance value, the next largest at one-third the significance value, and so on. If a significant value is reached, we reject all other tests with p-values smaller than that value. Significant contrasts and associated adjusted significance levels are bolded.

SUPPLEMENTARY TABLE 3. Summary of GLMM model output: non-zero density of Merkel cells (Mk) and Pacinian corpuscles (PC) across glabrous skin structures.

Type	Summary of Random and Fixed Effects				
Mk	*Random Effects*				
	Groups	*Fixed Effect within Group*	*Variance*	*Std. Dev.*	
	Otter (n=3)	Flipper	0.0761344	0.27592	
		Lips	0.0008581	0.02929	
		Paw	0.0909663	0.30161	
		Rhinarium	0.0208108	0.14426	
	Residual		0.6072153	0.77924	
	Number of observations: 102				
	Fixed Effects	*Estimate*	*Std. Error*	*t-value*	*Pr(>|z|)*
	Intercept	-0.8127	0.3192	-2.546	**0.0109**
	Lips	-0.8945	0.4699	-1.904	0.0570
	Paw	0.3581	0.2653	1.350	0.1771
	Rhinarium	-1.5634	0.6125	-2.553	**0.0107**
PC	*Random Effects*				
	Groups	*Fixed Effect within Group*	*Variance*	*Std. Dev.*	
	Otter (n=3)	Flipper	0.08313	0.288331	
		Lips	2.746e-07	0.000524	
		Paw	0.006841	0.082708	
		Rhinarium	1.102e-06	0.001050	
	Residual		0.5171	0.719123	
	Number of observations: 79				
	Fixed Effects	*Estimate*	*Std. Error*	*t-value*	*Pr(>|z|)*
	Intercept	-2.82313	0.01040	-271.45	**<2e-16**
	Lips	0.05085	0.70832	0.072	0.9428
	Paw	0.40334	0.01029	39.191	**<2e-16**
	Rhinarium	-1.49427	0.70835	-2.110	**0.0349**

This table lists the variance estimates and standard deviations for the random effects and the estimated coefficients, standard errors, t-values, and significance values for the fixed effects (Flipper, Lips, Paw, Rhinarium). Total unexplained variance is the sum of the residual variance and the variance of the fixed effects within the grouping of otter. The intercept represents the density under the default value of Flipper. Fixed effects with $p<0.05$ are bolded.

SUPPLEMENTARY TABLE 4. Summary of GLMM model output: presence of Merkel cells (Mk) and Pacinian corpuscles (PC) between left and right sides of the paw and flipper digit pads.

Type	Summary of Random and Fixed Effects				
Mk (PAW)	*Random Effects*				
	Groups	*Fixed Effect within Group*	*Variance*	*Std. Dev.*	
	Section:Otter (n=24)	Left	58.68	7.66	
		Right	3443.39	58.68	
	Number of observations: 88				
	Fixed Effects	*Estimate*	*Std. Error*	*t-value*	*Pr(>|z|)*
	Intercept	7.379	2.652	2.782	**0.0054**
	Right	7.217	6.506	1.109	0.2674
PC (PAW)	*Random Effects*				
	Groups	*Fixed Effect within Group*	*Variance*	*Std. Dev.*	
	Section:Otter (n=24)	Left	0.6703	0.8187	
		Right	0.7079	0.8414	
	Number of observations: 88				
	Fixed Effects	*Estimate*	*Std. Error*	*t-value*	*Pr(>|z|)*
	Intercept	1.7227	0.5931	2.904	**0.00368**
	Right	-0.4274	0.7947	-0.538	0.59072
Mk (FLIPPER)	*Random Effects*				
	Groups	*Fixed Effect within Group*	*Variance*	*Std. Dev.*	
	Otter (n=3)	Left	0.00	0.00	
		Right	0.001978	0.04447	
	Number of observations: 12				
	Fixed Effects	*Estimate*	*Std. Error*	*t-value*	*Pr(>|z|)*
	Intercept	1.609	1.095	1.469	0.142
	Right	18.957	11935.284	0.002	0.999
PC (FLIPPER)	*Random Effects*				
	Groups	*Fixed Effect within Group*	*Variance*	*Std. Dev.*	
	Otter (n=3)	Left	7.703e-19	8.777e-10	
		Right	6.561e-19	8.100e-10	
	Number of observations: 12				
	Fixed Effects	*Estimate*	*Std. Error*	*t-value*	*Pr(>|z|)*
	Intercept	4.279e-08	0.8165	0.00	1.000
	Right	1.609	1.366	1.178	0.239

This table lists the variance estimates and standard deviations for the random effects and the estimated coefficients, standard errors, t-values, and significance values for the fixed effects (Left, Right). Total unexplained variance is the sum of the residual variance and the variance of the fixed effects within the grouping of otter. The intercept represents the density under the default value of Left. Fixed effects with $p<0.05$ are bolded.

SUPPLEMENTARY TABLE 5. Summary of GLMM model output: non-zero density of Merkel cells (Mk) and Pacinian corpuscles (PC) between left and right sides of the paw and flipper digit pads.

Type	Summary of Random and Fixed Effects				
Mk (PAW)	*Random Effects*				
	Groups	*Fixed Effect within Group*	*Variance*	*Std. Dev.*	
	Section:Otter (n=23)	Left	0.1764	0.4200	
		Right	0.8185	0.9047	
	Residual		0.4137	0.6432	
	Number of observations: 82				
	Fixed Effects	*Estimate*	*Std. Error*	*t-value*	*Pr(>|z|)*
	Intercept	-0.5942	0.1568	-3.789	**0.00015**
	Right	-0.2867	0.3143	-0.912	0.3617
PC (PAW)	*Random Effects*				
	Groups	*Fixed Effect within Group*	*Variance*	*Std. Dev.*	
	Section:Otter (n=23)	Left	0.3296	0.5741	
		Right	0.3005	0.5482	
	Residual		0.5171	0.5647	
	Number of observations: 69				
	Fixed Effects	*Estimate*	*Std. Error*	*t-value*	*Pr(>|z|)*
	Intercept	-2.6537	0.1906	-13.925	**<2e-16**
	Right	-0.1857	0.1861	-0.998	0.318
Mk (FLIPPER)	*Random Effects*				
	Groups	*Fixed Effect within Group*	*Variance*	*Std. Dev.*	
	Otter (n=3)	Left	0.503324	0.70945	
		Right	0.006411	0.08007	
	Residual		0.330777	0.57513	
	Number of observations: 11				
	Fixed Effects	*Estimate*	*Std. Error*	*t-value*	*Pr(>|z|)*
	Intercept	-1.3156	0.7636	-1.723	0.0849
	Right	0.4064	0.8759	0.464	0.6427
PC (FLIPPER)	*Random Effects*				
	Groups	*Fixed Effect within Group*	*Variance*	*Std. Dev.*	
	Otter (n=3)	Left	0.2905	0.5390	
		Right	0.3728	0.6106	
	Residual		0.2537	0.5037	
	Number of observations: 8				
	Fixed Effects	*Estimate*	*Std. Error*	*t-value*	*Pr(>|z|)*
	Intercept	-2.8243	0.4806	-5.877	**4.19e-09**
	Right	-0.1404	0.7029	-0.200	0.842

This table lists the variance estimates and standard deviations for the random effects and the estimated coefficients, standard errors, t-values, and significance values for the fixed effects (Left, Right). Total unexplained variance is the sum of the residual variance and the variance of the fixed effects within the grouping of otter. The intercept represents the density under the default value of Left. Fixed effects with $p<0.05$ are bolded.

SUPPLEMENTARY TABLE 6. Summary of GLMM model output: non-zero density of Merkel cells (Mk) and Pacinian corpuscles (PC) within glabrous skin of the paw.

Type	Summary of Random and Fixed Effects				
	Random Effects				
	Groups	*Fixed Effect within Group*	*Variance*	*Std. Dev.*	
	Otter (n=3)	Digit 1	0.149	0.3866	
		Digit 2	0.0121	0.1102	
		Digit 3	0.0678	0.2604	
		Digit 4	0.0275	0.1657	
		Digit 5	0.151	0.3881	
		Upper Metacarpal pad	0.298	0.5462	
		Lower Metacarpal pad	0.320	0.5653	
		Carpal pad	0.0566	0.2380	
Mk	Residual		0.444	0.6662	
	Number of observations: 82				
	Fixed Effects	*Estimate*	*Std. Error*	*t-value*	*Pr(>|z|)*
	Intercept	-0.60855	0.38327	-1.588	0.1123
	Digit 2	0.37615	0.44538	0.845	0.3984
	Digit 3	0.01417	0.40136	0.035	0.9718
	Digit 4	0.12153	0.37410	0.325	0.7453
	Digit 5	0.33386	0.36022	0.927	0.3540
	Upper Metacarpal pad	0.09543	0.35901	0.266	**0.0477**
	Lower Metacarpal pad	-1.97816	0.99910	-1.98	0.9274
	Carpal pad	0.03646	0.40020	0.091	0.7904
	Random Effects				
	Groups	*Fixed Effect within Group*	*Variance*	*Std. Dev.*	
	Otter (n=3)	Digit 1	0.00378	0.06149	
		Digit 2	0.121	0.34847	
		Digit 3	0.074	0.27221	
		Digit 4	0.0583	0.24153	
		Digit 5	0.00680	0.08246	
		Upper Metacarpal pad	0.0632	0.25145	
		Lower Metacarpal pad	0.0489	0.22111	
		Carpal pad	0.0106	0.10313	
PC	Residual		0.252	0.50170	
	Number of observations: 69				
	Fixed Effects	*Estimate*	*Std. Error*	*t-value*	*Pr(>|z|)*
	Intercept	-2.7627	0.1883	-14.67	**<2e-16**
	Digit 2	0.3729	0.3752	0.994	0.320
	Digit 3	0.5553	0.3203	1.73	0.0830
	Digit 4	0.5000	0.2848	1.76	0.0792
	Digit 5	0.7091	0.2718	2.609	**0.00908**
	Upper Metacarpal pad	-0.1043	0.3663	-2.839	**0.00453**
	Lower Metacarpal pad	-0.9617	0.3388	-1.090	0.276
	Carpal pad	-0.6317	0.5797	-0.285	0.776

This table lists the variance estimates and standard deviations for the random effects and the estimated coefficients, standard errors, t-values, and significance values for the fixed effects (Digit 1, Digit 2,

Digit 3, Digit 4, Digit 5, Upper Metacarpal Pad, Lower Metacarpal Pad, Carpal Pad). Total unexplained variance is the sum of the residual variance and the variance of the fixed effects within the grouping of otter. The intercept represents the density under the default value of Digit 1. Fixed effects with $p<0.05$ are bolded.

SUPPLEMENTARY TABLE 7. Design of and results from *post-hoc* custom contrasts from GLMM model: proportional density of Merkel cells (Mk) and Pacinian corpuscles (PC) across and within glabrous skin structures.

Type	Sections included	Contrast	Estimate	Std. Error	p-value	Adjusted Sig.
Mk	Digits	**Distal (UQ) >= Non-distal (UMQ, LMQ, LQ)**	2.237	0.840	0.00397	**sig.**
		Distal (UQ, UMQ) >= Non-distal (LMQ, LQ)	2.46	0.949	0.008	**<0.1, sig.**
	Metacarpal and carpal pads	Distal (UQ) >= Non-distal (UMQ, LMQ, LQ)	1.038	0.837	0.17	>0.1, n.s.
		Distal (UQ, UMQ) >= Non-distal (LMQ, LQ)	0.543	0.863	0.38	>0.1, n.s.
	Lower metacarpal and carpal pads	Distal (UQ) >= Non-distal (UMQ, LMQ, LQ)	1.71	1.16	0.113	>0.1/2, n.s.
		Distal (UQ, UMQ) >= Non-distal (LMQ, LQ)	0.723	1.22	0.388	>0.1, n.s.
	Flipper pad	Distal (UQ) >= Non-distal (UMQ, LMQ, LQ)	7.17	302.27	0.981	>0.1/2, n.s.
		Distal (UQ, UMQ) >= Non-distal (LMQ, LQ)	-5.59	457.99	1.00	>0.1, n.s.
PC	Digits	**Distal (UQ) >= Non-distal (UMQ, LMQ, LQ)**	1.30	0.742	0.0587	**<0.1, sig.**
		Distal (UQ, UMQ) >= Non-distal (LMQ, LQ)	2.55	0.743	0.000521	**sig.**
	Metacarpal and carpal pads	Distal (UQ) >= Non-distal (UMQ, LMQ, LQ)	1.96	1.140	0.072	>0.1/2, n.s.
		Distal (UQ, UMQ) >= Non-distal (LMQ, LQ)	1.20	1.64	0.340	>0.1, n.s.
	Lower metacarpal and carpal pads	Distal (UQ) >= Non-distal (UMQ, LMQ, LQ)	1.46	1.33	0.193	>0.1/2, n.s.
		Distal (UQ, UMQ) >= Non-distal (LMQ, LQ)	1.35	1.89	0.326	>0.1, n.s.
	Flipper pad	Distal (UQ) >= Non-distal (UMQ, LMQ, LQ)	12.56	73.02	0.64	>0.1/2, n.s.
		Distal (UQ, UMQ) >= Non-distal (LMQ, LQ)	6.77	121.83	0.69	>0.1, n.s.

The estimate and standard error of the mean difference between contrasts and significance of the difference is reported. ">=" indicates "is greater than" and a one-sided test with significance level $p<0.1$. Adjusted significance represents the significance level based on a reversed sequential Bonferroni procedure to control family-wise Type 1 error. Shading separates each family of test. In this procedure the largest p-value is tested at the significance level, the next largest at half the

significance value, the next largest at one-third the significance value, and so on. If a significant value is reached, we reject all other tests with p-values smaller than that value. Significant contrasts and associated adjusted significance levels are bolded.

SUPPLEMENTARY TABLE 8. Summary of GLMM model output: proportional density of Merkel cells (Mk) and Pacinian corpuscles (PC) within glabrous skin of the paw digit pads.

Type	Summary of Random and Fixed Effects				
Mk	*Random Effects*				
	Groups	*Fixed Effect within Group*	*Variance*	*Std. Dev.*	
	Section:Otter (n=15)	Upper Quartile	1.0996	1.0486	
		Upper Middle Quartile	0.6121	0.7823	
		Lower Middle Quartile	0.7184	0.8476	
		Lower Quartile	0.7476	0.8646	
	Number of observations: 212				
	Fixed Effects	*Estimate*	*Std. Error*	*t-value*	*Pr(>|z|)*
	Intercept	-1.6592	0.4880	-3.400	**0.000674**
	Upper Quartile	0.8687	0.7428	1.169	0.095309
	Upper Middle Quartile	-0.2608	0.6669	-0.391	0.695721
	Lower Quartile	-2.6437	1.5849	-1.668	0.242205
PC	*Random Effects*				
	Groups	*Fixed Effect within Group*	*Variance*	*Std. Dev.*	
	Section:Otter (n=15)	Upper Quartile	0.060029	0.2450	
		Upper Middle Quartile	0.002591	0.0509	
		Lower Middle Quartile	0.000	0.000	
		Lower Quartile	0.239947	0.4898	
	Number of observations: 192				
	Fixed Effects	*Estimate*	*Std. Error*	*t-value*	*Pr(>|z|)*
	Intercept	-2.3979	0.5222	-4.592	**4.41e-06**
	Upper Quartile	0.9133	0.6533	1.398	0.1621
	Upper Middle Quartile	1.4067	0.6153	2.286	**0.0222**
	Lower Quartile	-0.4163	0.9901	-0.420	0.6742

This table lists the variance estimates and standard deviations for the random effects and the estimated coefficients, standard errors, t-values, and significance values for the fixed effects (Upper Quartile, Upper Middle Quartile, Lower Middle Quartile, Lower Quartile). The intercept represents the proportional density under the default value of the Lower Middle Quartile. Fixed effects with $p<0.05$ are bolded.

SUMMARY

This dissertation advances understanding of the sensory mechanisms underlying efficient foraging behavior in sea otters and builds on decades of field studies of population biology and foraging ecology in this species (Kenyon 1969; Riedman and Estes 1990; Estes et al. 2003; Tinker et al. 2007, 2008, 2012; Elliott Smith et al. 2015; Newsome et al. 2015; Thometz et al. 2016). Despite this substantial body of research, substantive observations of underwater search and detection strategies in foraging sea otters remain unavailable, while detailed descriptions readily exist for prey processing at the water's surface. The direct structural-functional relationships examined here for vision and touch expand the existing body of work on sensory biology in this species based on the few available experimental (Hammock 2005; Ghoul and Reichmuth 2014b, a) and anatomical investigations (Radinsky 1968; Murphy et al. 1990; Mass and Supin 2000; Levenson et al. 2006; Marshall et al. 2014).

Much of our foundational knowledge of vision and touch in mammals is based on classic "model" species, *i.e.*, primates and rodents. While highly useful to determine typical pathways of sensory transduction, this narrow phylogenetic approach limits our ability to connect functional and morphological variation with species-specific behavior and ecology. Since local environments directly influence the transmission of sensory cues, the inclusion of species adapted to different habitats and lifestyles can bolster the existing comparative framework. This dissertation's

focus on sea otters, a secondarily adapted amphibious marine mammal, has broader implications for our understanding of the feedback between evolution, ecology, and morphology in terrestrial-aquatic transitions and in a top predator that exerts strong direct and indirect effects on the coastal ecosystem (Estes and Palmisano 1974; Estes and Duggins 1995; Watson and Estes 2011; Hughes et al. 2013).

Chapter 1 of this dissertation contributes new research to understand the role of vision in the underwater foraging behavior of sea otters. The structural and functional approaches used in Chapter 1 address key data gaps to describe pupillary response, retinal morphology, and tapetal thickness within the constraints imposed by their method of accommodation. The structural results reveal that the sea otter eye contains elements that enhance low-light vision, including a tapetum lucidum and rod-rich retina comparable to nocturnal terrestrial carnivores. The functional results suggest that pupillary mobility in ambient light extremes is less than that measured in pinnipeds (Levenson and Schusterman 1999), which likely results from an accommodative mechanism that depends on pupil size for lens deformation to retain visual acuity under water (Balliet and Schusterman 1971; Schusterman and Barrett 1973; Murphy et al. 1990). Our findings in the visual domain build on previous work that places sea otters as intermediate between terrestrial and aquatic mammals (Estes 1989; Mass and Supin 2000, 2007), however, more comparative data are needed for other terrestrial and amphibious mustelids to rigorously determine whether the traits that contribute to amphibious vision in sea otters are derived. From an ecological perspective, the results from Chapter 1 suggest that best visual acuity under water is

likely achieved in shallow water during day dives for sea otters. Combined with their dichromatic color vision, underwater accommodation likely enables sea otters to discriminate between coastal habitat features and epifaunal prey in bright conditions. At night or during deep dives, vision likely becomes blurry due to a negative coupling between pupil size and accommodation ability, however the rod-rich retina may enable detection of large habitat features indicative of prey presence. On a broad level this chapter contributes to our understanding of how phylogenetic inertia and varying ecological pressures can drive species to different evolutionary solutions given the trade-off between acuity and low-light in amphibious vision.

Chapters 2 and 3 describe novel research to understand the role of touch in sea otter foraging behavior using behavioral and morphological methods, respectively. When paired with previous research on the processing of tactile cues via the vibrissal array and the central nervous system in sea otters (Radinsky 1968; Marshall et al. 2014), these chapters provide a comprehensive assessment of the tactile system for this species. Although the importance of touch for prey detection and capture has been suggested for decades (Kenyon 1969; Riedman and Estes 1990), the results reported in Chapter 2 comprise the first direct assessments of touch abilities in sea otters using behavioral methods. This chapter combines the results of four experiments to quantify tactile thresholds separately for the paws and vibrissae, both in air and under water, in a sea otter trained to participate in a cooperative texture discrimination task. The results from Chapter 2 reveal that both paw and vibrissal sensitivity in sea otters are comparable to those in other tactile specialists, including

terrestrial, amphibious, and fully aquatic mammals (Lamb 1983; Morley et al. 1983; Dehnhardt 1994; Dehnhardt and Dücker 1996; Dehnhardt et al. 1997, 1998; Bachteler and Dehnhardt 1999; Hille et al. 2001; Bauer et al. 2012). Paw sensitivity is especially acute in sea otters, similar to thresholds for humans tested in the same experimental paradigm using their hands. In addition to sensitivity metrics, Chapter 2 reveals rapid processing time of tactile cues for sea otters, which coincides with the high foraging efficiency observed for acquisition of infaunal prey in wild sea otters (Estes et al. 2003; Bodkin et al. 2004, 2007).

Chapter 3 complements the results from Chapter 2 by describing variation in morphological patterns in the glabrous skin of sea otters (*i.e.*, paw pads, flipper digit pads, rhinarium, and lips) and how these patterns may relate to differential perception of tactile cues. Chapter 3 uses established histological methods to confirm the presence of two mammalian mechanoreceptor types, Merkel cells and Pacinian corpuscles, and their high relative density in distal portion of the paw, which likely acts as a tactile fovea in sea otters relative to other glabrous skin. Sea otters appear to lack Meissner corpuscles, another mechanoreceptor described in a subset of terrestrial mammals (Winkelmann 1964; Ide 1977; Munger and Ide 1988; Tachibana and Fujiwara 1991; Hoffmann et al. 2004; Weissengruber et al. 2006; Verendeev et al. 2015), but show substantial, unclassified neural tissue in the shallow dermis that likely serves a similar mechanoreceptive function. These results indicate differential tactile sensitivity within the paw and parallel those for Chapter 2, in which the sea otter primarily used her distal paw to explore textured stimuli. Additionally, the low

relative densities of mechanoreceptors in the rhinarium and lips measured in Chapter 3 suggest that the skin surrounding the vibrissae contributes minimally to sensitivity measured in Chapter 2. Although Chapter 3 primarily focuses on anatomical comparisons within sea otters, the observed patterns in the paw show qualitative similarities to those described in other species for peripheral skin regions specialized for touch (Johansson and Vallbo 1979; Kumamoto et al. 1993b, a; Rasmussen and Munger 1996; Stark et al. 1998; Paré et al. 2002).

This dissertation emphasizes the value of approaching research questions in the field of sensory ecology from multiple perspectives. The behavioral methods used in Chapters 1 and 2 provide direct measures of sensory perception, including fine-scale metrics of sensitivity and strategy, however animal training for cooperative research requires considerable time and resources, which tends to limit sample size. In contrast, the histological methods used in Chapters 1 and 3 enable inferences of sensory ability based on sensory morphology. Such indirect methods can be made quickly across multiple individuals, however, they provide only a snapshot within each individual's lifetime, which can limit interpretation of results beyond broad patterns, and they require validation when used in previously unassessed species. The combination of direct and indirect approaches used in this dissertation balances the tradeoffs inherent to each method and represents a more complete framework to evaluate sensory abilities for species outside of traditional laboratory animal paradigms.

An overarching goal of sensory ecology is to integrate species-typical sensory capabilities with ecological data on free-ranging individuals. In the case of sea otters, a wealth of behavioral data has been collected for wild foraging individuals. However, significant data gaps in our understanding of sea otter sensory biology required attention to determine what questions to ask and how to ask them in a meaningful comparative way. The results presented within this dissertation fill some of the key data gaps, and in doing so, can direct future studies on both applied and comparative sensory ecology questions. For example, the results from Chapters 2 and 3 can support applied research on the prey cues sea otters attend to during foraging, *e.g.*, to examine whether sea otters use touch to detect typical flow rates measured from excurrent clam siphons. In addition, Chapter 1 points to the importance of integrating measures of species-specific perception to ground-truth interpretations of wild behavior; *e.g.*, future external animal-borne tags could incorporate sensors that monitor environmental cues at the level of the individual at the time of prey capture. This dissertation as a whole provides both quantitative and qualitative inspiration for future comparative work on how selection pressures shape interspecific variation in sensory abilities.

All organisms inhabit a multimodal world and need to sense the environment to behave appropriately and survive. Research on the basic biology of any species—like the body of work on sea otters presented here—provides the proximate perspective necessary to balance inferences made in ecological research. Since similar local physical environments are perceived differently across species, studies

that consider organisms at various levels of organization (*i.e.*, individuals, populations, communities) should account for unique species-specific sensory environments. Ultimately, such an understanding is required to decipher causal links between proximate mechanisms and ecological processes.

REFERENCES

Bachteler D, Dehnhardt G (1999) Active touch performance in the Antillean manatee: evidence for a functional differentiation of facial tactile hairs. Zoology 102:61–69

Balliet RF, Schusterman RJ (1971) Underwater and aerial visual acuity in the Asian "clawless" otter (Amblonyx cineria cineria). Nature 234:305–306

Bauer GB, Gaspard III JC, Colbert DE, et al (2012) Tactile discrimination of textures by Florida manatees (Trichechus manatus latirostris). Mar Mammal Sci 28:E456–E471 . doi: 10.1111/j.1748-7692.2012.00565.x

Bodkin JL, Esslinger GG, Monson DH (2004) Foraging depths of sea otters and implications to coastal marine communities. Mar Mammal Sci 20:305–321

Bodkin JL, Monson DH, Esslinger GG (2007) Activity budgets derived from time–depth recorders in a diving Mammal. J Wildl Manage 71:2034–2044 . doi: 10.2193/2006-258

Dehnhardt G (1994) Tactile size discrimination by a California sea lion (Zalophus californianus) using its mystacial vibrissae. J Comp Physiol A 175:791–800 . doi: 10.1007/BF00191851

Dehnhardt G, Dücker G (1996) Tactual discrimination of size and shape by a California sea lion (Zalophus californianus). Anim Learn Behav 24:366–374 . doi: 10.3758/BF03199008

Dehnhardt G, Friese C, Sachser N (1997) Sensitivity of the trunk of Asian elephants for texture differences of actively touched objects. Zeitschrift für Saugetierkd 62:37–39

Dehnhardt G, Mauck B, Hyvärinen H (1998) Ambient temperature does not affect the tactile sensitivity of mystacial vibrissae in harbour seals. J Exp Biol 201:3023–3029

Elliott Smith EA, Newsome SD, Estes JA, Tinker MT (2015) The cost of reproduction: differential resource specialization in female and male California sea otters. Oecologia 178:17–29 . doi: 10.1007/s00442-014-3206-1

Estes JA (1989) Adaptations for Aquatic Living by Carnivores. In: Gittleman JL (ed) Carnivore behavior, ecology, and evolution. Cornell University Press, Ithaca, pp 242–282

Estes JA, Duggins DO (1995) Sea Otters and Kelp Forests in Alaska: Generality and Variation in a Community Ecological Paradigm. Ecol Monogr 65:75–100

Estes JA, Palmisano JF (1974) Sea Otters: Their Role in Structuring Nearshore Communities. Science (80-) 185:1058–1060

Estes JA, Riedman ML, Staedler MM, et al (2003) Individual variation in prey selection by sea otters: patterns, causes and implications. J Anim Ecol 72:144–155

Ghoul A, Reichmuth C (2014b) Hearing in sea otters (Enhydra lutris): Audible frequencies determined from a controlled exposure approach. Aquat Mamm 40:243–251 . doi: 10.1578/AM.40.3.2014.243

Ghoul A, Reichmuth C (2014a) Hearing in the sea otter (Enhydra lutris): auditory profiles for an amphibious marine carnivore. J Comp Physiol A Neuroethol Sens Neural Behav Physiol 200:967–81 . doi: 10.1007/s00359-014-0943-x

Hammock J (2005) Structure, function and context: the impact of morphometry and ecology on olfactory sensitivity. Massachusetts Institute of Technology and Woods Hole Oceanographic Institution

Hille P, Becker-Carus C, Dücker G, Dehnhardt G (2001) Haptic discrimination of size and texture in squirrel monkeys (Saimiri sciureus). Somatosens Mot Res 18:50–61 . doi: 10.1080/08990

Hoffmann JN, Montag AG, Dominy NJ (2004) Meissner corpuscles and somatosensory acuity: the prehensile appendages of primates. Anat Rec Part A 281A:1138–1147 . doi: 10.1002/ar.a.20119

Hughes BB, Eby R, Van Dyke E, et al (2013) Recovery of a top predator mediates negative eutrophic effects on seagrass. Proc Natl Acad Sci U S A 110:15313–8 . doi: 10.1073/pnas.1302805110

Ide C (1977) Development of meissner corpuscle of mouse toe pad. Anat Rec 188:49–67

Johansson RS, Vallbo AB (1979) Tactile sensibility in the human hand: relative and absolute densities of four types of mechanoreceptive units in glabrous skin. J Physiol 286:283–300

Kenyon K (1969) The sea otter in the eastern Pacific ocean. Washington, D.C.

Kumamoto K, Senuma H, Ebara S, Matsuura T (1993a) Distribution of pacinian corpuscles in the hand of the monkey, Macaca fuscata. J Anat 183:149–154

Kumamoto K, Takei M, Kinoshita M, et al (1993b) Distribution of pacinian corpuscles in the cat forefoot. J Anat 182:23–28

Lamb GD (1983) Tactile discrimination of textured surfaces: psychophysical performance measurements in humans. J Physiol 338:551–565

Levenson DH, Ponganis PJ, Crognale M a, et al (2006) Visual pigments of marine carnivores: pinnipeds, polar bear, and sea otter. J Comp Physiol A 192:833–43 . doi: 10.1007/s00359-006-0121-x

Levenson DH, Schusterman RJ (1999) Dark adaptation and visual sensitivity in shallow and deep-diving pinnipeds. Mar Mammal Sci 15:1303–1313

Marshall CD, Rozas K, Kot B, Gill VA (2014) Innervation patterns of sea otter (Enhydra lutris) mystacial follicle-sinus complexes. Front Neuroanat 8:1–8 . doi: 10.3389/fnana.2014.00121

Mass AM, Supin AY (2007) Adaptive features of aquatic mammals' eye. Anat Rec 290:701–715 . doi: 10.1002/ar.20529

Mass AM, Supin AY (2000) Ganglion cells density and retinal resolution in the sea otter, Enhydra lutris. Brain Behav Evol 55:111–119 . doi: 10.1159/000006646

Morley JW, Goodwin AW, Darian-Smith I (1983) Tactile discrimination of gratings. Exp Brain Res 49:291–299

Munger BL, Ide C (1988) The structure of cutaneous sensory receptors. Arch Histol Cytol 51:1–34

Murphy CJ, Bellhorn RW, Williams T, et al (1990) Refractive state, ocular anatomy, and accommodative range of the sea otter (Enhydra lutris). Vision Res 30:23–32

Newsome SD, Tinker MT, Gill VA, et al (2015) The interaction of intraspecific competition and habitat on individual diet specialization: a near range-wide examination of sea otters. Oecologia 178:45–59

Paré M, Smith AM, Rice FL (2002) Distribution and terminal arborizations of cutaneous mechanoreceptors in the glabrous finger pads of the monkey. J Comp Neurol 445:347–359 . doi: 10.1002/cne.10196

Radinsky LB (1968) Evolution of somatic sensory specialization in otter brains. J Comp Neurol 134:495–506 . doi: 10.1002/cne.901340408

Rasmussen LEL, Munger BL (1996) The sensorineural specializations of the trunk tip (finger) of the Asian elephant, Elephas maximus. Anat Rec 246:127–134

Riedman ML, Estes JA (1990) The sea otter (Enhydra lutris): behavior, ecology, and natural history. Biol Rep 90:1–136

Schusterman RJ, Barrett B (1973) Amphibious nature of visual acuity in the Asian "clawless" otter. Nature 244:518–519

Stark B, Carlstedt T, Hallin RG, Risling M (1998) Distribution of human pacinian corpuscles in the hand: A cadaver study. J Hand Surg (British Eur Vol 23B:370–372

Tachibana T, Fujiwara N (1991) Mechanoreceptors of the hard palate of the mongolian gerbil include special junctions between epithelia and Meissner lamellar cells: A comparison with other rodents. Anat Rec 231:396–403

Thometz NM, Staedler MM, Tomoleoni JA, et al (2016) Trade-offs between energy maximization and parental care in a central place forager, the sea otter. Behav Ecol 27:1552–1566 . doi: 10.1093/beheco/arw089

Tinker MT, Bentall G, Estes JA (2008) Food limitation leads to behavioral diversification and dietary specialization in sea otters. PNAS 105:560–565

Tinker MT, Costa DP, Estes JA, Wieringa N (2007) Individual dietary specialization and dive behaviour in the California sea otter: Using archival time–depth data to detect alternative foraging strategies. Deep Res II 54:330–342 . doi: 10.1016/j.dsr2.2006.11.012

Tinker MT, Guimarães PR, Novak M, et al (2012) Structure and mechanism of diet specialisation: testing models of individual variation in resource use with sea otters. Ecol Lett 15:475–83 . doi: 10.1111/j.1461-0248.2012.01760.x

Verendeev A, Thomas C, Mcfarlin SC, et al (2015) Comparative analysis of meissner's corpuscles in the fingertips of primates. J Anat 227:72–80 . doi: 10.1111/joa.12327

Watson J, Estes JA (2011) Stability, resilience, and phase shifts in rocky subtidal communities along the west coast of Vancouver Island, Canada. Ecol Monogr 81:215–239 . doi: 10.1890/10-0262.1

Weissengruber GE, Egger GF, Hutchinson JR, et al (2006) The structure of the cushions in the feet of African elephants (Loxodonta africana). J Anat 209:781–792 . doi: 10.1111/j.1469-7580.2006.00648.x

Winkelmann RK (1964) Nerve endings of the North American opossum (Didelphis virginia): A comparison with nerve endings of primates. Am J Phys Anthropol 22:253–258

BIBLIOGRAPHY

Abrahams VC, Hodgins M, Downey D (1987) Morphology, distribution, and density of sensory receptors in the glabrous skin of the cat rhinarium. J Morphol 191:109–114

Adams T, Hunter WS (1969) Modification of skin mechanical by eccrine sweat gland activity properties. J Appl Physiol 26:417–419

Adelman S, Taylor CR, Heglund NC (1975) Sweating on paws and palms: what is its function? Am J Physiol 229:1400–1402

Andres KH, v Düring M (1990) Comparative and functional aspects of the histological organization of cutaneous receptors in vertebrates. In: Zenker W, Neuhuber WL (eds) The Primary afferent neuron: a survey of recent morpho-functional aspects. Plenum Press, New York, NY, pp 1–17

Bachteler D, Dehnhardt G (1999) Active touch performance in the Antillean manatee: evidence for a functional differentiation of facial tactile hairs. Zoology 102:61–69

Ballard K., Sivak JG, Howland HC (1989) Intraocular muscles of the Canadian river otter and Canadian beaver and their optical function. Can J Zool 67:469–474 . doi: 10.1139/z89-068

Balliet RF, Schusterman RJ (1971) Underwater and aerial visual acuity in the Asian "clawless" otter (Amblonyx cineria cineria). Nature 234:305–306

Banks MS, Munsinger H (1974) Pupillometric measurement of difference spectra for three color receptors in an adult and a four-year-old. Vision Res 14:813–817

Bartoń K (2016) MuMIn: Multi-Model Inference

Bates D, Maechler M, Bolker B, Walker S (2015) Fitting linear mixed-effects models using lme4. J Stat Softw 67:1–48

Bauer GB, Gaspard III JC, Colbert DE, et al (2012) Tactile discrimination of textures by Florida manatees (Trichechus manatus latirostris). Mar Mammal Sci 28:E456–E471 . doi: 10.1111/j.1748-7692.2012.00565.x

Bell J, Bolanowski S, Holmes MH (1994) The structure and function of Pacinian corpuscles: A review. Prog Neurobiol 42:79–128

Berta A, Sumich JL (1999) Integumentary, Sensory, and Urinary Systems. In: Marine Mammals: Evolutionary Biology. Academic Press, San Diego, CA, pp 130–172

Berta A, Sumich JL, Kovacs KM (2015) Marine Mammals: Evolutionary Biology, 3rd edn. Academic Press, London

Bodkin JL (2015) Historic and Contemporary Status of Sea Otters in the North Pacific. In: Larson SE, Bodkin JL, VanBlaricom GR (eds) Sea Otter Conservation. Academic Press, London, pp 43–61

Bodkin JL, Esslinger GG, Monson DH (2004) Foraging depths of sea otters and implications to coastal marine communities. Mar Mammal Sci 20:305–321

Bodkin JL, Monson DH, Esslinger GG (2007) Activity budgets derived from time–depth recorders in a diving Mammal. J Wildl Manage 71:2034–2044 . doi: 10.2193/2006-258

Bolanowski SJ, Pawson L (2003) Organization of Meissner corpuscles in the glabrous skin of monkey and cat. Somatosens Mot Res 20:223–231 . doi: 10.1080/08990220310001622915

Bolanowski SJ, Verrillo RT (1982) Temperature and criterion effects in a somatosensory subsystem: a neurophysiological and psychophysical study. J Neurophysiol 48:836–855

Bouley DM, Alarcón CN, Hildebrandt T, O'Connell-Rodwell CE (2007) The distribution, density and three-dimensional histomorphology of Pacinian corpuscles in the foot of the Asian elephant (Elephas maximus) and their potential role in seismic communication. J Anat 211:428–435 . doi: 10.1111/j.1469-7580.2007.00792.x

Braekevelt CR (1986) Fine structure of the tapetum cellulosum of the grey seal (Halichoerus grypus). Arcta anat 127:81–87

Braekevelt CR (1989) Fine structure of the retinal epithelium and tapetum lucidum of the ranch mink Mustela vison. Acta Anat 135:296–302

Braekevelt CR (1981) Fine structure of the tapetum lucidum of the domestic ferret. Anat Embryol (Berl) 163:201–214

Brenowitz GL (1980) Cutaneous mechanoreceptor distribution and its relationship to behavioral specializations in squirrels. Brain Behav Evol 17:432–453 . doi: 10.1159/000121813

Calderone JB, Jacobs GH (2003) Spectral properties and retinal distribution of ferret cones. Vis Neurosci 20:11–7

Cartmill M (1979) The volar skin of primates: its frictional characteristics and their functional signif icance. Am J Phys Anthropol 50:497–510

Carvell GE, Simons DJ (1990) Biometric Analyses of Vibrissal Tactile Discrimination in the Rat. J Neurosci 10:2638–2648

Catania KC (2006) Underwater "sniffing" by semi-aquatic mammals. Nature 444:1024–1025 . doi: 10.1038/nature4441023a

Catania KC, Hare JF, Campbell KL (2008) Water shrews detect movement, shape, and smell to find prey underwater. Proc Natl Acad Sci U S A 105:571–6 . doi: 10.1073/pnas.0709534104

Catania KC, Kaas JH (1997) Somatosensory fovea in the star-nosed mole: Behavioral use of the star in relation to innervation patterns and cortical representation. J Comp Neurol 387:215–233 . doi: 10.1002/(SICI)1096-9861(19971020)387:2<215::AID-CNE4>3.0.CO;2-3

Catania KC, Remple FE (2004) Tactile foveation in the star-nosed mole. Brain Behav Evol 63:1–12 . doi: 10.1159/000073755

Catania KC, Remple FE (2005) Asymptotic prey profitability drives star-nosed moles to foraging speed limit. Nature 433:519–522 . doi: 10.1038/nature03106.1.

Cauna N (1985) Nature and functions of the papillary ridges of the digital skin. Anat Rec 119:449–468

Chinn SM, Miller MA, Tinker MT, et al (2016) The high cost of motherhood: end-lactation syndrome in southern sea otters (Enhydra lutris nereis) on the central California coast, USA. J Wildl Dis 52:307–318 . doi: 10.7589/2015-06-158

Cornsweet TN (1962) The Staircase-Method in Psychophysics. Am J Psychol 75:485–491

Costa DP, Kooyman GL (1982) Oxygen consumption, thermoregulation, and the effect of fur oiling and washing on the sea otter, Enhydra lutris. Can J Zool 60:2761–2767 . doi: 10.1139/z82-354

De Groot SG, Gebhard JW (1952) Pupil size as determined by adapting luminance. J Opt Soc Am 42:492–495 . doi: 10.1364/JOSA.42.000492

Dehnhardt G (1994) Tactile size discrimination by a California sea lion (Zalophus californianus) using its mystacial vibrissae. J Comp Physiol A 175:791–800 . doi: 10.1007/BF00191851

Dehnhardt G (1990) Preliminary Results from Psychopysical Studies on the Tactile Sensitivity in Marine Mammals. In: Thomas JA, Kastelein RA (eds) Sensory Abilities of Cetaceans. Plenum Press, New York, pp 435–446

Dehnhardt G, Dücker G (1996) Tactual discrimination of size and shape by a California sea lion (Zalophus californianus). Anim Learn Behav 24:366–374 . doi: 10.3758/BF03199008

Dehnhardt G, Friese C, Sachser N (1997) Sensitivity of the trunk of Asian elephants for texture differences of actively touched objects. Zeitschrift für Saugetierkd 62:37–39

Dehnhardt G, Hanke W, Bleckmann H (2001) Hydrodynamic trail-following in harbor seals (Phoca vitulina). Science (80-) 293:102–104

Dehnhardt G, Hyvärinen H, Palviainen A, Klauer G (1999) Structure and innervation of the vibrissal follicle-sinus complex in the Australian water rat, Hydromys chrysogaster. J Comp Neurol 411:550–562 . doi: 10.1002/(SICI)1096-9861(19990906)411:4<550::AID-CNE2>3.0.CO;2-G

Dehnhardt G, Kaminski A (1995) Sensitivity of the mystacial vibrissae of harbour seals (Phoca vitulina) for size differences of actively touched objects. J Exp Biol 198:2317–2323

Dehnhardt G, Mauck B (2008) Mechanoreception in Secondarily Aquatic Vertebrates. In: Thewissen JGM, Nummela S (eds) Sensory Evolution on the Threshold: Adaptations in secondarily adapted vertebrates. University of California Press, Berkeley, CA, pp 295–314

Dehnhardt G, Mauck B, Hyvärinen H (2003) The Functional Significance of the Vibrissal System of Marine Mammals. In: Baumann KI, Halata Z, Moll I (eds) The Merkel Cell. Springer, Berlin, Heidelberg, pp 127–135

Dehnhardt G, Mauck B, Hyvärinen H (1998) Ambient temperature does not affect the tactile sensitivity of mystacial vibrissae in harbour seals. J Exp Biol 201:3023–3029

Denwood MJ (2016) runjags: An R Package Providing Interface Utilities, Model Templates, Parallel Computing Methods and Additional Distributions for MCMC Models in JAGS. J Stat Softw 71:1–25 . doi: doi:10.18637/jss.v071.i09

Dunstone N, Sinclair W (1978) Comparative aerial and underwater visual acuity of the mink, Mustela vison Schreber, as a function of discrimination distance and stimulus luminance. Anim Behav 26:6–13 . doi: 10.1016/0003-3472(78)90002-7

Elliott Smith EA, Newsome SD, Estes JA, Tinker MT (2015) The cost of reproduction: differential resource specialization in female and male California sea otters. Oecologia 178:17–29 . doi: 10.1007/s00442-014-3206-1

Erdsack N, Dehnhardt G, Hanke W (2014) Thermoregulation of the vibrissal system in harbor seals (Phoca vitulina) and Cape fur seals (Arctocephalus pusillus pusillus). J Exp Mar Bio Ecol 452:111–118 . doi: 10.1016/j.jembe.2013.12.011

Esslinger GG, Bodkin JL, Breton AR, et al (2014) Temporal patterns in the foraging behavior of sea otters in Alaska. J Wildl Manage 78:689–700 . doi: 10.1002/jwmg.701

Estes JA (1989) Adaptations for Aquatic Living by Carnivores. In: Gittleman JL (ed) Carnivore behavior, ecology, and evolution. Cornell University Press, Ithaca, pp 242–282

Estes JA, Duggins DO (1995) Sea Otters and Kelp Forests in Alaska: Generality and Variation in a Community Ecological Paradigm. Ecol Monogr 65:75–100

Estes JA, Hatfield BB, Ralls K, Ames J (2003a) Causes of mortality in California sea otters during periods of population growth and decline. Mar Mammal Sci 19:198–216

Estes JA, Jameson RJ, Rhode EB (1982) Activity and prey selection in the sea otter: influence of population status on community structure. Am Nat 120:242–258

Estes JA, Palmisano JF (1974) Sea Otters: Their Role in Structuring Nearshore Communities. Science (80-) 185:1058–1060

Estes JA, Riedman ML, Staedler MM, et al (2003b) Individual variation in prey selection by sea otters: patterns, causes and implications. J Anim Ecol 72:144–155

Fay FH (1982) Ecology and biology of the Pacific walrus, Odobenus rosmarus divergens, North Amer. U.S. Fish and Wildlife Service, Washington, D.C.

Feldkamp SD, DeLong RL, Antonelis GA (1989) Diving patterns of California sea lions, Zalophus californianus. Can J Zool 67:872–883

Fitts PM (1966) Cognitive aspects of information processing: III. Set for speed versus accuracy. J Exp Psychol 71:849–857

Fujii JA, Ralls K, Tinker MT (2015) Ecological drivers of variation in tool-use frequency across sea otter populations. Behav Ecol 26:519–526 . doi: 10.1093/beheco/aru220

Garshelis DL, Garshelis JA, Kimker AT (1986) Sea otter time budgets and prey relationships in Alaska. J Wildl Manage 50:637–647

Gelatt TS, Siniff DB, Estes JA (2002) Activity patterns and time budgets of the declining sea otter population at Amchitka Island, Alaska. J Wildl Manage 66:29–39

Gellermann LW (1933) Chance orders of alternating stimuli in visual discrimination experiments. J Genet Psychol 42:206–208

Gentry R, Peterson R (1967) Underwater vision of the sea otter. Nature 216:435–436

Gescheider GA (1997) Psychophysics: the fundamentals, 3rd edn. Lawrence Erlbaum Associates, Mahwah, New Jersey

Gescheider GA, Thorpe JM, Goodarz J, Bolanowski SJ (1997) The effects of skin temperature on the detection and discrimination of tactile stimulation. Somatosens Mot Res 14:181–188 . doi: 10.1080/08990229771042

Ghoul A, Reichmuth C (2014a) Hearing in sea otters (Enhydra lutris): Audible frequencies determined from a controlled exposure approach. Aquat Mamm 40:243–251 . doi: 10.1578/AM.40.3.2014.243

Ghoul A, Reichmuth C (2014b) Hearing in the sea otter (Enhydra lutris): auditory profiles for an amphibious marine carnivore. J Comp Physiol A Neuroethol Sens Neural Behav Physiol 200:967–81 . doi: 10.1007/s00359-014-0943-x

Gibson JJ (1962) Observations on active touch. Psychol Rev 69:477–491

Ginter CC, DeWitt TJ, Fish FE, Marshall CD (2012) Fused traditional and geometric morphometrics demonstrate pinniped whisker diversity. PLoS One 7:1–10 . doi: 10.1371/journal.pone.0034481

Gislen A, Dacke M, Kröger RHH, et al (2003) Superior underwater vision in a human population of sea gypsies. Curr Biol 13:833–836 . doi: 10.1016/S

Gittleman JL (1991) Carnivore olfactory bulb size: allometry, phylogeny and ecology. J Zool 225:253–272 . doi: 10.1111/j.1469-7998.1991.tb03815.x

Gonzalez-Martinez T, Germana GP, Monjil DF, et al (2004) Absence of Meissner corpuscles in the digital pads of mice lacking functional TrkB. Brain Res 1002:120–128 . doi: 10.1016/j.brainres.2004.01.003

Goodge WR (1960) Adaptations for amphibious vision in the dipper (Cinclus mexicanus). J Morphol 107:79–91

Grant R, Wieskotten S, Wengst N, et al (2013) Vibrissal touch sensing in the harbor seal (Phoca vitulina): How do seals judge size? J Comp Physiol A 199:521–533. doi: 10.1007/s00359-013-0797-7

Green J (1977) Sensory perception in hunting otters, Lutra lutra. Otters, J Otter Trust 13–16

Guillemain M, Martin GR, Fritz H (2002) Feeding methods, visual fields and vigilance in dabbling ducks (Anatidae). Funct Ecol 16:522–529

Halata Z (1990) Sensory innervation of the hairless and hairy skin in mammals including humans. In: Zenker W, Neuhuber WL (eds) The Primary afferent neuron: a survey of recent morpho-functional aspects. Plenum Press, New York, NY, pp 19–34

Halata Z, Munger BL (1983) The sensory innervation of primate facial skin. II. Vermilion border and mucosa of lip. Brain Res Rev 5:81–107

Hall KRL, Schaller GB (1964) Tool-using behavior of the California sea otter. J Mammal 45:287–298

Hammock J (2005) Structure, function and context: the impact of morphometry and ecology on olfactory sensitivity. Massachusetts Institute of Technology and Woods Hole Oceanographic Institution

Hamrick MW (2001) Morphological diversity in digital skin microstructure of didelphid marsupials. J Anat 198:683–688 . doi: 10.1017/S0021878201007750

Hanke F, Dehnhardt G (2009) Aerial visual acuity in harbor seals (Phoca vitulina) as a function of luminance. J Comp Physiol A 195:643–650 . doi: 10.1007/s00359-009-0439-2

Hanke FD, Peichl L, Dehnhardt G (2009) Retinal ganglion cell topography in juvenile harbor seals (Phoca vitulina). Brain Behav Evol 74:102–109 . doi: 10.1159/000235612

Hanke W, Wieskotten S, Marshall C, Dehnhardt G (2013) Hydrodynamic perception in true seals (Phocidae) and eared seals (Otariidae). J Comp Physiol A Neuroethol Sensory, Neural, Behav Physiol 199:421–440 . doi: 10.1007/s00359-012-0778-2

Hille P, Becker-Carus C, Dücker G, Dehnhardt G (2001) Haptic discrimination of size and texture in squirrel monkeys (Saimiri sciureus). Somatosens Mot Res 18:50–61 . doi: 10.1080/08990

Hines AH, Loughlin TR (1980) Observations of sea otters digging for clams at Monterey Harbor, California. Fish Bull 78:159–163

Hochberg Y (1988) A sharper Bonferroni procedure for multiple tests of significance. Biometrika 75:800–802

Hoffmann JN, Montag AG, Dominy NJ (2004a) Meissner corpuscles and somatosensory acuity: The prehensile appendages of primates and elephants. Anat Rec - Part A Discov Mol Cell Evol Biol 281:1138–1147 . doi: 10.1002/ar.a.20119

Hoffmann JN, Montag AG, Dominy NJ (2004b) Meissner corpuscles and somatosensory acuity: the prehensile appendages of primates. Anat Rec Part A 281A:1138–1147 . doi: 10.1002/ar.a.20119

Hothorn T, Bretz F, Westfall P (2008) Simultaneous Inference in General Parametric Models. Biometrical J 50:346–363

Howland HC, Merola S, Basarab JR (2004) The allometry and scaling of the size of vertebrate eyes. Vision Res 44:2043–65 . doi: 10.1016/j.visres.2004.03.023

Hughes A (1977) The topography of vision in mammals of contrasting lifestyle: comparative optics and retinal organisation. In: Crescitelli F (ed) Handbook of Sensory Physiology, VII-5. Springer-Verlag, Berlin, pp 613–756

Hughes BB, Eby R, Van Dyke E, et al (2013) Recovery of a top predator mediates negative eutrophic effects on seagrass. Proc Natl Acad Sci U S A 110:15313–8 . doi: 10.1073/pnas.1302805110

Hyvärinen H (1989) Diving in darkness: whiskers as sense organs of the ringed seal (Phoca hispida saimensis). J Zool London 218:663–678

Hyvärinen H, Palviainen a, Strandberg U, Holopainen IJ (2009) Aquatic environment and differentiation of vibrissae: comparison of sinus hair systems of ringed seal, otter and pole cat. Brain Behav Evol 74:268–79 . doi: 10.1159/000264662

Ide C (1977) Development of meissner corpuscle of mouse toe pad. Anat Rec 188:49–67

Iggo A, Andres KH (1982) Morphology of cutaneous receptors. Ann Rev Neurosci 5:1–31

Iggo A, Muir AR (1969) The structure and function of a slowly adapting touch corpuscle in hairy skin. J Physio 200:763–796

Jacobs GH (1993) The distribution and nature of colour vision among the mammals. Biol Rev 68:413–471

Jamieson GS, Fisher HD (1972) The pinniped eye: a review. In: Harrison RJ (ed) Functional Anatomy of Marine Mammals, Vol. 1. Academic Press, London, pp 245–261

Jamieson GS, Fisher HD (1971) The retina of the harbour seal, Phoca vitulina. Can J Zool 49:19–23 . doi: 10.1139/z71-005

Johansson RS, Vallbo AB (1979) Tactile sensibility in the human hand: relative and absolute densities of four types of mechanoreceptive units in glabrous skin. J Physiol 286:283–300

Johnson GL (1901) Contributions to the comparative anatomy of the mammalian eye, chiefly based on ophthalmoscopic examination. Philos Trans R Soc Biol Charact 1941–82 194:1–82

Johnson GL (1968) Opthalmoscopic studies on the eyes of mammals. Philos Trans R Soc B Biol Sci 254:207–220

Johnson KO (2001) The roles and functions of cutaneous mechanoreceptors. Curr Opin Neurobiol 11:455–461 . doi: 10.1016/S0959-4388(00)00234-8

Johnson KO, Hsiao SS (1992) Neural mechanisms of tactual forma and texture perception. Annu Rev Neurosci 15:227–50

Jolly J (1997) Foraging ecology of the sea otter, Enhydra lutris, in a soft-sediment community. University of California Santa Cruz

Kastelein R, Stevens S, Mosterd P (1990) The tactile sensitivity of the mystacial vibrissae of a Pacific Walrus (Odobenus rosmarus divergens). Part 2: Masking. Aquat Mamm 16:78–87

Kastelein R, van Gaalen M (1988) The sensitivity of the vibrissae of a Pacific walrus (Odobenus rosmarus divergens) Part 1. Aquat Mamm 14:123–133

Kastelein RA, Zweypfenning CVJ, Spekreijse H, et al (1993) The anatomy of the Walrus head (Odobenus rosmarus). Part 3: The eyes and their function in Walrus ecology. Aquat Mamm 19.2:61–92

Katzir G, Howland HC (2003) Corneal power and underwater accommodation in great cormorants (Phalacrocorax carbo sinensis). J Exp Biol 206:833–841 . doi: 10.1242/jeb.00142

Kenyon K (1969) The sea otter in the eastern Pacific ocean. Washington, D.C.

Kirchner H, Thorpe SJ (2006) Ultra-rapid object detection with saccadic eye movements : Visual processing speed revisited ☭. 46:1762–1776 . doi: 10.1016/j.visres.2005.10.002

Kollmeier B, Gilkey RH, Sieben UK (1988) Adaptive staircase techniques in psychoacoustics: A comparison of human data and a mathematical model. J Acoust Soc Am 83:1852–1862 . doi: 10.1121/1.396521

Kreuder C, Miller MA, Jessup DA, et al (2003) Patterns of mortality in southern sea otters (Enhydra lutris nereis) from 1998-2001. J Wildl Dis 39:495–509

Kuhn RA, Ansorge H, Godynicki S, Meyer W (2010) Hair density in the Eurasian otter Lutra lutra and the Sea otter Enhydra lutris. Acta Theriol (Warsz) 55:211–222 . doi: 10.4098/j.at.0001-7051.014.2009

Kumamoto K, Senuma H, Ebara S, Matsuura T (1993a) Distribution of pacinian corpuscles in the hand of the monkey, Macaca fuscata. J Anat 183:149–154

Kumamoto K, Takei M, Kinoshita M, et al (1993b) Distribution of pacinian corpuscles in the cat forefoot. J Anat 182:23–28

Kvitek R, Bretz C (2004) Harmful algal bloom toxins protect bivalve populations from sea otter predation. Mar Ecol Prog Ser 271:233–243 . doi: 10.3354/meps271233

Kvitek RG, Degange AR, Beitler MK (1991) Paralytic shellfish poisoning toxins mediate feeding behavior of sea otters. Limnol Oceanogr 36:393–404

Lacour JP, Dubois D, Pisani A, Ortonne JP (1991) Anatomical mapping of Merkel cells in normal human adult epidermis. Br J Dermatol 125:535–542 . doi: 10.1111/j.1365-2133.1991.tb14790.x

Lamb GD (1983) Tactile discrimination of textured surfaces: psychophysical performance measurements in humans. J Physiol 338:551–565

Le Boeuf BJ, Crocker DE, Costa DP, et al (2000) Foraging ecology of northern elephant seals. Ecol Monogr 70:353–382

Lederman SJ, Klatzky RL (1990) Haptic classification of common objects: Knowledge-driven exploration. Cogn Psychol 22:421–459 . doi: 10.1016/0010-0285(90)90009-S

Lederman SJ, Klatzky RL (1993) Extracting object properties through haptic exploration. Acta Psychol (Amst) 84:29–40 . doi: 10.1016/0001-6918(93)90070-8

Lesiuk TP, Braekevelt CR (1983) Fine structure of the canine tapetum lucidum. J Anat 136:157–164

Levenson DH, Ponganis PJ, Crognale M a, et al (2006) Visual pigments of marine carnivores: pinnipeds, polar bear, and sea otter. J Comp Physiol A 192:833–43 . doi: 10.1007/s00359-006-0121-x

Levenson DH, Schusterman RJ (1999) Dark adaptation and visual sensitivity in shallow and deep-diving pinnipeds. Mar Mammal Sci 15:1303–1313

Levenson DH, Schusterman RJ (1997) Pupillometry in seals and sea lions: ecological implications. Can J Zool 75:2050–2057 . doi: 10.1139/z97-838

Levy B, Sivak JG (1980) Mechanisms of accommodation in the bird eye. J Comp Physiol A 137:267–272

Liapunova RG, Miklukho NN (1996) Essays on the ethnography of Aleuts: at the end of the eighteenth and the first half of the nineteenth century. The University of Alaska Press, Fairbanks, Alaska

Ling JK (1966) The skin and hair of the southern elephant seal, Mirounga leonina. I. The facial vibrissae. Aust J Zool 14:855–866

Lowry L, Pearse J (1973) Abalones and sea-urchins in an area inhabited by sea otters. Mar Biol 23:213–219

Marshall CD, Amin H, Kovacs KM, Lydersen C (2006) Microstructure and innervation of the mystacial vibrissal follicle-sinus complex in bearded seals, Erignathus barbatus (Pinnipedia: Phocidae). Anat Rec Part A 288A:13–25 . doi: 10.1002/ar.a.20273

Marshall CD, Rozas K, Kot B, Gill VA (2014) Innervation patterns of sea otter (Enhydra lutris) mystacial follicle-sinus complexes. Front Neuroanat 8:1–8 . doi: 10.3389/fnana.2014.00121

Martin GR (2007) Visual fields and their functions in birds. J Ornithol 148:S547–S562 . doi: 10.1007/s10336-007-0213-6

Mass AM (2004) A High-Resolution Area in the Retinal Ganglion Cell Layer of the Steller's Sea Lion (Eumetopias jubatus): A Topographic Study. Dokl Biol Sci 396:187–190

Mass AM (2009) Localization of the highest retinal resolution area in the retinal ganglion cell layer of the caspian seal Phoca caspica: A topographic study. Dokl Biol Sci 429:575–578 . doi: 10.1134/S001249660906026X

Mass AM (1992) Retinal topography in the walrus (Odobenus rosmarus divergence) and fur seal (Callorhinus ursinus). In: Thomas JA, Kastelein RA, Supin AY (eds) Marine Mammal Sensory Systems. Plenum Press, New York, NY, pp 119–135

Mass AM, Supin AY (1992) Peak density, size and regional distribution of ganglion cells in the retina of the fur seal Callorhinus ursinus. Brain Behav Evol Evol 39:69–76

Mass AM, Supin AY (2010) Retinal ganglion cell layer of the caspian seal Pusa caspica: topography and localization of the high-resolution area. Brain Behav Evol 76:144–153 . doi: 10.1159/000320951

Mass AM, Supin AY (2007) Adaptive features of aquatic mammals' eye. Anat Rec 290:701–715 . doi: 10.1002/ar.20529

Mass AM, Supin AY (2000) Ganglion cells density and retinal resolution in the sea otter, Enhydra lutris. Brain Behav Evol 55:111–119 . doi: 10.1159/000006646

Mass AM, Supin AY (2005) Ganglion cell topography and retinal resolution of the Steller sea lion (Eumetopias jubatus). Aquat Mamm 31:393–402 . doi: 10.1578/AM.31.4.2005.393

McGovern KA, Marshall CD, Davis RW (2015) Are Vibrissae Viable Sensory Structures for Prey Capture in Northern Elephant Seals, Mirounga angustirostris? Anat Rec 298:750–760 . doi: 10.1002/ar.23061

Merkel F (1875) Tastzellen und Tastkörperchen bei den Hausthieren und beim Menschen. Arch für mikroskopische Anat 636–654

Meyer W, Bartels TI, Tsukise A, Neurand K (1990) Histochemical aspects of stratum corneum function in the feline foot pad. Arch Dermatol Res Res 281:541–543

Meyer W, Tsukise A (1995) Lectin histochemistry of snout skin and foot pads in the wolf and domesticated dog (Mammalia: Canidae). Ann Anat 177:39–49 . doi: 10.1016/S0940-9602(11)80129-9

Miller SN, Colitz CMH, Dubielzig RR (2010) Anatomy of the California sea lion globe. Vet Ophthalmol 13:63–71

Monson DH, DeGange AR (1995) Reproduction, preweaning, and survival of adult sea otters at Kodiak Island, Alaska. Can J Zool 73:1161–1169

Montagna W, Roman NA, Macpherson E (1975) Comparative study of the innervation of the facial disc of selected mammals. J Invest Dermatol 65:458–465 . doi: 10.1111/1523-1747.ep12608197

Moore BA, Tyrell LP, Kamilar JM, et al (2017) Structure and function of regional specializations in the vertebrate retina. In: Kaas JH (ed) Evolution of Nervous Systems, 2nd edn. Elsevier, Oxford, U.K., pp 351–372

Morley JW, Goodwin AW, Darian-Smith I (1983) Tactile discrimination of gratings. Exp Brain Res 49:291–299

Mowat FM, Breuwer AR, Bartoe JT, et al (2013) RPE65 gene therapy slows cone loss in Rpe65-deficient dogs. Gene Ther 20:545–555 . doi: 10.1038/gt.2012.63

Munger BL, Halata Z (1983) The sensory innervation of primate facial skin. I. Hairy Skin. Brain Res Rev 5:45–80

Munger BL, Ide C (1988) The structure of cutaneous sensory receptors. Arch Histol Cytol 51:1–34

Munger BL, Pubols LM (1972) The sensorineural organization of the digital skin of the raccoon. Brain Behav Evol 5:367–393

Munsinger H, Banks MS (1974) Pupillometry as a measure of visual sensitivity among infants, young children, and adults. Dev Psychol 10:677–682 . doi: 10.1037/h0036942

Munz FW, McFarland WN (1973) The significance of spectral position in the rhodopsins of tropical marine fishes. Vision Res 13:1829–1874

Murphy CJ, Bellhorn RW, Williams T, et al (1990) Refractive state, ocular anatomy, and accommodative range of the sea otter (Enhydra lutris). Vision Res 30:23–32

Mykytowycz R (1972) The behavioural role of the mammalian skin glands. Naturwissenschaften 59:133–139

Nagy AR, Ronald K (1970) The harp seal, Pagophilus groenlandicus (Emleben, 1777). VI. Structure of retina. Can J Zool 48:367–370

Neumann F, Schmidt H (1959) Optische Differenzierungsleistungen von Musteliden: Versuche an Frettchen und Iltisfrettchen. Z Vgl Physiol 42:199–205

Newsome SD, Tinker MT, Gill VA, et al (2015) The interaction of intraspecific competition and habitat on individual diet specialization: a near range-wide examination of sea otters. Oecologia 178:45–59

Niesterok B, Krüger Y, Wieskotten S, et al (2017) Hydrodynamic detection and localization of artificial flatfish breathing currents by harbour seals (Phoca vitulina). J Exp Biol 220:174–185 . doi: 10.1242/jeb.148676

Ollivier FJ, Samuelson D a., Brooks DE, et al (2004) Comparative morphology of the tapetum lucidum (among selected species). Vet Ophthalmol 7:11–22 . doi: 10.1111/j.1463-5224.2004.00318.x

Ostfeld RS (1982) Foraging strategies and prey switching in the California sea otter. Oecologia 53:170–178 . doi: 10.1007/BF00545660

Paré M, Smith AM, Rice FL (2002) Distribution and terminal arborizations of cutaneous mechanoreceptors in the glabrous finger pads of the monkey. J Comp Neurol 445:347–359 . doi: 10.1002/cne.10196

Peichl L, Behrmann G, Kröger RH (2001) For whales and seals the ocean is not blue: a visual pigment loss in marine mammals. Eur J Neurosci 13:1520–8

Piersma T, Aelst R V., Kurk K, et al (1998) A new pressure sensory mechanism for prey detection in birds: the use of principles of seabed dynamics? Proc R Soc B Biol Sci 265:1377–1383 . doi: 10.1098/rspb.1998.0445

Plummer M (2003) JAGS: A program for analysis of Bayesian graphical models using Gibbs sampling. In: Proceedings of the 3rd International Workshop on Distributed Statistical Computing

Plummer M (2016) rjags: Bayesian Graphical Models using MCMC

Pocock RI (1928) Some external characters of the sea-otter (Enhydra lutris). Proc Zool Soc London 98:983–991

R Core Team (2016) R: A language and environment for statistical computing. R Foundation for Statistical Computing, Vienna, Austria.

Radinsky LB (1968b) Evolution of somatic sensory specialization in otter brains. J Comp Neurol 134:495–506 . doi: 10.1002/cne.901340408

Radinsky LB (1968a) Evolution of somatic sensory specialization in otter brains. J Comp Neurol 134:495–506 . doi: 10.1002/cne.901340408

Raimondi P, Jurgens LJ, Tinker MT (2015) Evaluating potential conservation conflicts between two listed species: Sea otters and black abalone. Ecology 96:3102–3108 . doi: 10.1890/15-0158.1.sm

Ralls K, Hatfield BB, Siniff DB (1995) Foraging patterns of California sea otters as indicated by telemetry. Can J Zool 73:523–531

Rasband WS (1997) ImageJ. U. S. National Institutes of Health, Bethesda, Maryland, USA, https://imagej.nih.gov/ij/, 1997-2018

Rasmussen LEL, Munger BL (1996) The sensorineural specializations of the trunk tip (finger) of the Asian elephant, Elephas maximus. Anat Rec 246:127–134

Rice FL, Rasmusson DD (2000) Innervation of the digit on the forepaw of the raccoon. J Comp Neurol 417:467–490 . doi: 10.1002/(SICI)1096-9861(20000221)417:4<467::AID-CNE6>3.0.CO;2-Q

Riedman ML, Estes JA (1990) The sea otter (Enhydra lutris): behavior, ecology, and natural history. Biol Rep 90:1–136

Rothman S, Lorincz AL (1963) Defense mechanisms of the skin. Annu Rev Med 14:215–242

Schaeffel F, de Queiroz A (1990) Alternative Mechanisms of Enhanced Underwater Vision in the Garter Snakes Thamnophis melanogaster and T. couchii. Am Soc Ichthyol Herpetol 1:50–58

Schindelin J, Arganda-Carreras I, Frise E, et al (2012) Fiji: An open-source platform for biological-image analysis. Nat Methods 9:676–682 . doi: 10.1038/nmeth.2019

Schusterman RJ, Balliet RF (1970b) Conditioned vocalizations as a technique for determining visual acuity thresholds in sea lions. Science (80-) 169:498–501

Schusterman RJ, Balliet RF (1970a) Visual acuity of the harbour seal and the stellar sea lion under water. Nature 226:563–564

Schusterman RJ, Barrett B (1973) Amphibious nature of visual acuity in the Asian "clawless" otter. Nature 244:518–519

Shimek S (1977) The underwater foraging habits of the sea otter, Enhydra lutris. Calif Fish Game 63:120–122

Sills JM, Southall BL, Reichmuth C (2014) Amphibious hearing in spotted seals (Phoca largha): underwater audiograms, aerial audiograms and critical ratio measurements. J Exp Biol 217:726–734 . doi: 10.1242/jeb.097469

Sills JM, Southall BL, Reichmuth C (2015) Amphibious hearing in ringed seals (Phoca largha): underwater audiograms, aerial audiograms and critical ratio measurements. J Exp Biol 218:2250–2259 . doi: 10.1242/jeb.097469

Silverman RT, Munger BL, Halata Z (1986) The Sensory Innervation of the Rat Rhinarium. Anat Rec 210–225

Sinclair RJ, Burton H (1991) Tactile discrimination of gratings: psychophysical and neural correlates in human and monkey. Somatosens Mot Res Res 8:241–248 . doi: 10.3109/08990229109144747

Sinclair W, Dunstone N, Poole TB (1974) Aerial and underwater visual acuity in the mink Mustela vison shreber. Anim Behav 22:965–974

Sivak JG (1976) Optics of the eye of the "four-eyed fish" (Anableps anableps). Vision Res 16:521–534

Sivak JG, Hildebrand T, Lebert C (1985) Magnitude and rate of accomodation in diving and nondiving birds. Vision Res 25:925–933

Sivak JG, Lincer JL, Bobier W (1977) Amphibious visual optics of the eyes of the double-crested cormorant (Phalacrocorax auritus) and the brown pelican (Pelecanus occidentalis). Can J Zool 55:782–788 . doi: 10.1139/z77-102

Smodlaka H, Khamas WA, Palmer L, et al (2016) Eye histology and ganglion cell topography of northern elephant seals (Mirounga angustirostris). Anat Rec 299:798–805 . doi: 10.1002/ar.23342

Staedler M, Riedman M (1993) Fatal mating injuries in female sea otters (Enhydra lutris nereis). Mammalia 57:135–139

Stark B, Carlstedt T, Hallin RG, Risling M (1998) Distribution of human Pacinian corpuscles in the hand: A cadaver study. J Hand Surg (British Eur Vol 23B:370–372

Stebbins WC (1970) Principles of Animal Psychophysics. In: Stebbins WC (ed) Animal Psychophysics: The Design and Conduct of Sensory Experiments. Appleton-Century Crofts, New York, NY, pp 1–19

Stillman J (1989) A comparison of three adaptive psychophysical procedures using inexperienced listeners. Percept Psychophys 46:345–350

Stirling I, Latour PB (1978) Comparative hunting abilities of polar bear cubs of different ages. Can J Zool 56:1768–1772

Stokkan K-A, Folkow L, Dukes J, et al (2013) Shifting mirrors: adaptive changes in retinal reflections to winter darkness in Arctic reindeer. Proc Biol Sci 280:20132451 . doi: 10.1098/rspb.2013.2451

Strobel SM, Sills JM, Tinker MT, Reichmuth CJ (2018) Active touch in sea otters: in-air and underwater texture discrimination thresholds and behavioral strategies for paws and vibrissae. J Exp Biol 221:1–14

Stumpf P, Künzle H, Welsch U (2004) Cutaneous eccrine glands of the foot pads of the small Madagascan tenrec (Echinops telfairi, Insectivora, Tenrecidae): skin glands in a primitive mammal. Cell Tissue Res 315:59–70 . doi: 10.1007/s00441-003-0815-0

Supin AM, Mass AY (2003) Retinal topography of the harp seal Pagophilus groenlandicus. Brain Behav Evol 62:212–222 . doi: 10.1159/000073273

Tachibana T, Fujiwara N (1991) Mechanoreceptors of the hard palate of the mongolian gerbil include special junctions between epithelia and Meissner lamellar cells: A comparison with other rodents. Anat Rec 231:396–403

Taylor MM, Forbes SM, Creelman CD (1983) PEST reduces bias in forced choice psychophysics. J Acoust Soc Am 74:1367–1374 . doi: 10.1121/1.390161

Thometz NM, Kendall TL, Richter BP, Williams TM (2016a) The high cost of reproduction in sea otters necessitates unique physiological adaptations. J Exp Biol 219:2260–2264 . doi: 10.1242/jeb.138891

Thometz NM, Staedler MM, Tomoleoni JA, et al (2016b) Trade-offs between energy maximization and parental care in a central place forager, the sea otter. Behav Ecol 27:1552–1566 . doi: 10.1093/beheco/arw089

Tinker MT, Bentall G, Estes JA (2008) Food limitation leads to behavioral diversification and dietary specialization in sea otters. PNAS 105:560–565

Tinker MT, Costa DP, Estes JA, Wieringa N (2007) Individual dietary specialization and dive behaviour in the California sea otter: Using archival time–depth data to detect alternative foraging strategies. Deep Res II 54:330–342 . doi: 10.1016/j.dsr2.2006.11.012

Tinker MT, Guimarães PR, Novak M, et al (2012a) Structure and mechanism of diet specialisation: testing models of individual variation in resource use with sea otters. Ecol Lett 15:475–83 . doi: 10.1111/j.1461-0248.2012.01760.x

Tinker MT, Guimarães PR, Novak M, et al (2012b) Structure and mechanism of diet specialisation: testing models of individual variation in resource use with sea otters. Ecol Lett 15:475–83 . doi: 10.1111/j.1461-0248.2012.01760.x

Tjälve H, Frank A (1984) Tapetum lucidum in the pigmented and albino ferret. Exp Eye Res 38:341–351

Tucker VA (2000a) Gliding flight: drag and torque of a hawk and a falcon with straight and turned heads, an a lower value for the parasite drag coefficient. J Exp Biol 203:3733–3744

Tucker VA (2000b) The deep fovea, sideways vision and spiral flight paths in raptors. J Exp Biol 203:3745–3754

Tucker VA, Tucker AE, Akers K, Enderson JH (2000) Curved flight paths and sideways vision in peregrine falcons (Falco peregrinus). J Exp Biol 203:3755–3763

Valqui J (2012) The marine otter Lontra felina (Molina, 1782): A review of its present status and implications for future conservation. Mamm Biol 77:75–83 . doi: 10.1016/j.mambio.2011.08.004

Van Valkenburgh B, Curtis A, Samuels JX, et al (2011) Aquatic adaptations in the nose of carnivorans: evidence from the turbinates. J Anat 218:298–310 . doi: 10.1111/j.1469-7580.2010.01329.x

Vehtari A, Gelman A, Gabry J (2017) Practical Bayesian model evaluation using leave-one-out cross-validation and WAIC. Stat Comput 27:1413–1432 . doi: 10.1007/s11222-016-9696-4

Verendeev A, Thomas C, Mcfarlin SC, et al (2015) Comparative analysis of meissner's corpuscles in the fingertips of primates. J Anat 227:72–80 . doi: 10.1111/joa.12327

Verrillo RT, Bolanowski SJ (1986) The effects of skin temperature on the psychophysical responses to vibration on glabrous and hairy skin. J Acoust Soc Am 80:528–32 . doi: 10.1121/1.394047

Walls GL (1942) The vertebrate eye and its adaptive radiation. Hafner, New York

Watanabe JM (1983) Anti-predator defenses of three kelp forest gastropods: contrasting adaptations of closely-related prey species. J Exp Mar Bio Ecol 71:257–270 . doi: 10.1016/0022-0981(83)90119-3

Watson J, Estes JA (2011) Stability, resilience, and phase shifts in rocky subtidal communities along the west coast of Vancouver Island, Canada. Ecol Monogr 81:215–239 . doi: 10.1890/10-0262.1

Weiffen M, Mo B (2006) Effect of water turbidity on the visual acuity of harbor seals (Phoca vitulina). Vision Res 46:1777–1783 . doi: 10.1016/j.visres.2005.08.015

Weissengruber GE, Egger GF, Hutchinson JR, et al (2006) The structure of the cushions in the feet of African elephants (Loxodonta africana). J Anat 209:781–792 . doi: 10.1111/j.1469-7580.2006.00648.x

Welsch U, Ramdohr S, Riedelsheimer B, et al (2001) Microscopic anatomy of the eye of the deep-diving Antarctic weddell seal (Leptonychotes weddellii). J Morphol 248:165–174

Wen G, Sturman J, Shek J (1985) A comparative study of the tapetum, retina and skull of the ferret, dog and cat. Lab Anim Sci 35:200–210

Werner YL (1970) Extreme adaptatability to light, in the round pupil of the snake, Spalerosophis. Vision Res 10:1159–1164

Wichmann FA, Hill NJ (2001) The psychometric function: I. Fitting, sampling, and goodness of fit. Percept Psychophys 63:1293–1313 . doi: 10.3758/BF03194544

Wickelgren WA (1977) Speed-accuracy tradeoff processing and information processing dynamics. Acta Psychol (Amst) 41:67–85

Wight R, Milliken GW, Ward JP (1988) Assessment of visual acuity, the oblique effect, and the lateral mirror-image confusion effect in the ferret (Mustela putorius furo). Int J Comp Psychol 1:254–267

Wilcox JG, Barlow HB (1975) The size and shape of the pupil in lightly anaesthetized cats as a function of luminance. Vision Res 15:1363–5

Wilkin SM (2003) Nocturnal foraging ecology and activity budget of the sea otter (Enhydra lutris) in Elkhorn Slough, California. San Francisco State University

Williams TD, Allen DD, Groff JM, Glass RL (1992) An analysis of California sea otter (Enhydra lutris) pelage and integument. Mar Mammal Sci 8:1–18

Winkelmann RK (1964) Nerve endings of the North American opossum (Didelphis virginia): A comparison with nerve endings of primates. Am J Phys Anthropol 22:253–258

Yamaue Y, Hosaka YZ, Uehara M (2015) Spatial relationships among the cellular tapetum, visual streak and rod density in dogs. J Vet Med Sci 77:175–179 . doi: 10.1292/jvms.14-0447

Yeates LC, Williams TM, Fink TL (2007) Diving and foraging energetics of the smallest marine mammal, the sea otter (Enhydra lutris). J Exp Biol 210:1960–1970 . doi: 10.1242/jeb.02767

Young B, O'Dowd G, Woodford P (2014) Wheater's Functional Histology: A text and colour atlas, 6th edn. Elsevier Churchill Livingstone, Philadelphia, PA

Yu Wang F, Yun Tang M, Young Yan H (2011) A comparative study on the visual adaptations of four species of moray eel. Vision Res 51:1099–1108 . doi: 10.1016/j.visres.2011.02.025